MULTI-SCALE COMPARISON OF FLOOD SOCIOECONOMIC VULNERABILITY
FOR URBAN AND AGRICULTURAL COMMUNITIES

by

Tuğkan Tanır
A Thesis
Submitted to the
Graduate Faculty
of
George Mason University
in Partial Fulfillment of
The Requirements for the Degree
of
Master of Science
Civil, Environmental, and Infrastructure Engineering

Committee:

_____   Dr. Dr. Celso M. Ferreira, Thesis Director

_____   Dr. Viviana Maggioni, Committee Member

_____   Dr. Mark H. Houck, Committee Member

_____   Dr. Sam Salem, Department Chair

_____   Dr. Kenneth S. Ball, Dean, Volgenau School
of Engineering

Date:_____   Fall Semester 2020
George Mason University
Fairfax, VA

Multi-Scale Comparison of Flood Socioeconomic Vulnerability for Urban and
Agricultural Communities

A Thesis submitted in partial fulfillment of the requirements for the degree of Master of
Science at George Mason University

by

Tuğkan Tanır
Bachelor of Science
Middle East Technical University, Ankara, Turkey, 2016

Director: Celso M. Ferreira, Associate Professor
Civil, Environmental, and Infrastructure Engineering

Fall Semester 2020
George Mason University
Fairfax, VA

DEDICATION

This is dedicated to my family and many friends.

ACKNOWLEDGEMENTS

TABLE OF CONTENTS

LIST OF TABLES

LIST OF FIGURES

LIST OF EQUATIONS

LIST OF ABBREVIATIONS

ABSTRACT

MULTI-SCALE COMPARISON OF FLOOD SOCIOECONOMIC VULNERABILITY FOR URBAN AND AGRICULTURAL COMMUNITIES

Tuğkan Tanır, M.S.

George Mason University, 2020

Thesis Director: Dr. Celso M. Ferreira

Flood events are one of the common natural hazards causing a considerable amount of damage to different sectors and communities all around the world. Due to several factors, such as climate change, urbanization, and deforestation, the impacts of different flood types, including riverine flood, coastal storms, and urban pluvial, increase in urban and agricultural communities. Especially, the co-occurrence of flood drivers (i.e compound floods) cause severe damages on coastal metropolitan areas, such as DC. Riverine flood events can also have destructive effects on agricultural production and threaten food security on both national and local scales, such as Potomac River Watershed. In this context, this study proposes two separate modules to assess flood socio-economic vulnerability (FSOEVI) to quantify both urban compound and riverine flood risks on the residential population in Washington, DC metropolitan area and agricultural communities in the Potomac River Watershed (PRW), respectively. A combination of the HAZUS-MH flood damage estimation tool and the Social Vulnerability Index (SOVI) were used to quantify overall vulnerability for both

communities. For urban populations, two different compound flood scenarios were used to estimate socioeconomic losses, while 100-year riverine flood event was used for agricultural crop damage analysis. Although the agricultural communities in Highland and Prince George's were more vulnerable, they did not experience high flood damages in any scenarios. The spatiotemporal distribution of vulnerabilities indicated that agricultural populations in Shenandoah County were most vulnerable in September and October, which were months with the highest flood probability. The compound event with coastal surge and riverine flood caused high damage on the banks of the Potomac River. In addition, a high precipitation scenario led to severe damages in locations with denser infrastructures, such as DC and Arlington County. The block level analysis was more sensitive to vulnerability and flood damages compared to coarser scales i.e. group and tract. The distribution of the risk was found significantly dependent on the compound flood event type and scale of the analysis for urban populations, while time of the year of a flood event and dominant crop type were the main determinant of the risk for agricultural communities. The method presented in this study is a tool that can identify most vulnerable agricultural and urban communities in order to aid vulnerability reduction efforts in flood risk management.

INTRODUCTION

<u>Problem Statement</u>

Flood events are one of the most destructive naturally occurring hazards, causing a considerable amount of economic damage to economies and societies around the world (Sowmya et al. 2015; Remo et al. 2016; Chen et al. 2019b; Rehman et al. 2019) . The intensity and the frequency of all different flood types, including riverine, coastal, urban, and compound events, increase due to climate change, urbanization, growing population, and deforestation (Bradshaw et al. 2007; de la Paix et al. 2013; Hinkel et al. 2014). Therefore, damages from each flood type on various land uses are amplified (Zhou et al. 2012). Urban areas are one of the most susceptible locations to those different flood types because of high-value properties and dense populations (Balica et al. 2009; Yerramilli 2012; Cho and Chang 2017; Bertilsson et al. 2018; Eem et al. 2018). Thus, the impacts of flood events are intense and hard to manage in urban areas (Sowmya et al. 2015; Bertilsson et al. 2018). Moreover, flood events can have destructive effects on crop yield and threaten the sustainability of the agricultural economy and food security on national, regional, and local scales (Balica et al. 2009; FAO 2017; Rahman and Di 2020). Although these economic damages are relatively higher in residential areas with same event characteristics, the flood damage to crops is still responsible for a substantial portion of loss experienced every year in the agriculture sector (Merz et al. 2010; Chau et

1

al. 2015; FAO 2017; Rahman and Di 2020). The most effective way of mitigating the impacts of those damages from flood events on both land uses is to implement flood risk management approaches and evaluating each risk dimensions (De Risi et al. 2018). The hazard, exposure and vulnerability, which are the main terms that describe overall flood risk (Crichton 2002), need to be well-defined and evaluated to manage the risk efficiently (Crichton 2002; Wilby and Keenan 2012; Win et al. 2018).

Different flood types such as riverine, coastal, and pluvial floods have caused substantial damage in disparate locations, sectors and communities (Hinkel et al. 2014; Van Ootegem et al. 2015; Duy et al. 2019) throughout history. Additionally, the amount of severe flood damage is magnified (Zscheischler et al. 2018; Couasnon et al. 2020; Paprotny et al. 2020), when two (or more) co-occur (i.e. compound floods) (Couasnon et al. 2020), especially in the large coastal cities (Wahl et al. 2015). For example, Hurricane Harvey (Paprotny et al. 2020) and Hurricane Sandy (Zscheischler et al. 2018) caused $150 and $50 billion of damage on prominent urban areas in the U.S, respectively. In addition, riverine floods have substantially damaged crops around the world (FAO 2017). For instance, $30 million loss was compensated by grants because of flood damage on crops in Indiana after a severe flood event happened in 2007 (Pantaleoni et al. 2007). The estimation of those flood damages on urban and agricultural areas is one of the main components of the flood risk management practices for urban and agricultural communities (Van Ootegem et al. 2015). Whereas it is unlikely to prevent all possible losses, it is possible to estimate them and their impacts on infrastructure and crops (Magombeyi and Taigbenu 2008; Singh and Singh 2015; Remo et al. 2016; Win et al.

2018). Thus, there is a significant amount of studies focused on the flood damage estimation for different types of flood drivers such as river flood (Remo et al. 2016; Arrighi and Campo 2019; Muthusamy et al. 2019; Oubennaceur et al. 2019) and coastal storms (Xian et al. 2015; Karamouz et al. 2016; Prahl et al. 2018) on urban infrastructure and agricultural activities (Vozinaki et al. 2015; Shrestha et al. 2017, 2019). However, very few studies have aimed to quantify urban compound flood risk in urban areas (Jiménez-Jiménez et al. 2020; Yang et al. 2020). As the Washington, DC metropolitan area has an increasing precipitation rate and is under the risk of sea level rise (Ayyub et al. 2012), substantial losses from compound events are expected to increase in the future. Thus, it is essential to quantify compound flood damages due to its importance for flood risk management. Moreover, the agricultural economy is one of the most important sectors in most of the counties located in the Potomac River Watershed, including Rockingham, Shenandoah, Augusta, Hardy, and Grant (USDA 2019). Especially for the west and the middle part of the watershed, agricultural production is the primary source of income for a considerable portion of the population (USDA 2019). Since crop types, harvest and plantation costs vary significantly across the Potomac River Watershed, the impact of flood events indicates high spatial variation as well. Additionally, seasonality is identified as one of the important variables for flood damages on crops (Brémond et al. 2013). Hence, distribution of the risk of flooding on agricultural activities is significantly dependent on both spatial and temporal variables.

The impacts of flood damages are not evenly distributed on societies because of the differences in population characteristics and socioeconomic structures (Karagiorgos

et al. 2016; Munyai et al. 2019). Socio-economic conditions and population dynamics (Cutter et al. 2003; Eakin and Luers 2006; Gu et al. 2018; Kawasaki et al. 2020) are the main determinants of inequalities within society which define how consequences of flood loss are distributed across the communities (Cutter et al. 2003; Munyai et al. 2019; Chakraborty et al. 2020). Since both alterations on vulnerabilities of the population and the hazard extent can result in a change in the flood risk, both components need to be well understood (Bhattacharya et al. 2011). Therefore, it is crucial to quantify characteristics of socio-economic components of the flood risk, as well as the hazard component, in order to assess cumulative risk efficiently (Cutter et al. 2003). Vulnerability assessment, which is a comprehensive socio-economic risk drivers quantification method (Cutter et al. 2003), is applied to map out vulnerabilities and their related factors. The hazard of place model, which is introduced by Cutter et al (1996), is the most widely used technique to evaluate social vulnerabilities of the populations in both local and national scales (Clark et al. 1998; Tapsell et al. 2002; Rygel et al. 2006; Fekete 2009; Cutter et al. 2012; Monterroso et al. 2014; Remo et al. 2016; Bathi and Das 2016; Gu et al. 2018). Some studies have combined social vulnerabilities with flood hazard to assess flood vulnerabilities of the population at different scales (Barroca et al. 2006; Ouma and Tateishi 2014; Sowmya et al. 2015; Remo et al. 2016; Fernandez et al. 2016; Weerasinghe et al. 2018; Jha and Gundimeda 2019; Erena and Worku 2019; Khajehei et al. 2020). However, few studies evaluate flood vulnerabilities at multiple scales (Remo et al. 2016). In addition, there are very few studies that focus on compound urban flood damage and risk (Yang et al. 2020).

Although generally rural communities are defined as more vulnerable to hazards compared the urban populations (ILO 2017), flood vulnerability assessments are under reported in the literature. There are few studies particularly focused on agricultural communities around the world (Ma et al. 2007; Huang et al. 2012; Monterroso et al. 2014; Awere et al. 2016; Jose et al. 2017; Hoque et al. 2019; Baky et al. 2020). However, any of aforementioned studies have not merged the standardized damage estimation and socioeconomic risk drivers to evaluate overall vulnerability of agricultural communities.

Research Statement

This study aims to evaluate socio-economic drivers of the riverine and compound flood risk and combine those drivers with physical damage for agricultural and urban communities, respectively. An integrated flood socio-economic vulnerability assessment tool is introduced to assess overall risk of flood on both agricultural and urban communities in two different case studies separately.

The first case study intended to investigate spatiotemporal distributions of flood risk over agricultural activities and its impacts on agricultural communities by using the Flood Socio-Economic Vulnerability Index (FSOEVI) in the Potomac River Watershed. In order to quantify physical and socioeconomic dimensions of risk, the Social Vulnerability Index (SOVI) was developed for agricultural communities at the county scale. For the physical dimension of the risk, spatiotemporal flood damage distributions on crops were evaluated by a proposed script which replicates the widely used flood damage estimation tool HAZUS-MH method. Then, these two dimensions were combined to introduce an overall vulnerability index, FSOEVI, to highlight the most

vulnerable agricultural communities to flood both spatially and temporally in the Potomac River Watershed. The article investigates this case study in detail which was submitted to "Natural Hazards" with the title "Assessing the spatiotemporal socio-economic flood vulnerability of agricultural communities in the Potomac River Watershed" is currently under review (Tanir et al. 2020).

The second case study aimed to assess spatial distributions of the urban compound flood socioeconomic vulnerabilities of residential population in the Washington, DC metropolitan area for three different scales (tract, group, and block) and evaluate sensitivities of each scale to flood vulnerability. The social dimension of the risk was investigated by SOVI for urban populations with parameters defined by the extensive literature search. Compound flood damages on residential buildings and vehicles were estimated by HAZUS-MH flood module from two different compound flood scenarios to identify physical risk dimension on the residential population. These two dimensions were merged to identify FSOEVI which facilitate to illustrate overall compound flood risk for the residential population for three disparate scales. The article evaluate urban compound flood in the Washington, DC metropolitan area was submitted to " International Journal of Disaster Risk Reduction" journal with the title " Multi-Scale comparison of urban socio-economic vulnerability in the Washington DC Metropolitan Region resulting from compound flooding" (Tanir et al. 2020). The manuscript is currently under review.

Set of objectives

The set of objectives defined to achieve the research goals for the first case study are;

- Quantify social vulnerability levels of agricultural communities with SOVI at the county scale.

- Evaluate seasonality of the risk of flooding on agricultural communities.

- Assess spatiotemporal distributions of flood risk across agricultural communities in PRW.

The set of objectives defined to achieve the research goals for the second case study are:

- Quantify social vulnerability levels of urban populations with SOVI index for three different scales.

- Assess spatial distribution of compound flood exposure over the Washington, DC metropolitan area

- Evaluate the spatial distributions of combined FSOEVI results for three different scales and compare distributions among three scales in the Washington, DC Metropolitan area.

- Determine the most vulnerable locations to compound flood hazard in Washington, DC metropolitan area

CHAPTER 1 ASSESSING THE SPATIOTEMPORAL SOCIO-ECONOMIC FLOOD VULNERABILITY OF AGRICULTURAL COMMUNITIES IN THE POTOMAC RIVER WATERSHED

Abstract

Flood events are one of the most destructive and yet increasingly frequent natural hazards causing a considerable amount of economic losses in the United States (U.S.) and throughout the world. The agricultural sector is particularly vulnerable to flood hazards compared to other sectors of the economy. The representation of spatiotemporal distributions of the agricultural damage and the vulnerability of the agricultural communities are essential for flood risk management. Therefore, this study is intended to investigate spatiotemporal socio-economic flood vulnerability of the agricultural communities in the Potomac River Watershed (PRW), which is located at the East Coast of the U.S, where corn and soybeans cultivation are one of the important agricultural activities. In this context, a combination of the widely used flood damage estimation tool HAZUS-MH and the county-based Social Vulnerability Index (SOVI) were utilized for the vulnerability assessment. The spatial distribution of agricultural communities vulnerable to flood was evaluated for the extreme and average damage conditions for 365 days along with the monthly average damage from a 100-year flood event. The maximum crop damage and most likely months to experience major flood event were found in the same temporal periods. The spatial distributions of damage and SOVI

assessments suggested that the most vulnerable agricultural communities (Highland (VA) and Prince George's (MD) did not experience high flood damages in any scenarios. The agricultural community in Shenandoah County the most vulnerable in September and October, which were the months with the highest flood probability. This high risk that is highlighted spatiotemporally can aid decision makers regarding the resource allocation for mitigation efforts in the PRW. The method presented in this study can potentially be replicated throughout the country, thus helping efforts to mitigate flood hazards and protect vulnerable agricultural populations.

1.1 Introduction

Flood events are the costliest natural hazards in the world (Remo et al. 2016; Tella and Balogun 2020; Ullah et al. 2020). Although the total economic loss in the agricultural sector is comparatively lower than the residential areas with the same exposure (Merz et al. 2010), there is growing attention towards the estimation of these devastating damages prior to their occurrence (Chau et al. 2015). Floods can have destructive effects on agricultural production and threaten food security on both local and national scales (Balica et al. 2013; FAO 2017; Rahman and Di 2020) . The main impact of flood hazards on agricultural production is the decline in crop production due to the interruption of crop growth (UNDP 2004; Chen et al. 2017, 2019a; Shrestha et al. 2017). Several examples in a variety of scales show that a considerable amount of economic damage has occurred owing to flood hazards in agriculture areas (Myers 1997; Hall et al. 2005; Gonsalves 2014; Pinos et al. 2020). For example, at a national scale analysis, annual flood damages to the agricultural economy are calculated as $7.8 million in Great

Britain (Hall et al. 2005) and $3 billion in the U.S. (Myers 1997). Additionally, some local flood events that happened in India (Mandal 2014), Vietnam (Chau et al. 2015), and Saint Vincent & Grenadines (Gonsalves 2014) caused a substantial loss in crop production; respectively 3,747 million Indian Rupee (Rs) in 2004, 84.1 million Vietnamese dongs (VND) in 2007, and $1.4 million in 2011. In addition, $30 million aid was granted because of flood damage on crops in Indiana after a severe flood event (Pantaleoni et al. 2007). Since flood damage on crops is experienced across the world (Chau et al. 2015), agricultural flood damage estimation becomes a crucial tool to predict the risk of experiencing damage and be prepared for its consequences (Chau et al. 2015). While it is unlikely to fully prevent the consequences of flooding (Singh and Singh 2015) in rural communities (Magombeyi and Taigbenu 2008), it is possible to quantify the agricultural population under risk and mitigate its impacts by predicting potential losses. In order to better quantify risk, it is important to develop an integrated framework combining physical damage and the socio-economic features of the rural population (Cannon et al. 2003; Messner and Meyer 2006; Ma et al. 2007; Magombeyi and Taigbenu 2008; Brémond et al. 2013; Nga et al. 2018). Some agricultural flood exposure estimation studies have been conducted using remote sensing tools (Rosenzweig et al. 2002; Tapia-Silva et al. 2011; Shrestha et al. 2017), flood depth-crop damage functions (Vozinaki et al. 2015; Shrestha et al. 2019), as well as, publicly available potential loss estimation method from floods HAZUS-MH (FEMA 2013; Pinter et al. 2016; Antolini et al. 2020) HAZUS-MH stands out for being a standardized GIS-based agricultural damage estimation widely used in the U.S. (FEMA 2013).

The impact of the amount of damage experienced from flooding depends on the socio-economic features and dynamics of the population (Karagiorgos et al. 2016; Sam et al. 2017; Munyai et al. 2019; Spielman et al. 2020). For instance, Hurricane Katrina catastrophically demonstrated that the consequences of natural hazards are not evenly distributed across the different groups of populations (Spielman et al. 2020). Vulnerability assessments are used as a tool to evaluate the system and/or population features and characteristics (Adger 2006), by assessing socio-economic features of the population to define how society, population, or communities are affected by hazards (Cutter et al. 2003). Four different approaches are introduced to define vulnerability in the vulnerability assessment literature, including Risk-Hazard Approach (RHA), Political Economy Approach (PEA), Biophysical Approach (BPA), and Integrated Assessment Approach (IAA). As one of the most frequently used methods, Integrated Assessment Approach (IAA) is a comprehensive methodology which synthesizes biophysical and socio-economic dimensions of vulnerability (Füssel 2007; Zarafshani et al. 2016). The most well-known example of the IAA is the hazard of place model introduced by Cutter et al. (2003) who developed a social vulnerability index for the U.S. at the county level. The hazard of place model is also widely used to develop social vulnerability index for both local (Clark et al. 1998; Tapsell et al. 2002; Rygel et al. 2006; Fekete 2009; Cutter et al. 2012; Monterroso et al. 2014; Remo et al. 2016; Bathi and Das 2016; Gu et al. 2018) and national scales (Cannon et al. 2003; Cutter et al. 2003; Dwyer et al. 2004; Holand et al. 2011). Some of the studies combined these indexes with flood hazards to assess flood social vulnerability of the populations (Barroca et al. 2006; Ouma and Tateishi 2014;

Sowmya et al. 2015; Remo et al. 2016; Fernandez et al. 2016; Weerasinghe et al. 2018; Jha and Gundimeda 2019; Erena and Worku 2019; Khajehei et al. 2020). However, most of the aforementioned examples were concentrated on the general populations, not comprising agricultural communities. There are few studies particularly focused on the agricultural population around the world by using socio-economic parameters defining agricultural vulnerability factors (Ma et al. 2007; Huang et al. 2012; Monterroso et al. 2014; Awere et al. 2016; Jose et al. 2017; Hoque et al. 2019; Baky et al. 2020). Ma et al. (2007) evaluated farmers' vulnerability in the Poyang Lake Region of China, by combining GIS-based flood hazard estimation and socio-economic vulnerability factors of farmers, including cash income, rural population, and share of agricultural revenue in the economy etc. (Ma et al. 2007). Similarly, Suryanto and Rahman (2019) integrated livelihood vulnerability index and the statistical probability of flood events to scrutinize the overall flood vulnerability of farmers in Indonesia (Suryanto and Rahman 2019). However, any of the mentioned studies above have not used standardized crop flood damage methods to describe exposure terms and merge that with socio-economic risk drivers.

As seen above, most of the existing flood vulnerability assessment studies are focused on urban populations both in the U.S and other locations in the world whereas the flood vulnerabilities of agricultural communities are under reported. Therefore, there is a scientific gap for vulnerability assessment on agricultural populations and quantifying risk of flooding across rural communities during flood hazards. This study aims to fill the scientific gap by (a) developing a social vulnerability index to map out the

most vulnerable agricultural communities in the Potomac River Watershed at county scale; (b) assessing spatiotemporal flood damage distributions on crops to indicate flood exposure levels on the agricultural economy, and (c) combining social vulnerability assessment results with flood exposure to introduce the Flood Socio-Economic Vulnerability Index (FSOEVI) to highlight hot spots for both flood hazards and vulnerabilities within the PRW.

1.2 Study Area

The Potomac River Watershed (PRW) is located in the Mid-Atlantic region of the U.S with total coverage of 14,670 miles of the drainage area (Interstate Commission on the Potomac River Basin 2020). It is located in parts of the Commonwealth of Virginia, Maryland, West Virginia, and Pennsylvania states, as well as the District of Columbia (Figure 1). There are 6.11 million residences with different socio-economic features in the PRW. Elevation range varies between sea level to 1,482 meters within the basin (Interstate Commission on the Potomac River Basin 2018). Spatial distribution of precipitation pattern shows that the annual precipitation is lower (700-900 mm) in the west and south parts of the basin compared to the east part where close to Chesapeake Bay (1000-1200 mm) (Sridhar et al. 2019). Seasonal distribution of precipitation patterns indicates that the wettest seasons are May and June in the basin (Sridhar et al. 2019).
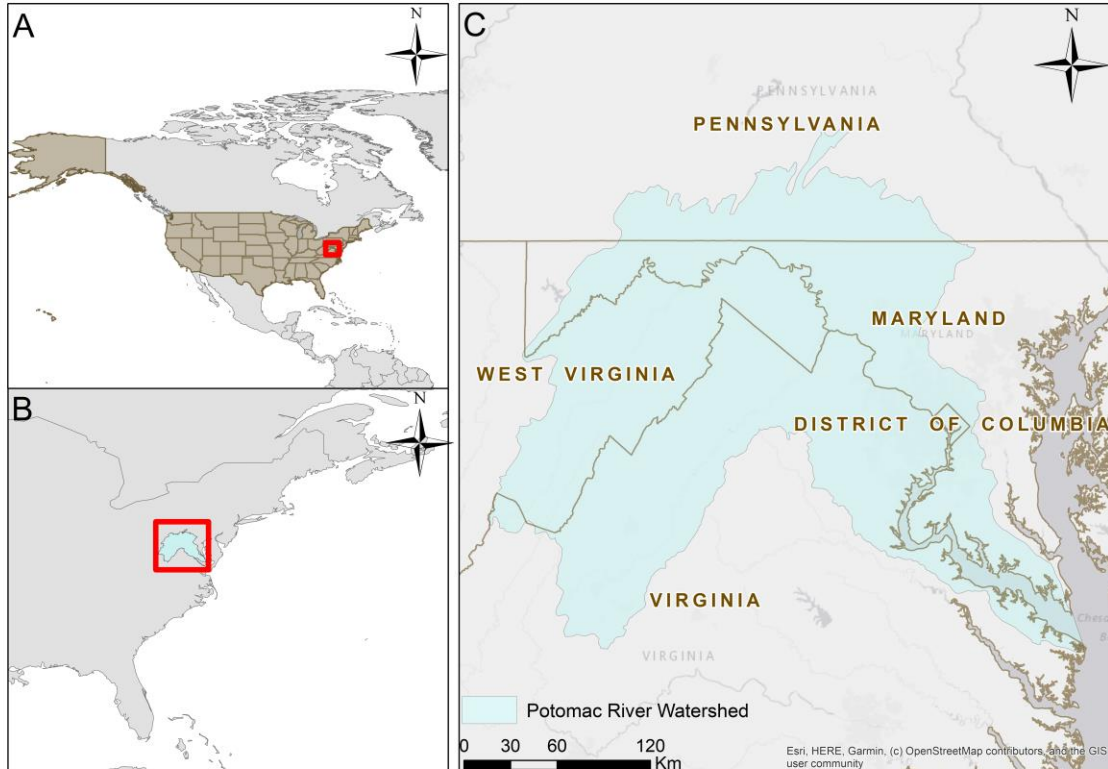
Figure 1 A) United States; B) East Coast of the U.S; C) Potomac River Watershed (PRW)

The majority of land uses are defined by the land cover map from National Land Cover Database (NCLD), as forests, agriculture, developed areas, and water with 54.6%, 26%, 14.1%, and 5.9%, respectively (Interstate Commission on the Potomac River Basin 2020). Agricultural activities are generally carried out in the western and central part of the watershed (Interstate Commission on the Potomac River Basin 2020). Additionally, most of those practices are observed around main rivers, streams, and branches in the basin (Battista et al. 1998). The agricultural economic activities play a significant role in the state economies in some counties in the PRW. For instance, counties of Rockingham (20%) and Augusta (7%) contain a considerable portion of Virginia's total agriculture

sales (USDA 2019). Hardy (25%), Pendleton (13%), and Grant (8%) are important for the agricultural economy of West Virginia, while Washington (6%) is for Maryland. Furthermore, Franklin (6%) county has an important percentage of total agriculture sales in Pennsylvania (USDA 2019). The highest number of producers are reported at Rockingham, Augusta, and Franklin counties which is 20% of all 46,400 producers recorded in the basin (USDA 2019).

The majority of the crops observed in the PRW are forage, corn, and soybeans. The distributions of those crops are not equal over the basin. For example, although Franklin (PA) county has the highest acreage of forage and corn, Frederick (MD) county has the highest share of soybeans cultivation in the basin (USDA 2019). Additionally, distributions of socio-economic characteristics, which are considered as vulnerability factors for farmers, vary within the PRW. All features of the PRW explained above make PRW a perfect candidate to demonstrate how both physical and social risks are distributed across the agricultural communities (USDA 2019).

1.3 Methodology

As depicted in Figure 2, there were three main parts of the overall framework applied in this research. The Social Vulnerability Index (SOVI) analysis quantitatively evaluated the overall vulnerability of the agricultural communities in the PRW. The relative social vulnerability levels of the agricultural communities in the PRW with respect to a national scale were assessed within the counties located in its borders and the entire U.S, including Puerto Rico. The comparison in the PRW demonstrated the actual distribution of vulnerabilities in the study area, while the U.S. scale analysis was only

used as a broad-scale comparison for reference in this study to contextualize results to a

national extent. The PRW scale comparison results were used as a social dimension of

the risk term in the rest of the study. As a result of the social dimension, the spatial

distributions of highly vulnerable agricultural populations were determined. The

spatiotemporal distribution of flood exposure index, which defines flood damage on the

crops, was obtained by using FEMA's 100-year flood map (FEMA 2020) and flood

damage functions in the PRW. Finally, these two indexes were combined to introduce a

FSOEVI to evaluate relative flood socio-economic vulnerability levels across the PRW.
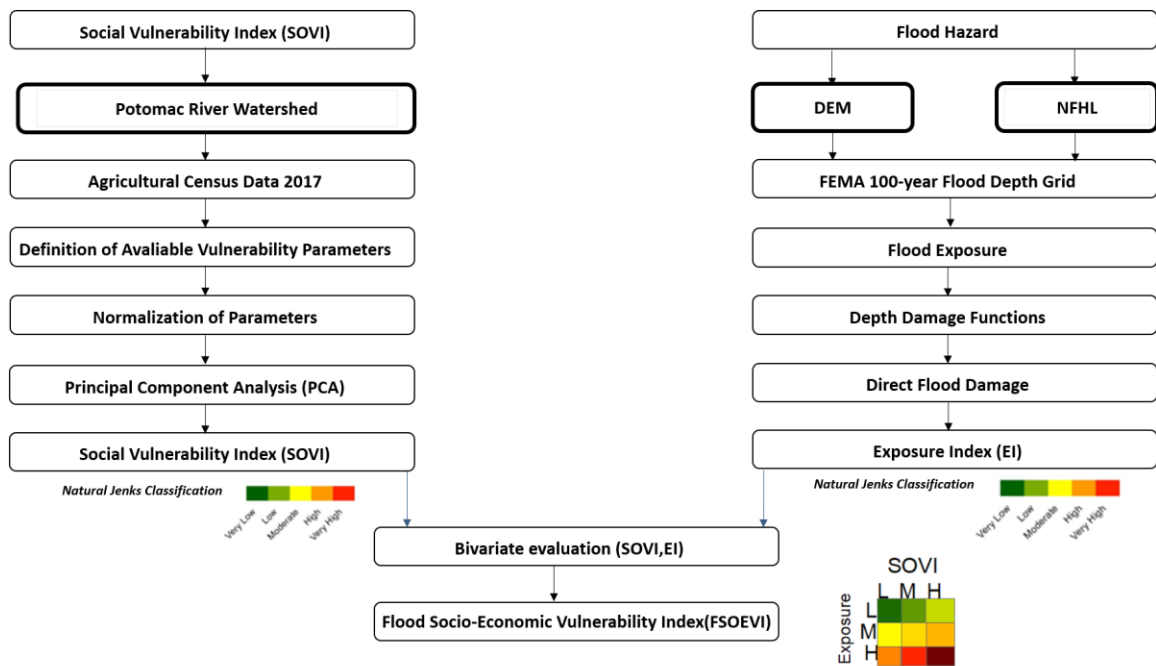
Figure 2 Overall methodology of agricultural flood socio-economic vulnerability

1.3.1 Social Vulnerability Index (SOVI)

1.3.1.1 SOVI parameters

The vulnerability factors for capturing the social vulnerability of the agricultural communities were determined by a detailed literature review. Table 1 summarized the selected variables, their correlations with vulnerability, years which data obtained, definitions as well as, articles that used them as vulnerability factors. All data related to the agricultural production and socio-economic features of producers were acquired from the United States Department of Agriculture (USDA) while the data which provides information for the general population, including poverty level and educational attainment, were obtained from the United States Census Bureau at a county level.

Table 1 List of parameters for the social agricultural vulnerability assessment

Parameter/Correlation/Year	Definition	Article
PerFemPro (+) (2017)	Percentage of Female Producers	(Nelson et al. 2002; Brooks et al. 2005; Abdur Rashid Sarker et al. 2013; Monterroso et al. 2014; Hoque et al. 2019)
Per65yrandOld (+) (2017)	Percentage of 65 years and older farmers	(Jose et al. 2017; Hoque et al. 2019)
PerInex (+) (2017)	Percentage of farms with New and Beginning Producers, (10 years or Less Experience)	(Reid et al. 2007; Nicholas and Durham 2012; Abdur Rashid Sarker et al. 2013; Jose et al. 2017; Khan et al. 2020)
PerMin (+) (2017)	Percentage of Minority Farmers	(Vásquez-León 2009; Monterroso et al. 2014; Bathi and Das 2016)
AvgAge (+) (2017)	Average Age of Producers	(Abdur Rashid Sarker et al. 2013; Hoque et al. 2019)
AgrSold (+) (2017)	Total Value of Agricultural Products Sold	(Jose et al. 2017; Hoque et al. 2019)
PerPopAgri (+) (2017)	Percentage of Population works in Agriculture, Fishing and Hunting	(Brooks et al. 2005; Ma et al. 2007; Hoque et al. 2019; Dumenu and Takam Tiamgne 2020; Khan et al. 2020)
PerPoverty (+) (2018)	Percentage of Population under	(Monterroso et al. 2014; Jose et al.

Parameter/Correlation/Year	Definition	Article
	poverty level	2017; Hoque et al. 2019)
PerInternet (-) (2017)	Percentage of Farmers Have Internet Connection	(Reid et al. 2007; Chauhan et al. 2020; Dumenu and Takam Tiamgne 2020)
PerHighEducated (-) (2018)	Percentage of the Population Have Completed 12th grade	(Abdur Rashid Sarker et al. 2013; Monterroso et al. 2014)
NetCash (-) (2017)	Net Cash Income of Farms	(Ma et al. 2007; Abdur Rashid Sarker et al. 2013)
PerFarm250K (-) (2017)	Percentage of Farms with Sales of $250,000 or more	(Ma et al. 2007)
LandofFarmers (-) (2017)	Acres of Land in Farms as Percent of Land Area in Acres: 2017	(Nelson et al. 2002; Abdur Rashid Sarker et al. 2013; Hoque et al. 2019)

1.3.1.2 Principal Component Analysis (PCA)

Principal Component Analysis (PCA) is a matrix factorization method commonly used to reduce the dimension of many variables to representative parameters which still define variation in the initial dataset (Alakkari and Dingliana 2018). As a result of the PCA, the most relevant information and variance are extracted with reduced dimensions (new orthogonal variables). Those new orthogonal dimensions are acquired by an orthogonal linear transformation to determine vectors containing some extent of the total variability of a dataset (Medina et al. 2020). PCA is a commonly applied tool in vulnerability studies to assign weights to parameters (Abson et al. 2012; Remo et al. 2016; Stafford and Abramowitz 2017; Medina et al. 2020) with other methods like expert judgements (Bjarnadottir et al. 2011) and equal weighting (Monterroso et al. 2014).

Since each parameter has different units and features, a normalization process is needed to be able to compare them before applying any statistical procedure like PCA. This process solves the incommensurability problem within datasets (Abson et al. 2012).

The data were normalized with maximum-minimum normalization with the Eq 1 in this study (Abson et al. 2012; Monterroso et al. 2014; Remo et al. 2016; Chakraborty et al. 2020).

Equation 1 Maximum-minimum normalization

$$\delta = (X - Xmin)/(Xmax - Xmin)$$

where δ is a normalized parameter, X is the original value, and Xmin and Xmax are the minimum and maximum values for each parameter in counties.

After the normalization process, the suitability of the datasets to factor analysis was controlled with the Bartlett's Test of Sphericity and the Kaiser-Mayer-Olkin (KMO) sampling adequacy tests (Abson et al. 2012; Monterroso et al. 2014; Remo et al. 2016; Kotzee and Reyers 2016; Chakraborty et al. 2020). The p-value of Bartlett's Test of Sphericity should be less than 0.05 to be sure that the dataset is suitable for factor analysis while KMO values should be higher than 0.5. All required tests, PCA, and visualization of results were performed in RStudio with the packages such as factoextra, FactoMiner, REdaS, corrplot, bartlett.test, and KMO.

1.3.1.3 Calculation of Social Vulnerability Index (SOVI)

After the required tests were applied to the datasets, the PCA procedure was utilized. Scree plots were used as a decision-making tool to select the number of principal components extracted from the PCA method (Rygel et al. 2006; Fekete 2009; Medina et al. 2020). By extracting these components, weights of each component and loadings of each variable in the components were obtained (Equation 2, Equation 3, Equation 4). Then, with the implementation of Equation 2, Equation 3, Equation 4 SOVI scores were calculated for each county.

Equation 2 SOVI (+)

$$\text{SOVIscore}(+) = (\text{PPCA1} * \text{Weight of PPCA1}) + \cdots (\text{PPCA8} * \text{Weight of PPCA8})$$

Equation 3 SOVI score (-)

$$\text{SOVIscore}(-) = (\text{NPCA1} * \text{Weight of NPCA1}) + \cdots (\text{NPCA8} * \text{Weight of NPCA8})$$

Equation 4 SOVI score

$$\text{SOVIscore} = (\text{PPCA1} * \text{Weight of PPCA1}) + \cdots (\text{PPCA8} * \text{Weight of PPCA8})$$

After the SOVI score was calculated for each county, the results were normalized

with the equation below so that results can be represented comparatively.

As a result, each county had a value between 0 to 1 indicating their vulnerability

levels compared to the rest of the domain. Finally, the Natural Jenks Classification

method was utilized to illustrate the results spatially because it maximizes the difference

between classes where the largest changes occur (Goodchild et al. 2007).

1.3.2 Flood Hazard

Flood depth grids for each county were derived from the National Flood Hazard

Layer (NFLH) in the PRW. Then, all grids were merged to represent flood hazard in the

study area. All depth grids were created for the riverine 100-year event (1% frequency),

which is defined as major flood event in remote areas (National Weather Service), using

DFRIM data from NFLH database (Cutrell et al. 2018). Flood depth information was

acquired for AE, AH, and AO riverine flood zones by following Cutrell et al. (2018)

(Cutrell et al. 2018). USGS 1/3 arc-second Digital Elevation Model (DEM) was used to

extract flood depth grid information for the study area.

1.3.3 Exposure Index (Flood Damage)

The flood depth grid derived from FEMA 100-year flood map was intersected

with the default HAZUS-MH library, which is developed by combining the National

Resources Inventory (NRI) and National Agriculture Statistical Service (NASS) (FEMA 2013). The data for the implementation of Eq (5), including crop type, average field, the unit price, and the harvest price were obtained from those datasets.

HAZUS-MH uses the Agricultural Flood Damage Analysis (AGDAM) method for the calculation of agricultural damage (5).

Equation 5 Agricultural crop damage

$$L = A(pYo - H) * D(t) * R(t)$$

where L is agricultural loss ($), A is cultivated areas (acres), P is the price ($/bushel), Y_0 is normal annual yield (bushels/acre), H is harvest cost ($/acre), D(t) is crop loss at day t of the year (% of maximum net revenue), and R(t) is the crop loss modifier for flood duration percent of the potential loss. For this study, instant loss, 3-day loss, 7-day loss, 14-day loss, and total maximum losses were calculated. Crop type, time of the year of analysis, the area flooded, and the net revenue from each crop type are significant factors for agricultural damage in AGDAM method (see Eq.1) (US Army Corps of Engineers 1985). Additionally, Brémond et al. (2013) reviewed the related literature and found that seasonality is one of the important variables for crop damage functions for many of the studies around the world (Brémond et al. 2013). Time of the year of analysis affects both production and harvesting cost which can be included to total loss values depending on crop maturity levels. Most of the crops are assumed to reach their maximum maturity in August and mid-September in the AGDAM method (US Army Corps of Engineers 1985). The beginning of the harvest period starts at the end of September and finishes before mid-October. The highest damage is observed in late September because all production expenses are included in the total damage. Additionally, since there is no

21

cultivation between mid-October and early March for most of the crops, the damage is

likely to lessen in between those times of the year (US Army Corps of Engineers 1985).

A python code replicating the HAZUS-MH crop damage loss function (eq 5) was

utilized to run multiple scenarios for PRW. All required information was obtained from

HAZUS-MH's library by SQL Server Management Studio (SSMS). Then, the inundation

layer for the 100-year storm event and the distributions of crop type, average yield,

harvest price, and the unit price were overlapped to simulate flood damage functions

spatially. The damage results were compared with HAZUS simulations for validation. It

was found that the proposed script can replicate total maximum loss values with less than

10% Relative Error in every county with an average of 4.5% in each scenario. Since this

method uses agricultural damage information comparatively, an average of 4.5% was

found acceptable. Total maximum loss results were used for each scenario. To compare

exposure levels of counties, the same normalization (1) procedure was applied for

exposure results as well. Therefore, each county had a value between 0-1 that shows how

large their exposure level is compared to maximum and minimum values of the study

domain. Sequentially, the spatial distribution of the Exposure Index was demonstrated by

Natural Jenks Method similar to SOVI results. The exposure indexes were presented for

the average, minimum and maximum scenarios in this framework. In addition,

probabilities of each month to experience flood events were analyzed to indicate the most

likely situation to happen among the scenarios. Frequencies of moderate, major, and total

flood events were evaluated to identify most likely months to experience flood events.

The dataset of the National Weather Service was used to investigate numbers of

moderate, major, and total events for each subbasin in the PRW (National Weather

Service 2016).

1.3.4 Calculation of Flood Social Vulnerability Index (FSOEVI)

Flood exposure and social vulnerability levels of the agricultural communities in

the PRW were combined to introduce FSOEVI. There are different ways to combine

exposure and social vulnerabilities in the flood vulnerability literature, such as using

weights by expert opinion (Sowmya et al. 2015), statistical analysis (Mansur et al. 2016;

Yang et al. 2018; Hadipour et al. 2019), equal weights (Remo et al. 2016; Lee and Choi

2018), and bivariate evaluation (Gu et al. 2018; Khajehei et al. 2020; Mohanty et al.

2020). A two-way cross tabular map was used to implement a bivariate mapping

methodology. In the bivariate mapping technique, two different parameters, which

describe a resultant parameter, were represented in a single map to display coincidence

(Gu et al. 2018). In this study, 3 different rows (Exposure) and columns (SOVI) were

used to construct a resultant FSOEVI color matrix. In order to highlight counties with

higher FSOEVI levels, very low and low classifications for Exposure and the SOVI were

reclassified as Low, while moderate levels were indicated as Moderate for bivariate

mapping. Finally, high and very high levels of exposure and SOVI values were grouped

as High.

<div align="center">

1.4 Results

</div>

1.4.1 SOVI results

The relative SOVI results in the PRW were compared among the 41 counties in

its borders and 3234 counties in the entire U.S. separately. The statistical tests (Bartlett's

Test for Sphericity and KMO) prior to PCA were applied to both data. For Bartlett's Test for Sphericity, both datasets acquired p-value 2.2e-16 by satisfying condition p<0.05. Also, the U.S and the PRW dataset passed the KMO tests by having 0.74 and 0.63 values, respectively. The numbers of the components to be extracted were selected by visual evaluation of the scree plots for both datasets. Eight components were extracted, which define 91.5% and 94% of the variances in the total dataset for the U.S and the PRW, respectively.

Figure 3 a) and b) illustrated the relationship between variables and the components. These correlation plots for both the U.S and the PRW datasets, represent which dimensions were expressed with which variables. Squares with darker color demonstrate the significant correlation of variables with the component. Also, red and blue colors indicate negative and positive correlations of variables with dimensions, respectively.
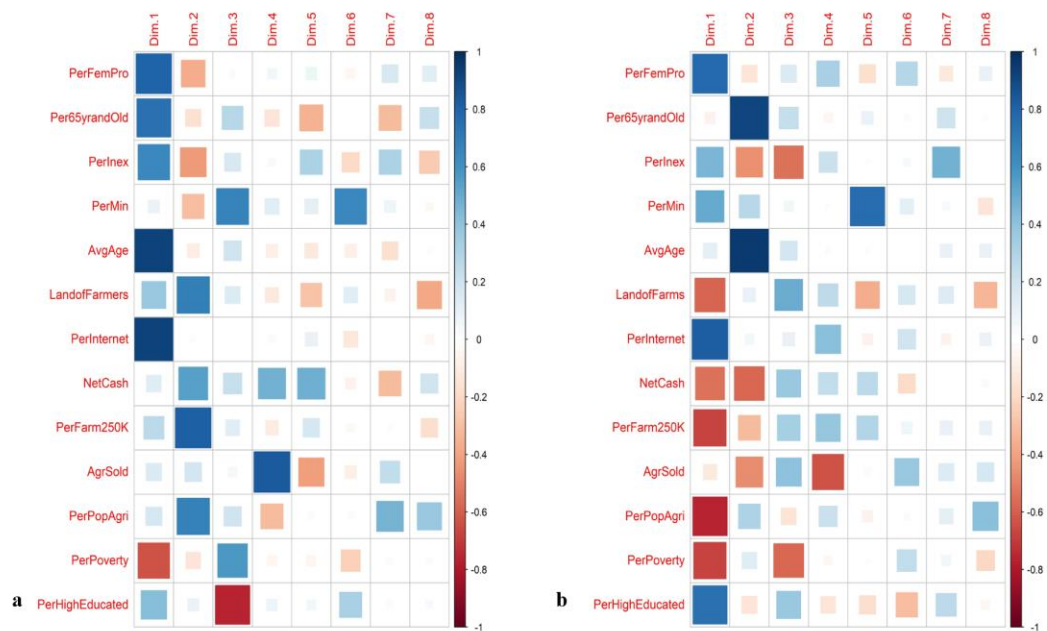
Figure 3 Correlation between variables and dimensions of agricultural populations within the a) U.S and b) Potomac River Watershed

Figure 3a) illustrated that variables, including average age (Average Age), percentage of female producers (PerFemPro), percentage of farmers have an internet connection (PerInternet), and percentage of population over 65 years age (Per65yrandOld), mostly represented the 1st dimension. Thus, it is fair to claim that the socio-economic demographic features of the agricultural communities were represented by the 1st dimension. For the second dimension, the correlation plot suggested that acres of land in farms, as a percent of land area in acres (LandofFarmers), percentage of the population working in the agriculture sector (PerPopAgri) and percentage of farms with sales of $250,000 or more (PerFarm250K) vulnerability factors were found as highest loadings. Therefore, it can be reported that dimension 2 describes the development of the

agriculture industry. Dimension 3, which defines demography and the educational status of the agricultural populations, contains the percentage of minority farmers (PerMin) and percentage of the population have completed 12th grade (PerHighEducated) parameters with the stronger loadings. Since dimension 4 is primarily explained by the total value of agricultural products sold (AgrSold) and net cash income of farms (NetCash), information of farming economy is represented with that. The 70% of the total variance was explained by those first 4 principal components in the U.S level analysis.

Figure 3b) provided a summary of the correlation of the variables with each dimension only in the PRW. The correlation column for the first dimension showed that vulnerability factors such as the percentage of farmers have an internet connection (PerInternet), percentage of female producers (PerFemPro), percentage of population under the poverty level (PerPoverty) and percentage of the population working in the agriculture sector (PerPopAgri) have the highest representation in the first component. Thus, dimension 1 depicted information accessibility, gender balance and significance of the agricultural economy shared in the community. The age distribution of the PRW was defined by the 2nd dimension because variables such as average age (AvgAge) and percentage of the population over 65 years of age (Per65yrandOld) mostly constitute the dimension 2. Moreover, dimension 3 was explained by the percentage of population under the poverty level (PerPov) and the percentage of farms with new and beginning producers (PerInex). It can be concluded that experienced farmers and socio-economic aspects of the agricultural populations were represented in dimension 3. For dimension 4, the total value of agricultural products sold (AgrSold) and the percentage of farmers who

have an internet connection (PerInternet) were dominant in the representation of the

components. Hence, it indicated the development of the agricultural economy and the

information accessibility in the PRW. Those four dimensions described the %77 of the

initial information in the dataset for the PRW.

The spatial distribution of the relative vulnerability of agricultural communities in

the PRW concerning all counties in the entire U.S. was demonstrated in Figure 4. Each

natural break was represented by different colors in the figure. The lower natural break

values had green and the higher ones had red colors. Therefore, the red colors highlighted

higher vulnerability among the agricultural communities while green colors showed

lower vulnerability levels.
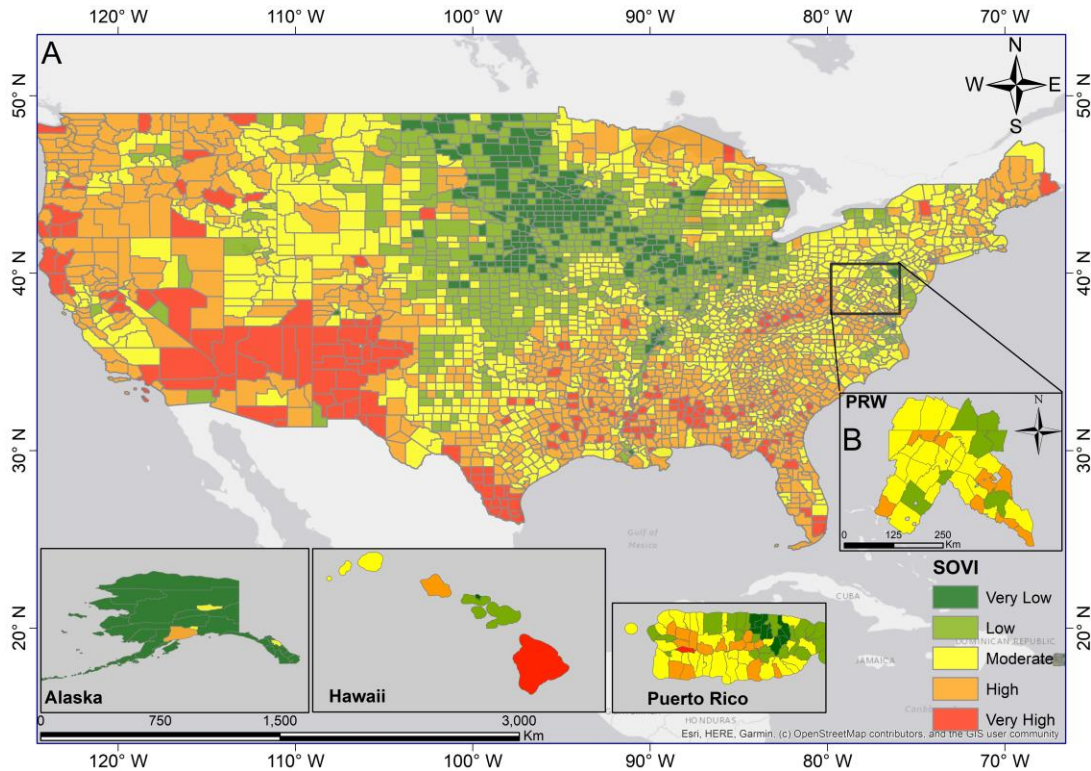
Figure 4 Spatial distribution of SOVI in the PRW compared to all counties in the entire U.S (county level): A) U.S and B) Potomac River Watershed

The comparison within the entire U.S indicated that the agricultural communities in the PRW mostly have moderate and high vulnerability levels relative to the entire U.S. The results demonstrated that counties in the PRW are less vulnerable than most of the counties in Arizona, Texas, and Georgia. However, some counties in the PRW are as vulnerable as counties in Florida, Alabama, Mississippi, Nevada, and California. In addition, most of the counties in the PRW have higher vulnerability levels compared to the ones in the mid-west. Distributions in the PRW suggested that the agricultural population in the south-west of the basin are more vulnerable, while the north-west side of the watershed generally has moderate vulnerable level (Figure 4 B).

All counties were numbered to demonstrate and discuss results better for the relative SOVI assessment within the PRW. Table 2 listed the county name and the corresponding number.

Table 2 Counties in the Potomac River Watershed

Number	County	Number	County	Number	County
1	Somerset (PA)	14	Stafford (VA)	27	Page (VA)
2	Bedford (PA)	15	Charles (MD)	28	Rockingham(VA)
3	Fulton (PA)	16	Pr. William (VA)	29	Augusta (VA)
4	Franklin (PA)	17	Fauquier (VA)	30	Highland (VA)
5	Adams (PA)	18	Loudoun (VA)	31	Pendleton (WV)
6	Carroll (MD)	19	Jefferson (WV)	32	Grant (WV)
7	Frederick (MD)	20	Washington (MD)	33	Garrett (MD)
8	Montgomery (MD)	21	Berkeley (WV)	34	Mineral (WV)
9	Prince George's (MD)	22	Morgan (WV)	35	Hampshire (WV)
10	St. Mary's (MD)	23	Allegany (MD)	36	Hardy (WV)
11	Northumberland (VA)	24	Frederick (VA)	37	Shenandoah(VA)
12	Westmoreland (VA)	25	Clarke (VA)	38	Fairfax (VA)
13	King George (VA)	26	Warren (VA)	39	Arlington(VA)

Figure 5 illustrated the spatial distribution of the SOVI results for the PRW. The cities were not included in the SOVI assessment because they do not have any agricultural practices and production. The same legend and colors were used for the same natural break values.
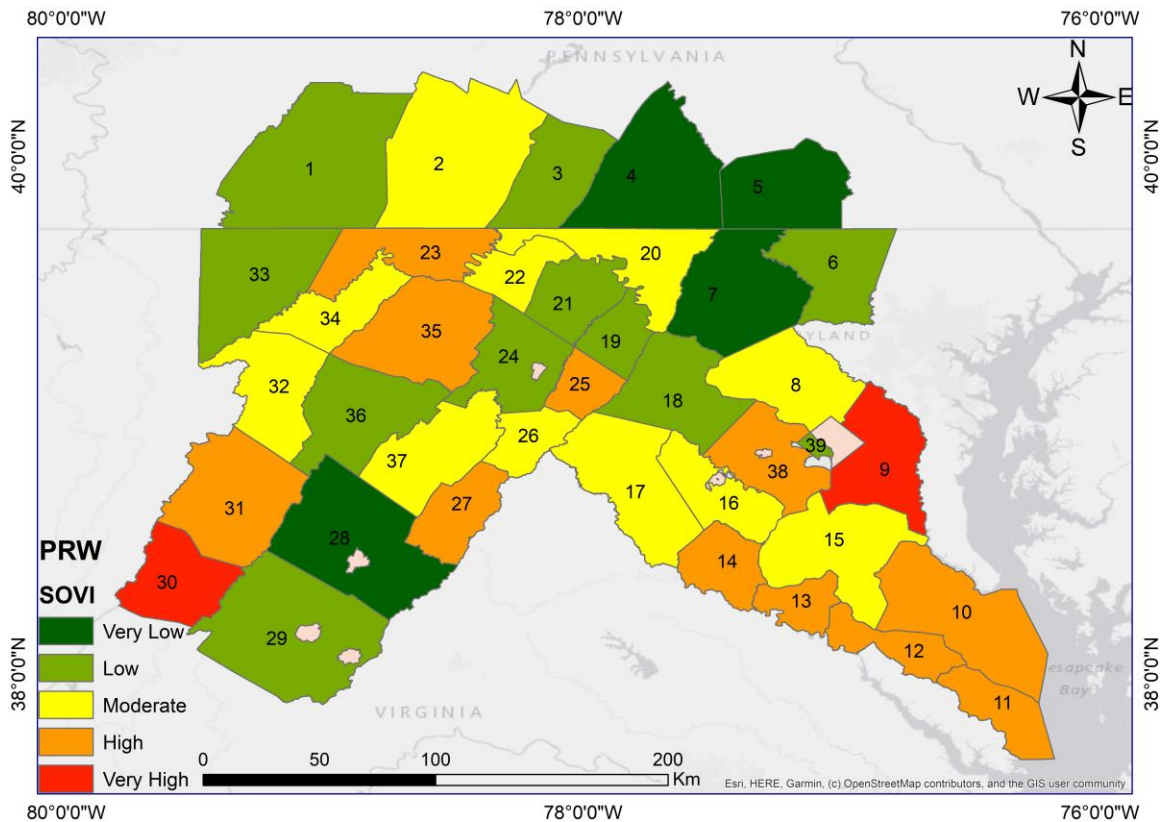
Figure 5 Spatial distribution of SOVI (county level PRW)

Figure 5 suggested that only 5% (2) of the counties have very high vulnerability levels. The agricultural communities in Highland (30) and Prince George's (9) were labeled as the most vulnerable in the PRW. High values of percentage of female producers (PerFemPro), the average age (AvgAge), the percentage of the population over 65 years of age (Per65yrandOld), low values of the percentage of farmers have an internet connection (PerInternet), and the percentage of the population who have completed 12th grade (PerHighEducated) led Highland (30) and Prince George's (9) to have a highly vulnerable population. In addition, 28% (11) of the counties indicated highly vulnerable agricultural populations. Therefore, it can be concluded that a total of

33% of the counties have highly or very highly vulnerable agricultural communities within the PRW. Similarly, 28% (11) of the counties demonstrated moderately vulnerable farmers. The rest of the study area had either very low or low vulnerability levels.

Figure 5 showed that nine (52%) counties located in Virginia were determined as highly and very highly vulnerable out of 17 of the total in the PRW. In Pennsylvania, all counties except Bedford (2) appeared to have low and very low vulnerable agricultural populations. Pendleton (37) and Hamisphere (36) were found as highly vulnerable in West Virginia. Lastly, three counties indicated high vulnerability levels in Maryland (MD).

1.4.2 Exposure Index results

1.4.2.1 Flood hazard results

As explained above, the flood hazard map was derived from FEMA 100-year flood maps. The flood depth grids for "A" flood zones, which are the areas with a 1% annual chance of flooding, were employed to evaluate a 100-year return period flood hazard for only riverine are used (Figure 6).
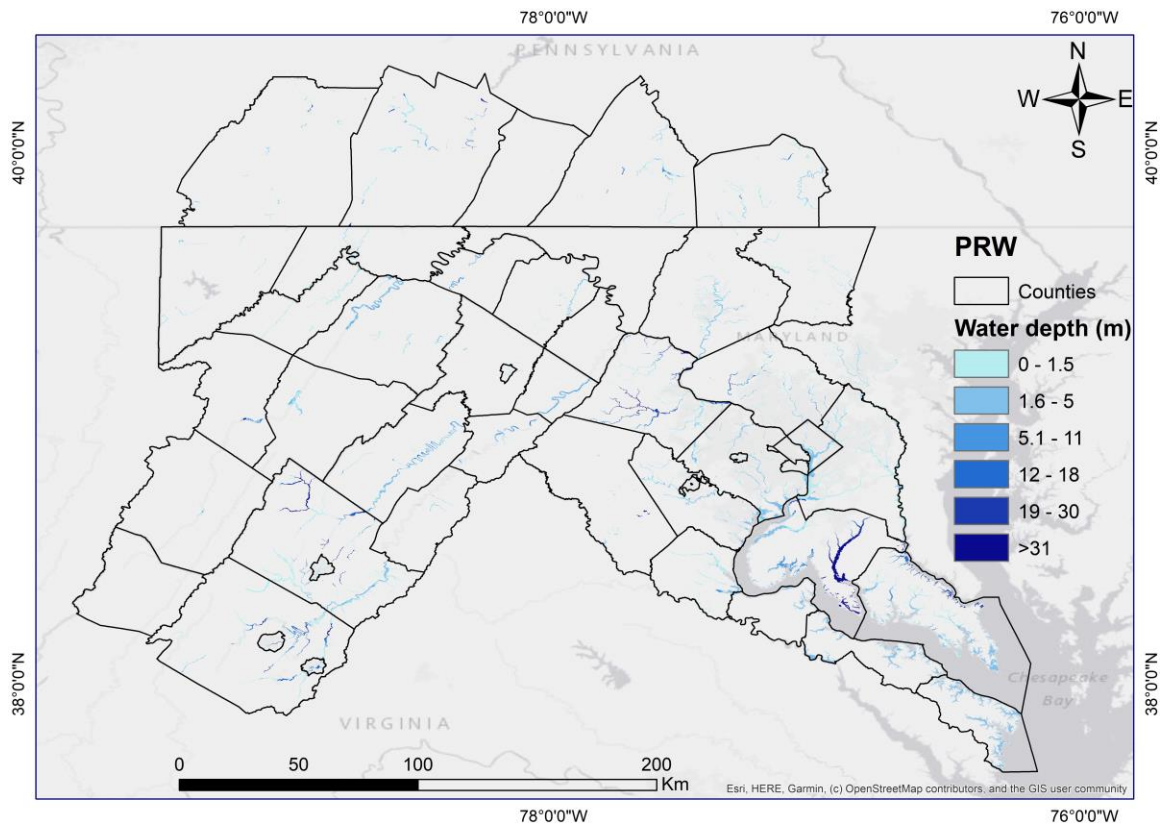
Figure 6 Flood hazard map (FEMA 100 year)

Since the AGDAM method only considers the inundation area for estimating flood damage, water depth information was not essential for the analysis. Thus, FEMA 100-year flood inundation layer was deemed as a good reference to use in this framework.

1.4.2.2 Flood exposure

The total maximum loss for different crops such as corn, corn silage, wheat, alfalfa hay, oats, and soybean was calculated. The analysis was performed for each day of the year since the crop damage percentages vary with the time of the year but assuming that the 100-year flood event was equally likely to occur any of these days.
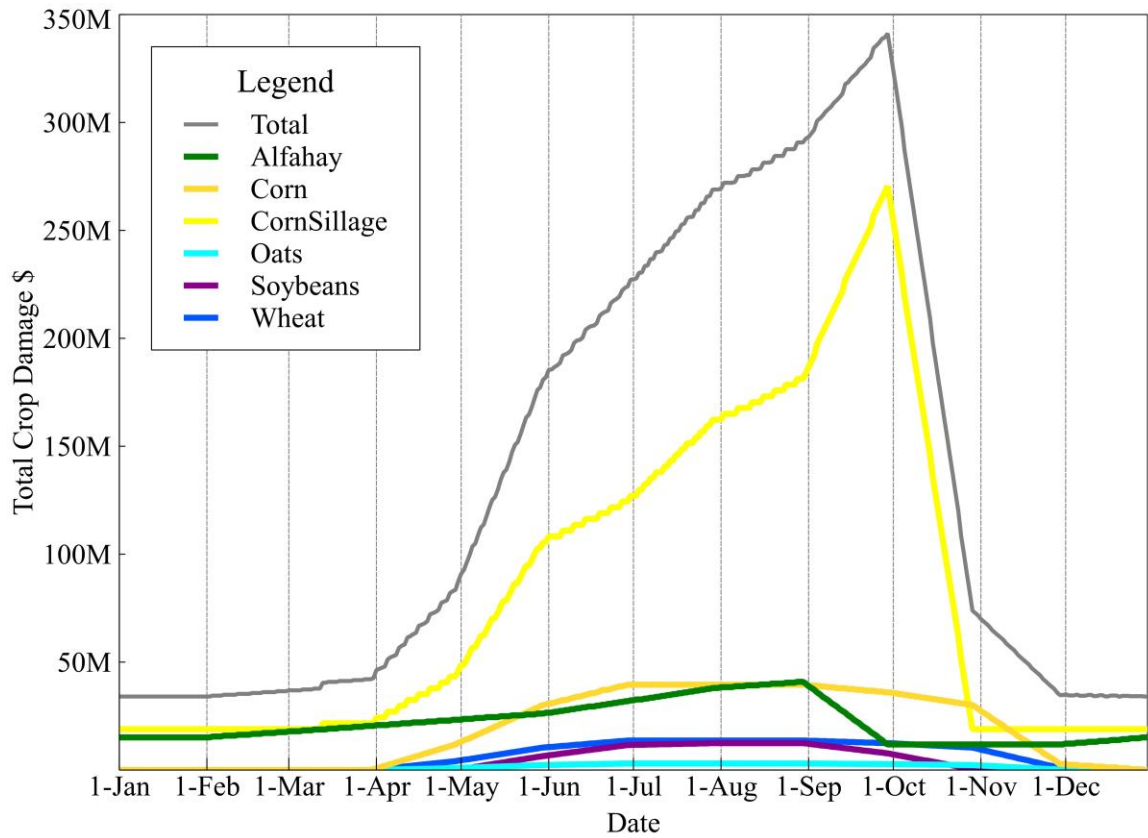
Figure 7 Seasonality variation of total maximum loss with 100-year FEMA flood map hazard layer in the PRW

As seen in Figure 7, the total maximum economic loss from a 100-year flood event was lowest in winter, however, highest in September and at the beginning of October. After observing the highest damages at the beginning of October, the possible total crop damages decreased because the harvest period started to end after that time of the year. Figure 7 suggested that the biggest portion of the total crop damages was experienced by corn silage. Corn and alfalfa hay were the other crops which shared a significant part of the losses. However, the damage occurred on corn silage is almost 5-

times larger than them. Oats had the least damage throughout the year. Table 3 and Table

4 explained minimum, maximum, and an average of 365 different scenarios and a

seasonal average of total maximum loss. Table 3 showed that maximum crop damage

was experienced on the 30th of September while the minimum was on the 21st of

December. There was more than a 10-time difference between maximum and minimum

scenarios. Table 4 suggested that the largest damage was experienced in the Summer and

Fall seasons.

Table 3 Minimum, average and maximum total economic loss scenarios

Scenario	Date	Total Maximum Loss ($)
Maximum	30 September	341,195,636
Average	17 May	137,318,256
Minimum	21 December	33,949,801

Table 4 Seasonal average of total maximum loss ($)

Season	Average Total Maximum Loss ($)
Winter	55,076,143
Spring	79,208,534
Summer	243,689,188
Fall	210,765,217

Flood exposure levels were analyzed for the scenarios in Table 3 and Table 4.

Moreover, the simulation of the scenarios which aim to assess the damage in the most

likely months to experience flood hazard were defined. Thus, the frequencies of

moderate, major, and total flooding events were evaluated for all basins within the PRW

(National Weather Service 2016). The results of the evaluation indicated that the most

likely months to have a moderate flood is March, while October and September are likely

to have major floods (Figure 8). 40% of the total flood events have happened in October,

March, and September in the PRW (National Weather Service 2016). Since the 100-year

flood event is considered as a major flood in remote areas (National Weather Service),

September and October were found to have the highest potential to experience flood

damage. Figure 7 illustrated that the most likely months to have major flood events

experienced the highest damages throughout the year. The seasonality of maximum

damage and the highest probability of having major flood event highlighted in the same

temporal period. Additionally, although most of the major flood events have occurred in

October and September in the PRW, Figure 8 demonstrated that there is a 75% chance of

experiencing flooding events in the other 9 months. Therefore, the Exposure and FSOEVI

analyses were performed for each the average total maximum loss for each month to

quantify risk for the whole year.
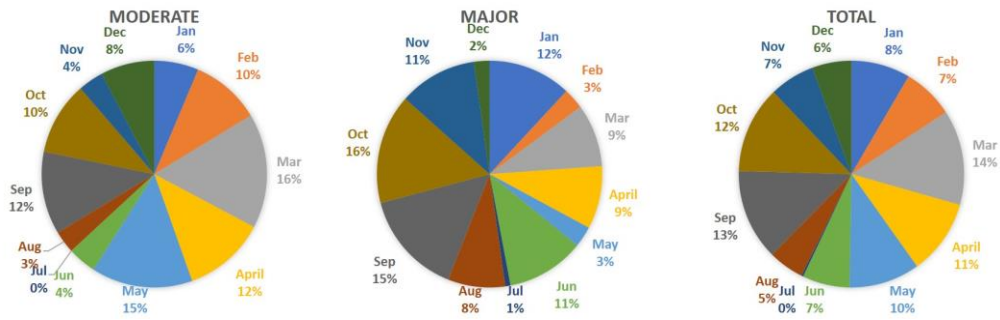
Figure 8 Percentages of moderate (a), major (b), and total (c) floods for each month in the Potomac River Watershed

1.4.2.3 Flood Socio-Economic Vulnerability results

Figure 9 and Table 5 showed the results of the scenarios from Error! Reference source not found.**.** The FSOEVI results were combinations of both exposure and SOVI results for each county. The results for FSOEVI components, which demonstrated high and very high exposure and the high FSOEVI levels, were summarized in Error! R eference source not found.**.** Comparative results indicated that the number of counties with very high exposure levels was larger in the average scenario than others. Augusta (29), Loudoun (18), and Rockingham (28) were found as having very high levels of exposure in every scenario. Unlike exposure, results of FSOEVI analysis demonstrated that Shenandoah (37) and Hampshire (35) are found as the highest FSOEVI scores compared to the rest of the study area.

Table 5 Results of the FSOEVI analysis

Scenario	High/ Very High Exposure	Highest FSOEVI
Maximum	Frederick (7), Berkeley (21), Hardy (36), Shenandoah (37), Augusta (29), Loudoun	Shenandoah (37)

	(18), Rockingham (28)	
Average	Bedford (2), Franklin (4), Adams (5), Carroll (6), Berkeley (21), Hampshire (35), Hardy (36), Shenandoah (37), Augusta (29), Loudoun (18), Rockingham (28)	Hampshire (35)
Minimum	Berkeley (21), Shenandoah (37), Frederick (7), Augusta (29), Loudoun (18), Rockingham (28)	Shenandoah (37)

Three plots represented three different scenarios, including minimum, average, and maximum damage. The left part of Figure 9 summarized the distribution of the exposure indexes, which were normalized crop damage values for each county. The lower natural jenks break values had green while higher values had a red color. Also, the counties with beige color did not experience any flood damage in the corresponding scenario. The right part illustrated FSOEVI results, which were a combination of exposure and SOVI distributions. The color scale indicated that the counties with red color have both very high or high exposure and SOVI results while the green ones have very low of both. The number of counties which had high and very high exposure increased from minimum to average damage scenario. The majority of the counties indicating low, very low, and moderate exposure levels in the minimum scenario had high exposure levels in the average scenario. For example, Bedford (PA) (2), Franklin (PA) (4), Adams (PA) (5), Carroll (MD) (6), Hampshire (WV) (35), and Hardy (WM) (36) experienced moderate levels of exposure in the minimum scenario, while they were labeled as high exposure in the average scenario. Figure 9 also showed that the average scenario has the highest number of counties, which had very high and high (12) flood

exposure. The minimum scenario 6 (15%) and maximum scenario 7 (18%) experience

contained high and very high exposure extent.
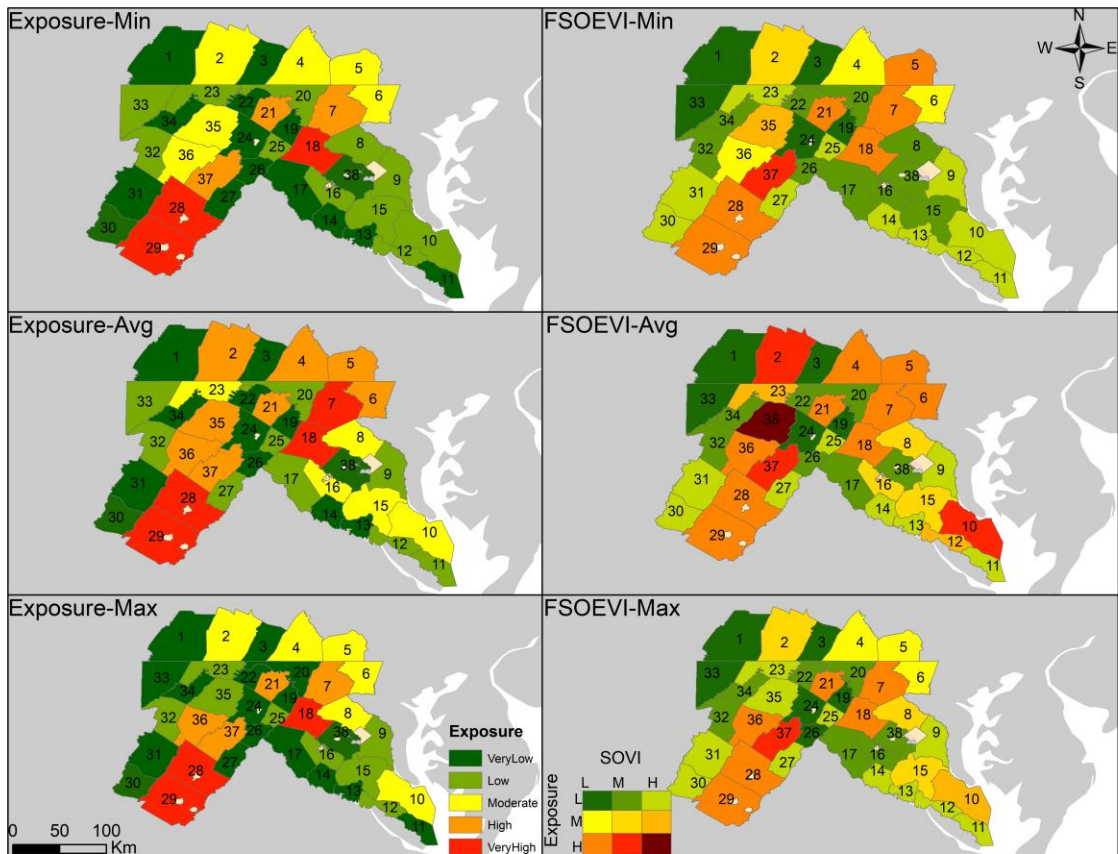
Figure 9 Spatiotemporal distributions of Exposure Index and FSOEVI

The spatiotemporal comparison (Figure 9) demonstrated that flood socio-

economic vulnerability of the agricultural communities in the south-east of the study area

varies significantly in each scenario. In the minimum loss scenario (21 December),

almost all counties obtained low levels of exposure and moderate levels of SOVI in the

south-east. Thus, the combined risk was lower compared to the south-west and north part of the study area. However, the results of the average loss scenario (17 May) reported that most of the counties have moderate exposure and high SOVI values. As a result, the overall FSOEVI levels were higher than counties located in the west and north. In addition, the spatiotemporal distribution of the FSOEVI results showed that in the maximum economic loss scenario (30 September), the northern half of the south-east of the study area had a higher risk than the southern half. The northern and western half of the study area had similar risk distributions in each scenario. Similar to exposure results, the average scenario contained more flood socio-economic vulnerable agricultural communities in the PRW.

As explained in the previous section, FSOEVI assessment was conducted for the exposure indexes for the average damage experienced each month in Figure 10. Twelve different plots, which were the combinations of SOVI and average exposure values in each month, aimed to show spatiotemporal distributions of flood socio-vulnerability levels of agricultural communities in the PRW.

The number of counties experienced flood damage in April, May, June, July, August, September, October, and November was more than in the rest of the year. Hampshire (35), Shenandoah (37), and St. Mary's (10) appeared to have the highest FSOEVI levels in monthly average scenarios. Hampshire county was highlighted in December, April, May, and November, while St. Mary's (10) county only classified as high FSOEVI among all scenarios. Moreover, in January, February, March, July, August, September and October, Shenandoah (37) county was indicated as high FOSEVI.

Shenandoah (37) county had the most vulnerable agricultural communities in most likely months to experience major flood hazard. There was no county found to have high FSOEVI in June. However, Shenandoah(37), Augusta (29), Rockingham (28), Frederick (7) and Loudoun (18) had high-very high exposure and moderate SOVI levels in that scenario and were classified as the most vulnerable agricultural population in that simulation. Highland (30), Pendleton (31), Mineral (34), Warren (26), and Fairfax (38) did not show any exposure for some scenarios throughout the year. In the summer and fall seasons, there were more counties experiencing flood damage compared to winter and spring. The spatiotemporal distributions of risk for each month illustrated that the risk varies significantly in everywhere in the PRW except the west side of the study area. Most of the counties in the western part of the PRW indicated low levels of flood socio-economic vulnerabilities of the farmers. The rest of the year generally demonstrated moderate and low levels of risk for farmers.
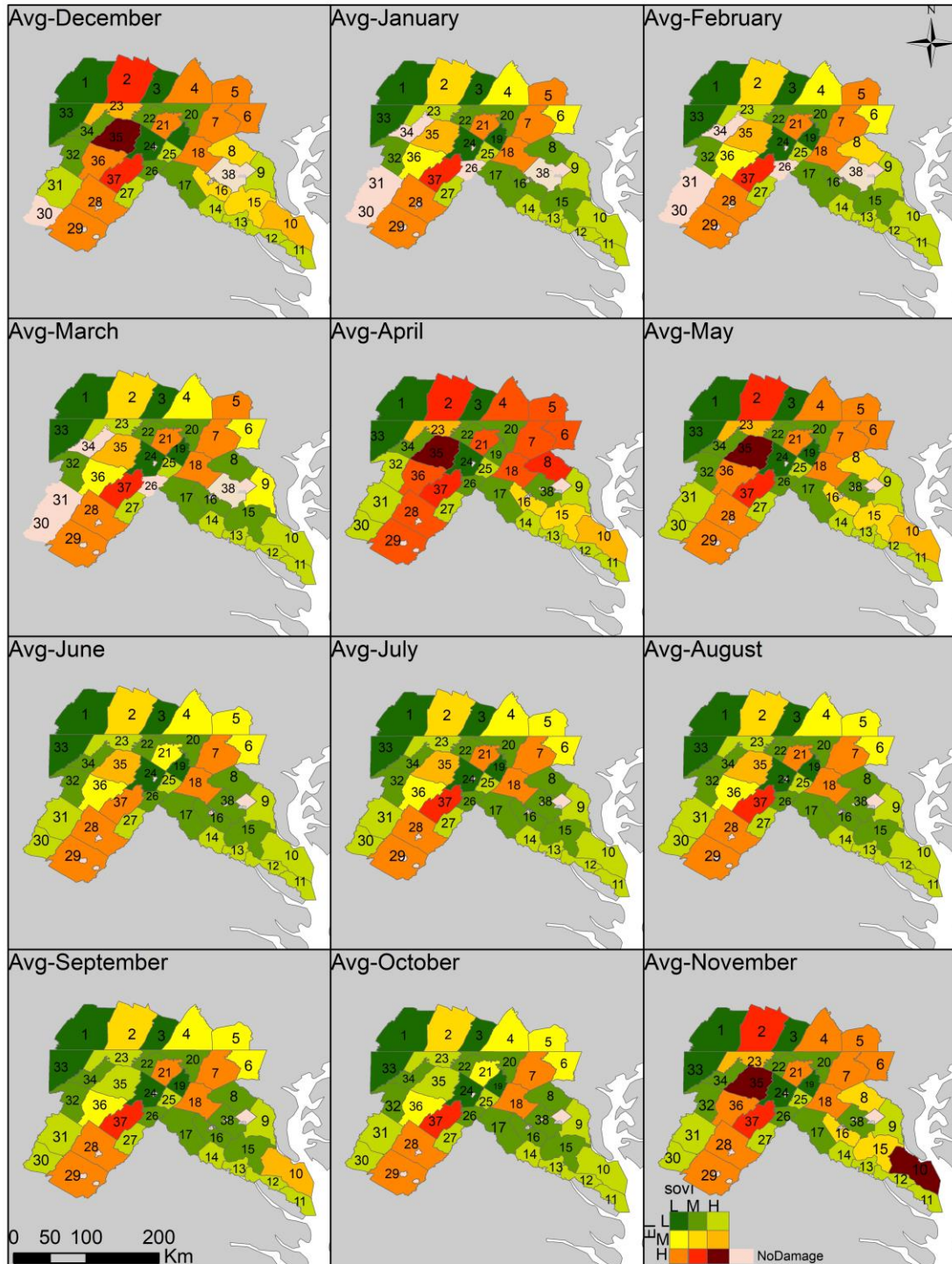
Figure 10 FSOEVI results for average economic loss scenarios for each month

41

1.5 Discussion

In the Potomac River Watershed, the spatial distribution of the multidimensional social vulnerability index of agricultural communities illustrated a high-level of spatial variability. Our findings showed that population under poverty, percentages of female producers, the minority producers, internet accessibility rate within the producers, a portion of the population works in the agricultural sector as a primary job, percentage of farms with sales of $250,000 or more, and net cash income of farmers were the most important vulnerability factors defining overall vulnerability levels in the Potomac River Watershed. Several counties, including south-west, south-east and middle parts were highlighted as having vulnerable agricultural communities. Agricultural communities in Highland (30) and Prince George's (9) were found as the most vulnerable within the Potomac River Watershed. The comparison in the context of the U.S. demonstrated that the most of the counties (64%) were found as moderately vulnerable compared to all 3234 counties in the U.S., while nine of them (23%) appeared as highly vulnerable. This result suggested that 23% of the counties are as vulnerable as most of the counties located in the southern states, known for having a large number of disadvantaged rural population groups in terms of ethnicity, poverty, gender and socio-economic status, including Texas, Florida, Mississippi, and Georgia (Oxfam America 2009). Consistent with these studies, the distributions of high SOVI results were also found to be similar by two different comparisons performed in this study. Almost all counties which had vulnerable

agricultural communities in the PRW for countywide analysis also found as highly vulnerable within its borders.

Similar to literature (Brémond et al. 2013; Klaus et al. 2016; Bathrellos et al. 2018), seasonality was found as the main factor for the spatiotemporal distribution of the crop damages in this study. This study demonstrated that the 100-year flood event happening in summer and fall season causes more severe damage to crops than winter and spring. The temporal distribution of the crop damage values indicated that the lowest values were observed in most of the winter season because the damage was only estimated on alfa hay and corn silage with the lowest percentage damages of 32% and 7%, respectively. The losses started to be observed after 1st of April for wheat, oat, and corn plants. Moreover, soybean crops experience losses only between 1st of May and the 25th of November. For most of the crops cultivated in the PRW, the highest percentage loss was observed in the late Summer except for corn silage. Corn silage crop damage function indicated that the maximum percentage losses are in late September. The maximum of total flood damage was observed in late September since corn silage is one of the highest acreage values in the PRW, and its unit and harvest prices are higher than other crops. According to the US Army Corps of Engineers (1985) (US Army Corps of Engineers 1985), this might be due to the fact that it coincides with the beginning of the harvesting period for the corn silage (FEMA 2013). Hence almost all crops reached their maturity levels until that time, and all production costs were also included in the economic damage. Although it is stated that the seasonality of the flood damage on crops changes depending on the hemisphere and latitude (Huizinga et al. 2017), the maximum

damage was found to be occurring between August and the early-October in Germany (Klaus et al. 2016), Mexico (Vega-Serratos et al. 2018), and Greece (Bathrellos et al. 2018) as consistent with our results.

Socio-economically sustainable agricultural communities can adopt the impacts of biophysical risk easier than the vulnerable, unsustainable communities because their wealth, socioeconomic status, and levels of accessibility to resources facilitate mitigation efforts (Ma et al. 2007; Cutter et al. 2012). However, generally, the most vulnerable population and the locations which have the highest biophysical risk do not overlap (Cutter et al. 2012). Similarly, our findings indicated that counties which have highest SOVI results did experience lower damages compared to the rest of the PRW in all scenarios. The average unit price of the main crops and average yields were lower in Highland and Prince George's counties. Therefore, the agricultural communities were not highlighted as vulnerable to flood in those counties. However, several counties, which have high SOVI values, also experienced high levels of flood exposure, including St Mary's and Hampshire. The counties with high and very high exposure levels mainly located in the south and middle part of the PRW such as Augusta, Rockingham, Shenandoah, Hampshire, and Hardy. This finding can be explained by the fact that agricultural activities are mainly carried out around main rivers, streams and the branches in the western and the central part of the basin (Battista et al. 1998; Interstate Commission on the Potomac River Basin 2020). The rivers which have greater size like Shenandoah River may cause more damage to the agricultural activities around its banks.

The findings of the flood socioeconomic vulnerability assessment results demonstrated that spatiotemporal distributions of the risk vary significantly depending on the time of the year. For instance, although St Mary's (10) had low/moderate FSOEVI levels in 11 months, it had high FSOEVI levels in November. Therefore, St Mary's (10) county had a higher risk when the 100-year flood event happened in November. Additionally, flood socioeconomic vulnerability levels of the agricultural communities located in the north side of the study area generally increased substantially in April, May, and December. These results suggested that mitigation efforts should be focused on different locations at a different time of the year. To the best of our knowledge, this is the first study evaluating spatiotemporal distributions of farmers' flood vulnerabilities, not only in Potomac River Watershed, but also in the world. However, methodologically similar studies are found in the literature such as the studies of Ma et al. (2007), Awere et al. (2016), and Suryanto and Rahman (2019). The main difference of this study is the consideration of the spatiotemporal variation of the risk in the agricultural communities. Additionally, Suryanto and Rahman (2019) and Ma et al. (2007) did not define the exposure as the actual impact of a flood on the agricultural communities. The reason may be the data scarcity and lack of institutional capacities in those study areas which are located in underdeveloped and developing countries. The common vulnerability factors used in those studies mentioned above is the percentage of households working in the agriculture sector as a primary job out of 24 parameters (Ma et al. 2007; Awere et al. 2016; Suryanto and Rahman 2019). The crop damage functions are represented in the Huizinga et al. (2017) for each continent in the world except Oceania, South America, and Central

America. Therefore, the presented methodology in this study can be replicated by using those crop damage functions to define exposure and population data for the social vulnerability of the farmers anywhere in the world.

Vulnerability reduction is one of the main elements of disaster risk mitigation procedures, which aims to both reduce the physical and the social vulnerabilities of the risk areas (McEntire 2011; Gu et al. 2018). Although some researches highlight the shortcomings of the studies which quantitatively assess the social vulnerabilities, quantifying vulnerability with multidimensional index can facilitate to identify most vulnerable locations and people as well as the main contributors to the overall vulnerability (Rufat et al. 2015; Chakraborty et al. 2020). Simplified and combined information about social vulnerabilities and the hazard, make vulnerability assessment suitable to be used in the prioritization of emergency planning, resource allocation and decision making processes (Cutter et al. 2012; Rufat et al. 2015). Therefore, the findings of this study facilitate the understanding of the spatiotemporal distribution of the flood socioeconomic vulnerability in the Potomac River Watershed. The represented methodology can easily be applied in any location in the world to quantify and evaluate the spatiotemporal nature of the flood risk of flooding across agricultural communities at any scale.

In addition, the main limitation and possible improvements in the study are investigated. Firstly, this study was carried out by replicating HAZUS-MH crop-damage functions for agricultural flood damage analysis. However, there are some studies stating that (Crow 2014; Maroof 2016; Rahman and Di 2020) functions used for calculation of

agricultural damage do not effectively predict the damage because it does not consider some parameters that may affect the damage, including flood depth, flow, sediment etc. There are also some uncertainty issues with the social vulnerability assessment methodology since the number of available data was the restricted parameter for defining population features as well. Also, as mentioned in the (Remo et al. 2016) study, there are some parameters that are correlated with each other, although they are assumed to be independent. Finally, since there are not many studies focusing on vulnerabilities aiming at agricultural communities in the U.S., parameters employed to define vulnerability factors are coming from studies that have been conducted around the world. This comes with some drawbacks like the fact that some parameters may not define the features of the agricultural population in the U.S. well. For future work, both flood hazard and exposure terms can be further investigated with hydrological and hydraulics modelling for the entire PRW area. Additionally, storm surge analysis can be included in the coastal areas in the PRW to explain the compound flood impacts. The presented method can be easily applied to states leading the agricultural economy in the U.S. such as California, Iowa, Texas, Nebraska etc., to evaluate possible flooding effects on agricultural populations. In addition, SOVI analysis results for the entire U.S. can be combined with hydrological flooding model output for the whole country. In that way, not only SOVI but also FSOEVI results can be analyzed within the U.S. Furthermore, climate change effects can be integrated with further analysis, to observe possible future changes in both agricultural damage and FSOEVI levels in the PRW or new applied study areas.

1.6 Conclusion

This paper aimed to construct a social vulnerability index for agricultural populations and evaluate the PRW to aid planners to understand the socio-economic dimension of the flood risk. With an extensive literature search, 13 different parameters were defined to identify social vulnerability levels. After the assessment methodology, results were interpreted spatially. In addition, an integrated FSOEVI methodology, which aims to quantify risk as a combination of the social vulnerabilities and physical damage to crops, was introduced in this paper for the PRW.

The SOVI results showed that Highland (30) and Prince George's (9) were more vulnerable comparatively than the rest of the counties in the watershed. It was found that the majority of the agricultural communities in the PRW were less vulnerable than the ones in the southern states in the U.S. However, 23% of the counties were found as vulnerable as several agricultural communities in Texas, Florida, Georgia, Arizona, and Mississippi.

The 100-year FEMA flood map was used to define major flood event. The exposure term was evaluated by combining the inundation area with cropland information to calculate the agricultural damage from a flood event. 365 different damage loss, exposure, and FSOEVI scenarios were evaluated for considering a 100-year flood to happen each day. By doing so, the seasonality of both exposure and risk was examined. Flood damages were higher in the fall and summer seasons compared to winter and spring. The seasonality of exposure indicated that major flood event in late September caused the highest damage in the PRW. This finding suggests that the agricultural

activities are significantly affected from major floods occurring in fall and summer seasons, especially in late September. Therefore, more resources should be allocated for mitigation efforts for that time of the year.

Agricultural communities in Shenandoah County were identified as the producers with the highest risk in September and October, which are the months when major flood events are most likely to occur in the Potomac River Basin. In addition, the findings of most results suggested that Hampshire, Shenandoah, and St Mary's counties, which have 12% of the total producers in the Potomac River Watershed, are more vulnerable to flood hazard among the others. Therefore, it can be concluded that 12% of the producers in the entire Potomac River Watershed is under high flood risk at different times of the year. The spatiotemporal distributions of flood vulnerabilities suggested that some socially vulnerable agricultural communities may experience severe flood damages only in specific times of the year. Therefore, the communities who need the largest resources to mitigate flood risk varies throughout the year. Our findings can be used as a temporal guidance to plan mitigation actions for agricultural communities.

CHAPTER 2 MULTI-SCALE COMPARISON OF URBAN SOCIO-ECONOMIC VULNERABILITY IN THE WASHINGTON DC METROPOLITAN REGION RESULTING FROM COMPOUND FLOODING

Abstract

The co-occurrence of different flood drivers (i.e. compound floods), such as coastal storms, riverine flow, and urban pluvial runoff, can cause severe damage to urban areas. Like many U.S. metropolitan regions along the coast, the Washington, DC metropolitan area, where increasing precipitation rates and sea-level rise have been observed, is vulnerable to the impacts from such events because of its complex demographics and socioeconomics structure. This study aims to evaluate urban socio-economic vulnerability in the Washington, DC Metropolitan Region resulting from compound flooding at multiple scales. The socioeconomic damages from riverine flood and coastal surges, which is defined as Exposure Index, were combined with the Social Vulnerability Index (SOVI) in order to detect vulnerable populations to compound flood events at range of scales (tract, group, and block). The results of each index were compared among each scale to evaluate their sensitivities. The highest damage was found on the banks of Potomac River in the compound scenario. A high-precipitation scenario was also performed, leading to severe damages in locations with denser infrastructures, such as DC and Arlington County. The multiscale comparison suggested that block scale analysis is more sensitive to vulnerability and flood damages compared to coarser scales

i.e. group and tract. Distribution of the risk was found significantly dependent on both the type of the compound flood event and scale of the analysis. From a flood management perspective, coarser scale assessments can mislead efforts as it is not able to highlight specific locations with substantial vulnerable populations. The method presented in this study is a tool that can potentially aid decision makers to identify the vulnerable populations to compound flood in large coastal metropolitan areas.

2.1 Introduction

Flood events are one of the costliest natural hazards impacting societies around the world (Deely et al. 2010; Remo et al. 2016). Flooding is especially a problem in urban areas, which is intensifying by an increase in storms intensity and frequency(Fernandez et al. 2016; Abebe et al. 2018; Gu et al. 2018; Wu et al. 2019; Oubennaceur et al. 2019; Chakraborty et al. 2020; Khajehei et al. 2020). In addition, growing population and urbanization amplify the flood-related losses in both economic and social dimensions (De Risi et al. 2018; Chakraborty et al. 2020). However, the impacts of flood events are unequally distributed across infrastructure and communities due to their characteristics (Gu et al. 2018). Conditions such as infrastructure characteristics, including age, foundation type, elevation (FEMA 2013), and demographic information, such as socio-economic conditions leading to inequalities between people are some of the determinant factors for how consequences of flood damage are distributed within society and structures (Cutter et al. 2003; Eakin and Luers 2006; Karagiorgos et al. 2016; Gu et al. 2018; Kawasaki et al. 2020). Therefore, it is essential to assess the characteristics of construction and vulnerability factors of the community to

51

quantify risk on assets and communities better (Zahran et al. 2008; Fernandez et al. 2016; Munyai et al. 2019; Chakraborty et al. 2020; Walkling and Haworth 2020).

Social vulnerability assessment is a comprehensive tool that aims to measure those socio-economic factors, which defines sensitivity and the adaptive capacity of the population to the hazard (Gu et al. 2018). Hence, susceptibilities of population subgroups, such as limited resources to cope with the consequences of hazards, low well-being levels, and disabilities, are evaluated, quantified, and documented (Fatemi et al. 2017). Multiple studies have mapped out socio-economic vulnerability factors and quantified them around the world at both national and local scales (Rufat et al. 2015). The hazards-of-place model of vulnerability introduced by Cutter (Cutter 1996), a specific method to perform place-based vulnerability analysis to any hazard, is applied in many social vulnerability assessment studies (Cutter et al. 2003; Ahsan and Warner 2014; Monterroso et al. 2014; Remo et al. 2016; Gu et al. 2018; Khajehei et al. 2020). In one example, the spatial distribution of the social vulnerabilities in the entire U.S. is assessed (Cutter et al. 2003) at the county scale by using vulnerability factors, such as age, gender, race, education level, social dependence, family structure, and socioeconomic status as in most of the vulnerability studies (Cutter et al. 2003; Rufat et al. 2015; Pricope et al. 2019; Khajehei et al. 2020; Walkling and Haworth 2020). Although this county scale social vulnerability index results illustrate the broad vulnerability distribution for regional study areas, several studies used the same approach to evaluate social vulnerability levels in finer scales and within their study areas in the U.S. (Rygel et al. 2006; van Zandt et al. 2012; Remo et al. 2016). It is very important to identify the most vulnerable

neighborhoods to flood hazards in order to analyze impacts spatially (Yang et al. 2018; Chakraborty et al. 2020) . According to (Rufat et al. 2015), the number of studies focused on social vulnerability to floods is highest in the U.S., followed by Western Europe and Southeast Asia. Flood vulnerability is a specific term for measuring the social vulnerability based on exposure, sensitivity, and adaptive capacity of a population to flood hazard particularly (Lee and Choi 2018). In most studies, exposure is defined as a potential loss, while sensitivity and adaptive capacities are fragilities and abilities of the population to cope with damage, respectively (Lee and Choi 2018). Some particular studies combine the hazard of place social vulnerability model with exposure, such as flood damages, to quantify risk (Zhou et al. 2012; Remo et al. 2016; Chen et al. 2019a), while some others utilize flood hazard information using statistical flood probability (Thakuy et al. 2011; Hoque et al. 2019; Khajehei et al. 2020), and satellite imagery (Zheng et al. 2008). Since both hazard and exposure are the components of the risk definition in the widely accepted risk triangle approach (Crichton 2002), they both need to be well represented in the description of the risk.

Different flood drivers, such as coastal storms, riverine flow, and urban pluvial runoff can cause severe damage to urban areas. However, whenever co-occurring, the amount of severe flood damage can be magnified (Couasnon et al. 2020), as observed during Hurricane Harvey (Zscheischler et al. 2018) and Cyclone Idai (Couasnon et al. 2020). In a study conducted in the entire U.S., it is reported that the frequency of the compound flood events has increased in the majority of the coastal cities (Wahl et al. 2015). In addition, Couasnon et al. (Couasnon et al. 2020) stated that the large

metropolitan areas in the U.S., such as Washington DC and Baltimore MD, are susceptible to compound flooding. It is also important to estimate future flood damages due to its importance for flood risk management methods (Middelmann-Fernandes 2010). Thus, several studies have shown efforts to quantify urban flood damage from riverine and urban runoff (Remo et al. 2016; Arrighi and Campo 2019; Muthusamy et al. 2019; Oubennaceur et al. 2019), and coastal storms (Xian et al. 2015; Karamouz et al. 2016; Prahl et al. 2018) by applying various methodologies, including depth-damage functions and remote sensing techniques. There are very few studies that focus on compound urban flood damage and risk (Yang et al. 2020). Since the quantification of urban compound flood risk is an essential component of risk management in coastal metropolitan areas, there is a clear need to further improve this subject in order to support flood resilience of communities (Shen et al. 2019). Therefore, this study aims to quantify both social and physical dimensions of compound urban flood risk in the Washington, DC metropolitan area by: (a) evaluating the spatial distribution of the social vulnerability within the Washington, DC metropolitan area at multiple scales (census tract, group, and block levels); (b) investigating the impacts of different flood drivers and their consequences; (c) assessing the urban compound flooding hazard in the Washington, DC metropolitan area for 7 different compound flooding scenarios; (d) estimating compound flood damages to residential buildings; and (e) combining social vulnerability assessment with damage results to introduce the Flood Socio-Economic Vulnerability Index (FSOEVI) to illustrate compound flood risk for the residential population.

2.2 Study Area

As one of the most prominent locations in the U.S., the Washington, DC metropolitan area (Figure 11) is located in the Mid-Atlantic region of the U.S. with 6.2 million residences. It encompasses the counties of Alexandria, Arlington, Fairfax, and the Falls Church City from the State of Virginia, some portions of Montgomery and Prince George's counties from the State of Maryland and the District of Columbia (DC) within its borders. Washington, DC experienced significant floods in history, such as Hurricane Agnes (1972) and the Federal Triangle Flash Flood (2006). Different types of floods, including coastal, riverine, and pluvial were observed in those events (Commission 2008). For instance, streets and buildings including some important federal agencies were flooded and caused $10 million damage in the Flash Flood event (Commission 2008). These kinds of events, with substantial losses, are expected to increase in the future, since the Washington, DC metropolitan area has an increasing precipitation rate and is under the risk of sea-level rise (Ayyub et al. 2012).

On the other hand, the Washington, DC metropolitan area has complex demographics and socio-economic. In addition to differences in the distribution of population density in the study area, there are noticeable differences between the common indicators of socio-economic features, such as age, educational attainment, the median value of a house, and poverty (U.S. Census Bureau 2019a). Some parts of the area have the most educated people, but some have less-educated ones compared to the entire U.S. (U.S. Census Bureau 2019b). Hence, these main differences in population

structures lead to highly variant spatial social vulnerabilities (Gu et al. 2018). This was

one of our motivations to further investigate this area.
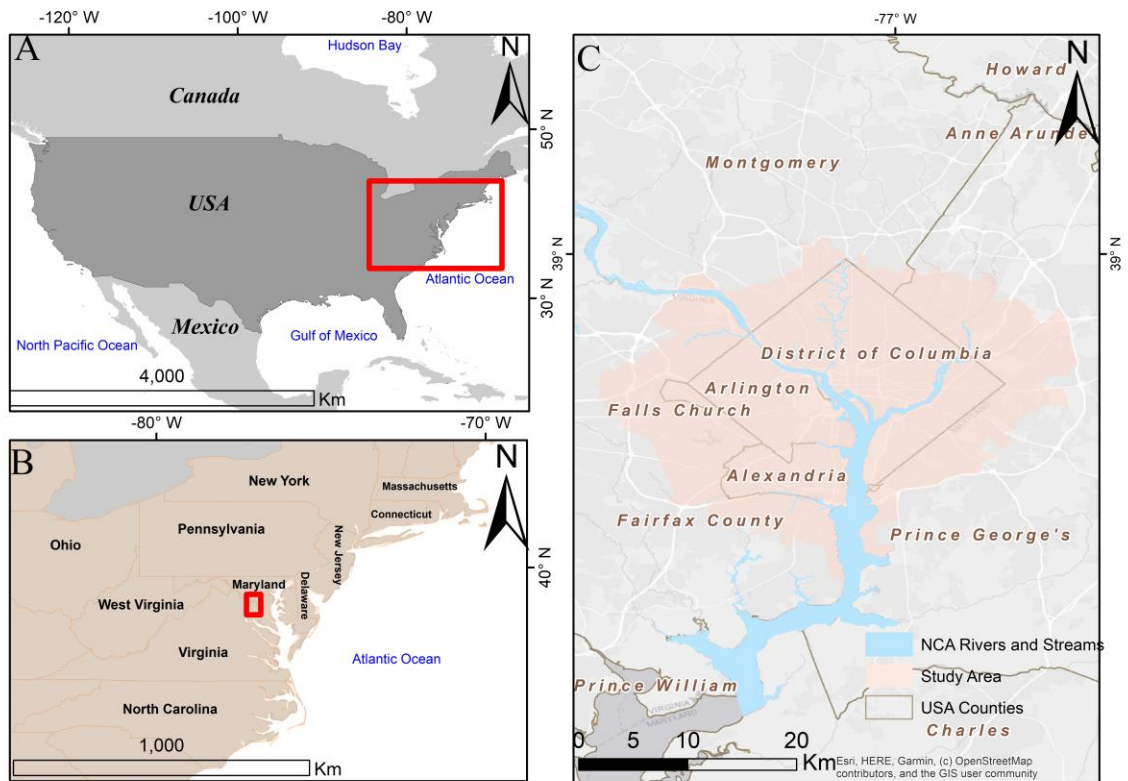
Figure 11 Study area A) U.S; B) East coast of the U.S.; C) Washington, DC metropolitan region

2.3 Methodology

Figure 12 summarizes the overall method showing how the flood socioeconomic

vulnerability of the residential population was assessed. In the left part of the figure, the

social vulnerability assessment module was presented, which utilized Principal

Component Analysis (PCA) with vulnerability factors defined from census data for tract,

group, and block scales. The right part computes the flood exposure index by applying

the flood damage estimation tool of HAZUS-MH to compute flood damages from

compound urban flood scenarios. Finally, the results of social vulnerability assessment

and exposure index were combined to evaluate the overall flood socioeconomic

vulnerabilities in tract, group, and block scales. Each step of the general method was

described in detail over the following sections.
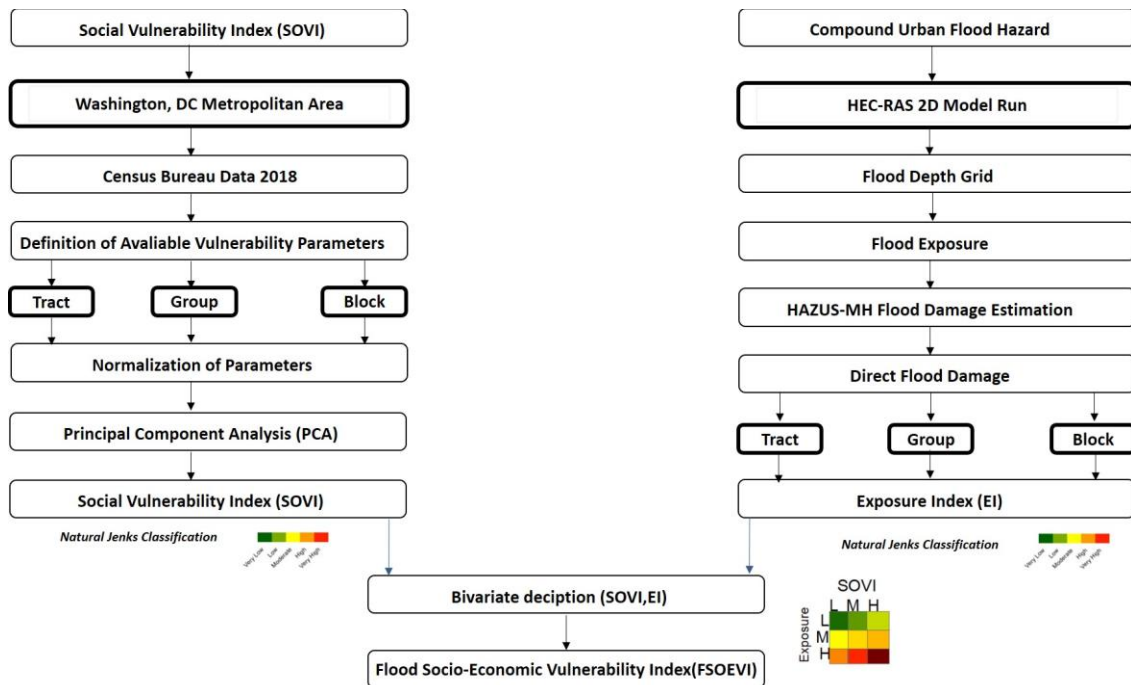
Figure 12 Overall method to calculate Flood Socio-Economic Vulnerability Index (FSOEVI)

2.3.1 Social Vulnerability Assessment (SOVI)

The hazards-of-place model is a popular model applied in the vulnerability

assessment frameworks which combines social and biophysical dimensions of

vulnerabilities to introduce the overall vulnerability of a location (Fernandez et al. 2016).

The Social Vulnerability Index (SOVI) generated by this approach helps to map out the

vulnerability distribution of the population. In this study, the method represented in

(Cutter et al. 2003) was employed by adding some vulnerability factors from studies on

flood social vulnerability (Remo et al. 2016; Khajehei et al. 2020). The study by (Cutter

et al. 2003) not only demonstrates the SOVI levels spatially in the entire U.S. at the

county level for environmental hazards, but also introduces a comprehensive method for

assessing social vulnerability. The spatial distribution of socially vulnerable populations

in the U.S. (Cutter et al. 2003) suggests that the counties in the Washington, DC

metropolitan area have medium, medium-low, and low levels of SOVI compared to other

counties in the U.S. However, their results are not appropriate to be applied for this study

area because it performs SOVI analysis comparatively within the entire U.S.

Additionally, the county scale is too coarse to be used in this study area since there are

only 7 different counties and cities. Thus, the SOVI analyses were performed using some

additional variables that focus on flood vulnerability at the finest scales possible. SOVI

analyses were conducted at three different scales: i) tract, ii) group, and iii) census block

levels. Block, the finest scale in which population data is available, is generally bounded

by roads, highways, rivers, and means city block in the urbanized areas (United States

Census Bureau 2019). A group contains between 600 and 3,000 people while tract level

generally contains between 1,000 and 8,000 people (United States Census Bureau 2019).

The variables used for the definition of social vulnerabilities, which are found by

considering data availability and their correlation with vulnerability, are demonstrated in

Table 9A (Appendix A). Although common vulnerability factors utilized in the literature are similar, there is still some subjectivity in choosing vulnerability indicators (Roder et al. 2017). Therefore, it is necessary to analyze the study area well and then decide which parameters to define vulnerability (Roder et al. 2017). Different representative variables (41 total) for social, cultural, and demographic features of the study area were chosen for three different geographic aggregation levels. There are different numbers of variables available for disparate geographic aggregation levels due to the availability of datasets for block, group, and tract level. The 2010 decennial census survey results were used to analyze the census block level, while 2018 (5-year estimates) of the American Community Survey (ACS) dataset were employed for tract and group level analysis. The 5-year estimates were selected because the statistical reliability of the dataset for the less populated areas is higher in 5-year estimates of the United States Census Bureau (Bureau n.d.). The number of variables utilized was less for block (18) and group (27) levels when they are compared to tract (31). However, the socioeconomic factors of vulnerability were described by selecting variables to quantify the differentiation of those factors including advantages and disadvantages, capacities to cope with hazard, as well as sensitivity to exposure.

   After collecting all related data, the normalization procedure was performed to solve the incommensurability problem of using different data with various units. The maximum-minimum normalization technique was applied by Equation 1. (Abson et al. 2012; Monterroso et al. 2014; Remo et al. 2016; Chakraborty et al. 2020):

Principal Component Analysis (PCA) is a factor analysis method that aims to reduce the number of variables by the matrix factorization process (KC et al. 2015; Jha and Gundimeda 2019). After PCA, fewer representative variables are acquired by storing the optimum portion of the information (KC et al. 2015; Jha and Gundimeda 2019). The first dimension of the principal component has the highest amount of information from the initial dataset. The total information explained by principal components decreases with each component (Jha and Gundimeda 2019). Since social vulnerability assessments contain many parameters, PCA is widely used as an effective way of combining variables and reducing dimensions(Cutter et al. 2003; Fekete 2009; Monterroso et al. 2014; KC et al. 2015; Remo et al. 2016; Gu et al. 2018; Jha and Gundimeda 2019; Rufat et al. 2019; Khajehei et al. 2020). Some statistical tests need to be applied prior to any factor analysis to evaluate if the dataset is appropriate for the procedure. Bartlett's Test of Sphericity and Kaiser-Meyer Olkin (KMO) measure of sampling adequacy tests are commonly performed before PCA in the literature (Fekete 2009; Mavhura et al. 2017; Jha and Gundimeda 2019; Pricope et al. 2019; Chakraborty et al. 2020). The acceptable p-value for Bartlett's Test of Sphericity is less than 0.05. KMO values that facilitate the assessment of interdependencies of initial variables should be greater than 0.5 (Gu et al. 2018). Several RStudio packages, including factoextra, FactoMiner, REdaS, corrplot, bartlett.test, and KMO were employed for simulating all required tests and PCA.

After the PCA application, a scree plot was used as a decision tool to select a number of representative principal components retained from the analysis. The information about the percentage of variance explained by each component and the total

explained variance were obtained. In addition to component extraction, loadings of all variables on every component were derived. Then, SOVI scores were calculated by applying the Equation 2, Equation 3, Equation 4 (Remo et al. 2016):

After the SOVI values were computed for each geographic aggregation level, they are normalized again to represent results of the SOVI scores. Lastly, the Natural Jenks classification method was applied to show results spatially.

2.3.2   Compound Flood

The spatial and temporal variability of the compound urban flooding in Washington, DC resulting from riverine flow, coastal storm surges, and urban rainfall/runoff were investigated (Sumi 2020). The impacts of the flood drivers in different urban locations were explored to understand how the flood propagates into inland areas and what are the consequences associated with such flooding. The storm surge and river discharge values used for the analysis are representative of the low-probability and high-probability events occurring in the study area. The results of a hydrodynamic model for the region with synthetic time series of flood drivers and by generating a set of runoff data from design rainfall depths were utilized. The synthetic events were evaluated for understanding the patterns of flood inundation extent, flood depth, and ultimately the flood risk in the area (Sumi 2020).

A 2D hydrodynamic model, using the River Analysis System (HEC-RAS) software from the Hydrologic Engineering Center's (HEC), was implemented for the flood simulation along the Potomac River. The HEC-RAS 2D software is capable of modelling unsteady-flow routing with Saint-Venant and diffusion wave equations by

solving implicit finite volume (U.S. Army Corps of Engineering 2016). A total of 7 scenarios were selected for this analysis out of 28 scenarios implemented based on historical extreme and non-extreme values of flow and surge at Little Falls, DC, and Alexandria, VA, respectively (Sumi 2020). The 100-year, 25-year, and 5-year 6-hour duration design rainfalls were used to generate storm runoffs. Runoffs were generated for each rainfall based on two Curve Numbers (CN): CN 65 and CN 85 based on the minimum and maximum area coverage of CN values in the study area (Sumi 2020). Two of selected synthetic 7 compound events which are defined as High Flow High Surge with and without rain, are seen in Figure 13.
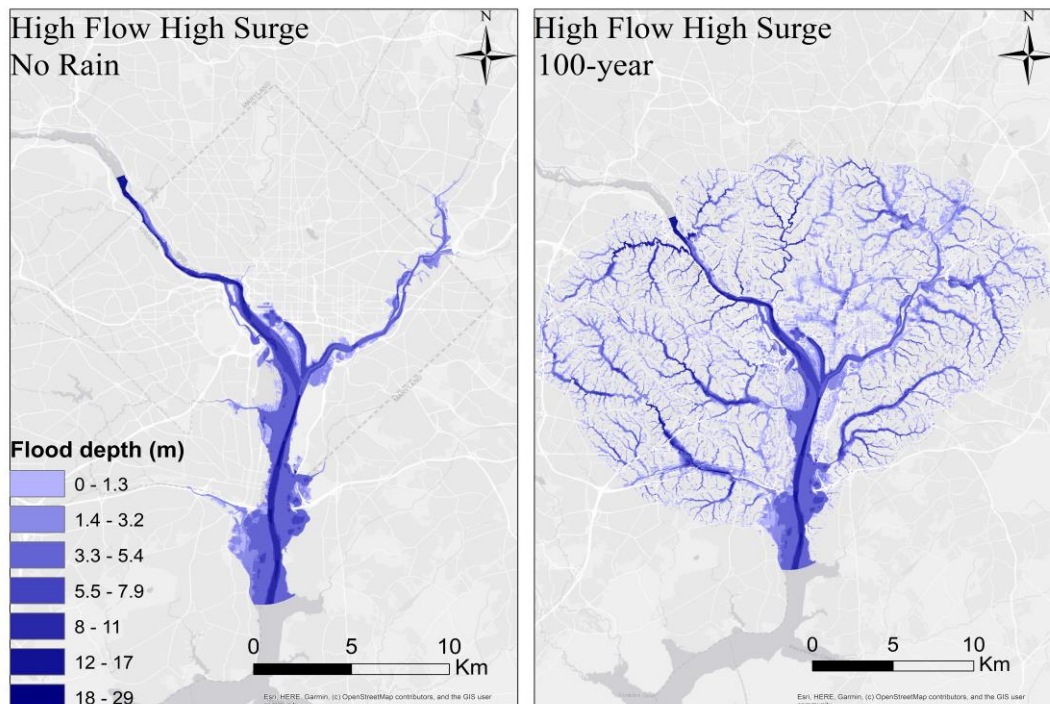
Figure 13 Compound flood hazard scenarios (Sumi 2020)

2.3.3 Flood Exposure (HAZUS-MH)

The flood exposure index term was introduced as flood damage from the previously described 7 different urban compound flood scenarios. Flood damage estimation was performed by using HAZUS-MH, which is a comprehensive, standardized damage estimation tool for multi-hazards (FEMA 2013). The flood module of HAZUS-MH has been used for decision-makers and floodplain managers to quantify potential losses and flood risks to protect citizens and properties (FEMA 2013). There are three different levels of flood damage simulations available in HAZUS-MH. Level 2 analysis, which requires modification of both inventory and hazard data (FEMA 2013), was performed importing the HEC-RAS2D flood depth grids to HAZUS-MH.

HAZUS-MH has the ability to calculate flood damage for different building occupancies, such as residential, commercial, industrial, governmental, educational, religious, and agricultural, as well as transportation, motor vehicles, essential infrastructure (i.e. bridges, roads, oil stations, wastewater treatment facilities), and indirect losses (FEMA 2013). All building-related losses were computed for all specific occupancies. However, this study intends to assess the socio-economic vulnerability of the residential urban population. Thus, socioeconomic losses, which are defined as residential buildings-related losses (structural, content, inventory, relocation, income, rental income, wage), and vehicles, were only included in the flood exposure definition in this study (Table 6).

Table 6 Specific occupancies included in exposure analysis

Specific Occupancy	General Occupancy	Description	Specific Occupancy	General Occupancy	Description
RES1	SingleFam.	Single Fam. Dwelling	**RES3E**	Residential	Multi-dwellings (20 to 49 units)
RES2	Residential	Manufactured Housing	**RES3F**	Residential	Multi-dwellings (+50 units)
RES3A	Residential	Duplex	**RES4**	Residential	Temporary Lodging
RES3B	Residential	Triplex/Quads	**RES5**	Residential	Institutional Dormitory
RES3C	Residential	Multi-dwellings (5 to 9 units)	**RES6**	Residential	Nursing Home
RES3D	Residential	Multi-dwellings (10 to 19 units)	**Vehicle**	Vehicle Loss	Cars, Light Truck, Heavy Truck

Foundation type, building age, first-floor elevation, and building type are some essential components of the flood damage estimation procedure used for structural, content, and inventory losses in HAZUS-MH. Depth-damage functions are mainly derived from those components (FEMA 2013). There are also different depth-damage functions for rental income, relocation, income, and wage losses, such as disruption cost, restoration time, etc. Moreover, parking demand rates, expected daily utilization at commercial parking lots, parking distribution by parking area type are the information needed to estimate flood damage on vehicles (FEMA 2013). Vehicle ages and types also affect the related function implemented for vehicle loss evaluation. Information about three different vehicle classes; automobiles, light trucks, and heavy trucks were estimated for each geographic aggregation level by combining the National Automobile Dealers

Association (NADA), U.S. Department of Transportation's Truck Size and Weight Study (TSWS), and National Personal Transportation Survey (NPTS) in HAZUS-MH (FEMA 2013).

All residential building-related and vehicle losses were calculated for census block level and summed for the group, and tract levels as full replacement costs. Then, all losses were summed to define total economic damage for each aggregation level. In order to compare exposure indexes within the study area, the same maximum-minimum normalization technique was applied (Equation 1). Finally, the Natural Jenks classification method was implemented again to show the spatial distribution of exposure indexes.

2.3.4 Flood Socio-Economic Vulnerability (FSOEVI) Calculation

Two scenarios were chosen to implement the FSOEVI calculation. The scenarios indicating compound flood events with and without rain were selected to indicate the impacts of precipitation as an additional flood driver to riverine flow and storm surge. The Exposure Index was evaluated for the most and least intense compound flood scenarios to observe the effect of high intensity rain in overall risk distributions. The most intense scenario was defined as High Flow High Surge with 100-year return period with CN of 85, while High Flow High Surge without rain was identified as the least intense scenario. After the evaluation of both SOVI and Exposure indexes, each geographic aggregation level had one value representing social vulnerability and one for exposure intensity from the flood events. Both have their own five Natural Jenks break values to classify results as "Very Low", "Low", "Moderate", "High" and "Very High".

In order to evaluate the Flood Socio-economic Vulnerability Index, both results were merged. Some studies combine both terms using weights defined by expert opinion (Sowmya et al. 2015), equal weighting (Remo et al. 2016; Lee and Choi 2018), statistical procedure (Mansur et al. 2016; Yang et al. 2018; Hadipour et al. 2019), and cross tabular bivariate (Gu et al. 2018; Khajehei et al. 2020) method. A two-way cross-tabulation was chosen to apply the bivariate method to illustrate the relationship between two different indexes (Gu et al. 2018). Three different rows (exposure) and columns (SOVI) were used to develop the FSOEVI scores for each geographic aggregation level. Very low and low values of Exposure and SOVI were reclassified as low while moderate values of both were considered as moderate FSOEVI. For the high FSOEVI, high and very high exposure and SOVI results were combined to highlight high risk areas in the Washington, DC metropolitan area.

2.4 Results and Discussion

2.4.1 SOVI Results

The SOVI analysis was conducted at three contrasting scales with different variables due to data availability. The variables indicating the same population features were chosen for each scale. The statistical tests (Bartlett-Sphericity, KMO) were performed before the PCA procedure. The datasets passed both tests for each geographic aggregation level for the study area (Table 7) with acceptable values defined in the related literature (Remo et al. 2016; Fatemi et al. 2017; Roder et al. 2017; Chakraborty et al. 2020). This finding suggested that all datasets are reliable, consistent, and the multicollinearity problem is under accepted levels for any factor analysis.

Table 7 Results of statistical tests prior to PCA

Aggregation Level	Bartlett-Sphericity(p)	KMO value
Tract	2.2e-16	0.85
Group	2.2e-16	0.89
Block	2.2e-16	0.80

The selection of the number of principal components to be used for the representation of the initial data is a subjective decision. However, there are some common standards and requirements for that decision. In this paper, visual assessment with scree plots, which optimize the selection process for the percentage of variance explained of the initial dataset, was utilized. Scree plots in Figure 14 were an illustration of the contributions of each dimension which intend to identify the total dataset.
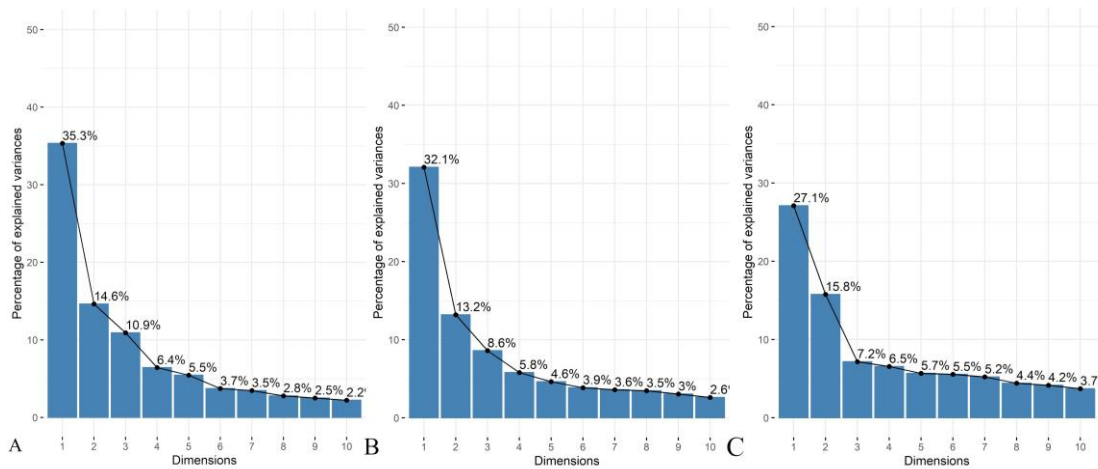
Figure 14 Scree plots for A) tract; B) group; C) block levels

In this study, it was aimed to describe 75-80% of total information with principal components to be consistent with the related literature (Cutter et al. 2003; Fekete 2009; Chakraborty et al. 2020). Therefore, after examining scree plots, 8 principal components were extracted. The total percentage of described variance was 82.7%, 75.3%, and 77.4% for tract, group, and block levels, respectively (Figure 14). The percentage variance explained by the first dimensions were the greatest for all geographic aggregation levels again similar to the literature (Rygel et al. 2006; Fekete 2009; Ganguly et al. 2019; Chakraborty et al. 2020). The explanation percentage declined with an increasing component number. In coarser scale scree plots (Figure 14), the first dimensions had more information about variance than block level.

Correlation plots in Figure 15 indicated the relationships between each variable and the principal components. The squares had darker colors showing a strong correlation and strong representation of variables in a specific dimension. Thus, the darker colors showed the most significant variables which had the dominant loadings in the components. Additionally, blue and red colors indicated different signs of each relationship of variables to each dimension.
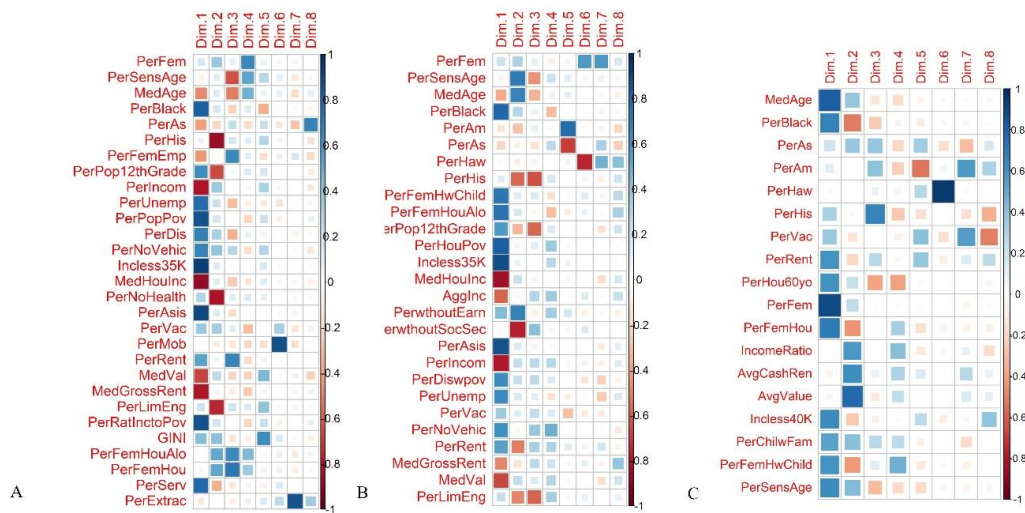
Figure 15 Correlation between variables and dimensions at A) Tract; B) Group; C) Block for Washington DC, metropolitan area

The parameters define the first dimension of each scale, which explains the biggest portion of initial datasets, which were similar for tract and group levels. Yet, the results for block level indicated different parameters as important ones for the first dimension. These differences could be explained by the usage of disparate census datasets for block level. For tract and group levels, parameters which mostly represent economic aspects of vulnerability factors had the highest loading in the first dimension. In block level, age and gender were the parameters, which have the highest explanation in the results.

Only a few studies found similar variables as the main determinant of the vulnerability in the related literature (Fernandez et al. 2016; Rufat et al. 2019). For instance, in a research conducted to validate different social vulnerability models for Hurricane Sandy in New York and New Jersey (Rufat et al. 2019), similar parameters

were used to define social vulnerabilities of the population by principal components and weighted methods. In both methods, the variables defining economic aspects of the population, such as per capita income, population under the poverty level, unemployment rate, and income levels of the households were determined as having the highest weights and loadings for the explanation of the overall vulnerability levels. In the study of (Cutter et al. 2003), the variables embedded in the personal wealth indicator were found as the most influential to the overall vulnerability results. In addition, the social vulnerability assessment carried out in the metropolitan area of Hampton Roads, Southeast Virginia, by principal component analysis and the significantly loaded first component was again defined by the poverty term. Some other studies also reported poverty term as the main contributor to social vulnerability (Kaźmierczak and Cavan 2011; Armaș and Gavriș 2013). Consistent with all those studies, the results of the principal component analysis in this study suggested that the variables, which represent the economic status of the population, were generally highly loaded in first components in each geographic aggregation level in this study. On the other hand, in another studies conducted in different locations, variables related to age (Kaźmierczak and Cavan 2011; Zhang and Huang 2013; Remo et al. 2016), minorities (Zhang and Huang 2013; Remo et al. 2016; Pricope et al. 2019; Chakraborty et al. 2020), housing (Fekete 2009; Jha and Gundimeda 2019; Medina et al. 2020), family structure (Armaș and Gavriș 2013; Pricope et al. 2019), employment (Armaș and Gavriș 2013; Roder et al. 2017), vehicles available (Jha and Gundimeda 2019; Medina et al. 2020), insurance (Medina et al. 2020), and education level (Armaș and Gavriș 2013; Kotzee and Reyers 2016; Ganguly et al. 2019), were

determined as having the highest impact on the resultant vulnerability term. These

findings suggested that the main determinants of the overall vulnerability significantly

depend on both the distribution of vulnerability data over the study area and scale. As a

result of all information depicted above in Figure 15 the spatial distributions of SOVI

were represented in Figure 16.
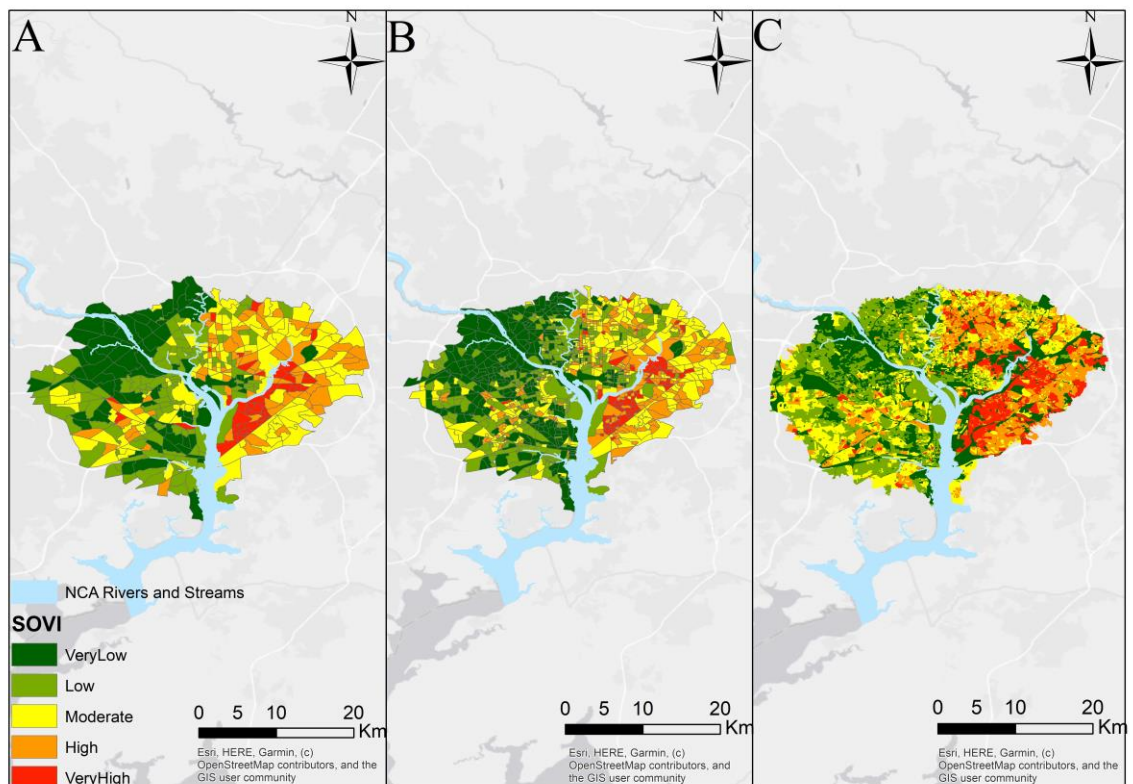
Figure 16 SOVI results for Washington DC, Metropolitan area (A)Tract; (B)Group; (C)Block

Figure 16 illustrated the spatial distribution of the SOVI results at tract(a),

group(b), and block(c) levels. Each of the geographic aggregation levels demonstrated a

similar spatial distribution of the SOVI. Moreover, the block level analysis highlighted

more locations with high and very high vulnerability levels. The population at the north-west of the study area had mostly "Very Low" and "Low" vulnerability levels since the population living in that area were wealthier than the average of the study area. The population located in the south-east and the north part of the study area had more "High" and "Very High" vulnerable populations. Additionally, it can be depicted that the population in the inner city are more vulnerable than the surrounding suburban areas (Figure 16). This may be due to the fact that the wealthier population generally lives in suburbs and exurbs, which explains why the population in the inner city are more vulnerable. However, several locations were also found that had low levels of vulnerability in the city and high levels in the surrounding suburbs. This finding was consistent or contrasting with some of the urban vulnerability studies conducted in different cities of the world (Gu et al. 2018). For instance, population groups in suburban places were found more vulnerable in Bucharest (Armaș and Gavriș 2013), Beijing (Zhang and Huang 2013), and Sao Paulo (Roncancio and Nardocci 2016), whereas population groups in inner cities are found more vulnerable in Manchester (Kaźmierczak and Cavan 2011) and Mumbai (Sherly et al. 2015). In addition, Shanghai (Gu et al. 2018) by demonstrating more mixed vulnerability levels in the inner city was found similar to the Washington, DC Metropolitan area in terms of distributions.
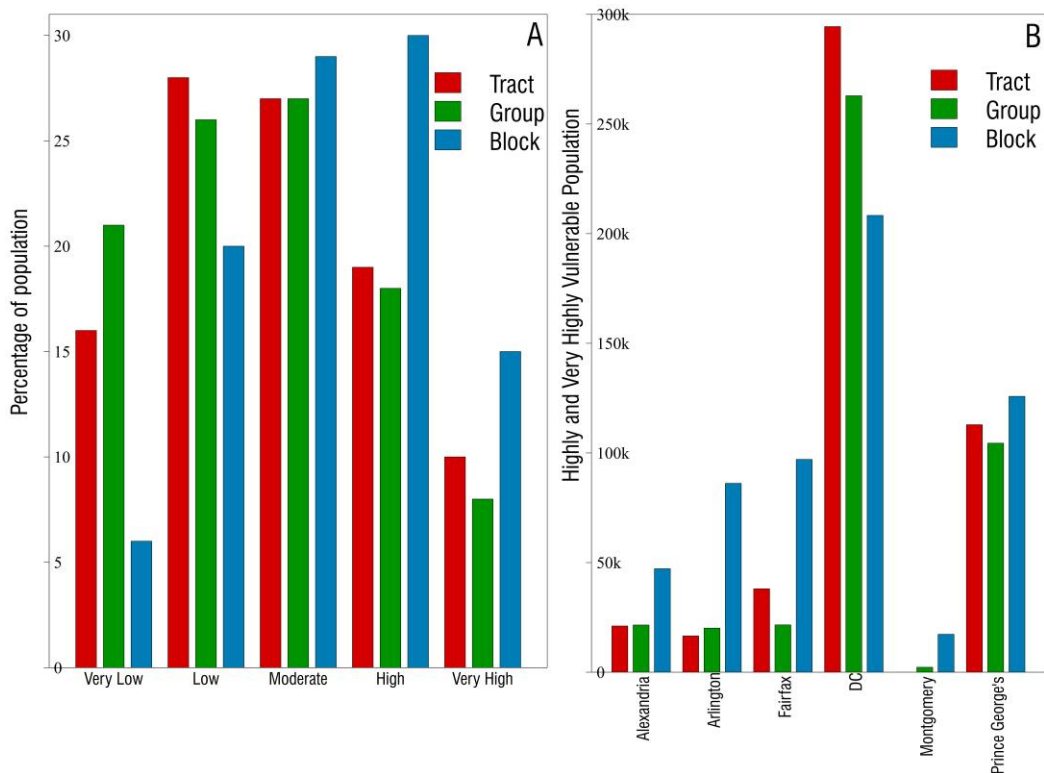
Figure 17 Distribution of vulnerability levels in the Washington, DC Metropolitan Area A) in tract, group and block scales; B) spatial distributions of highly and very highly vulnerable populations

Generally, residents of the Commonwealth were less socially vulnerable than residents of Maryland and DC for each scale (Figure 17). Among all areas, DC had the highest portion of the vulnerable population (Figure 17). Most of the population located in DC labelled as very highly vulnerable for each scale (Tract: 88%, Group 86%, Block 76%). These vulnerability distributions in the Washington, DC metropolitan area were consistent with the literature although the studies found have different scales, aims and extent of comparison. The study aimed to illustrate the spatial distribution of the vulnerable population in the entire U.S (Cutter et al. 2003) indicated that the residents of DC and Prince George's County were more vulnerable (Medium-low) than the residents

of Montgomery, Fairfax, Arlington counties, and Alexandria City (Low). Similarly, the number of geographic aggregation levels, which had a high and very highly vulnerable population, were found to be higher in DC and Prince George's County in this paper. However, since this study was conducted on a much finer scale than the county, findings revealed that there are some locations in Alexandria City, Arlington, Fairfax, and Montgomery counties which had highly and very highly vulnerable populations. Another reason for that difference was the extent of the comparative evaluation. In the (Cutter et al. 2003) study, SOVI results were analyzed within the entire U.S. Thus, the other hotspots, which have a vulnerable population, suppress the possible substantial vulnerable population in the borders of our study area. Likewise, consistent with our findings, the country-wide tract scale SOVI map, which was constructed by the Centers for Disease Control and Prevention (CDC), indicated that the south-east DC and Prince George's County have a more vulnerable population than Montgomery, Arlington and Fairfax counties (Centers for Disease for Control and Prevention 2015). CDC's study also found highly vulnerable tracts in Alexandria and Fairfax since it assessed the vulnerability levels on a finer scale than counties (Centers for Disease for Control and Prevention 2015). However, tract level countywide comparison again was not able to capture some vulnerable populations not only in Arlington and Montgomery counties but also in the rest of the study area. Yet, several locations with vulnerable populations were detected with block and group level analysis in this study.

Figure 17 indicated that the percentage of the vulnerable (highly and very highly) population was larger in the block level compared to the coarser scale analysis.

Additionally, 15% of the total population in the study area appeared had "Very High" vulnerability level in block level which is the largest compared to group (8%) and tract (10%) scales. Finer scale assessment indicated a higher level of spatial variability on a vulnerable population compared to others. For instance, there was no tract found as highly or very highly vulnerable in the portion of Montgomery County located in the study area. Reversely, group and block levels demonstrated some vulnerable populations in residences of Montgomery County in the study area (Figure 17). Furthermore, especially in the block level, the highly vulnerable population was more evenly distributed to the study area compared to two other scales. The complex demographics and socioeconomic structure of the metropolitan areas are hard to detect with coarser scale analysis because the distribution of vulnerability factors varies highly in even in geographically close neighborhoods (Lawrence 2002; Boulant et al. 2016; Nijman and Wei 2020). This suggests that the finer scale assessment is able to capture more locations with vulnerable populations. Therefore, finest scale comparison should be performed in order not to overlook some possible considerable vulnerable population.

2.4.2 Flood Exposure

The results of the total flood damage from the HAZUS-MH simulations for 7 different compound flood scenarios were shown in Figure 18. Each scenario contained high flow and surge conditions represented with HQ and HS, respectively. All scenarios were numbered as in Table 8.

Table 8 Representation of each scenario

Scenario	Definition	Number
HQHS100year85CN	High Flow High Surge 100-year 85CN	1
HQHS25year85CN	High Flow High Surge 25-year 85CN	2
HQHS5year85CN	High Flow High Surge 5-year 85CN	3
HQHS100year85CN	High Flow High Surge 100-year 65CN	4
HQHS25year85CN	High Flow High Surge 25-year 65CN	5
HQHS5year85CN	High Flow High Surge 5-year 65CN	6
HQHS-No Rain	High Flow High Surge No Rain	7
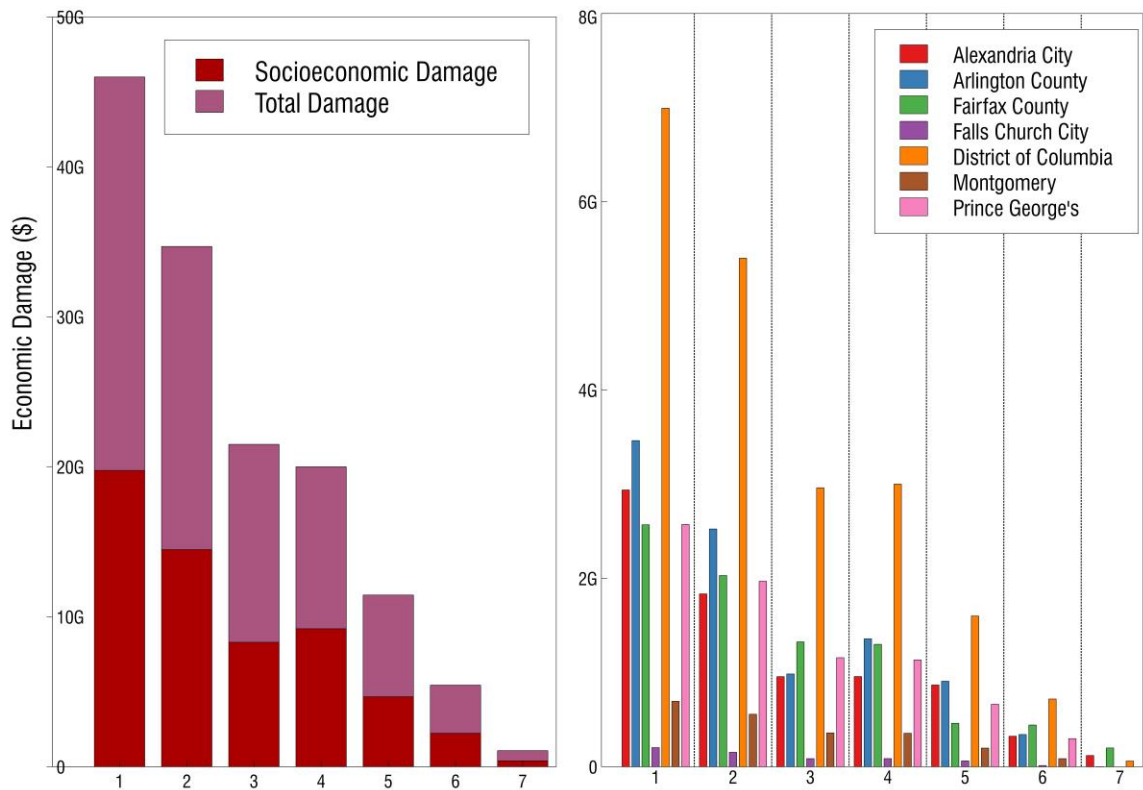
Figure 18 Economic damage from different compound flood scenarios A) Social and total economic damages B) spatial distributions of social damage values across the counties and cities

As expected, the highest damage was estimated in "High Flow High Surge 100 year return period with 85CN (1)" with 46 billion dollars while the lowest one in "High Flow High Surge without Rain (7)" scenario with approximately 1 billion dollars when all building-related and vehicle losses were included. Estimated flood damages on residential buildings, which were identified as socioeconomic losses, showed a similar pattern with all building losses. The highest (High Flow High Surge 100-year return period with 85CN) and lowest (High Flow High Surge without Rain) total damages were found to be 20 billion dollars and 396 million dollars, respectively for socioeconomic losses. The findings of damage estimation indicated that when precipitation event occurred as a third component of the compound flood event, in addition to riverine and coastal floods, the total damage is magnified for both total and socioeconomic losses. The damage differences caused by the intensifying precipitation events were larger in locations with denser infrastructure, such as DC, Prince George's, and Arlington. Alexandria and Fairfax counties indicated lower differences of damage among the scenarios because coastal storm surge, which causes the biggest portion of damage in those locations, was constant for each scenario.

The results of the spatial distribution of flood damages (Figure 18) suggested that DC had the highest damage amount in all scenarios with rain. In a scenario without rain, Fairfax County, which has the longest coastline to Potomac River in the study area, appeared as having the maximum damage. Arlington, Prince George's, and Alexandria counties experienced more damage than Montgomery County and Falls Church City in each scenario. The low levels of damage in Montgomery and Prince George's County

were not surprising since only a small part of their area was included in the study area. Figure 9 illustrated the spatial distribution of exposure index results for each scale and two selected scenarios.
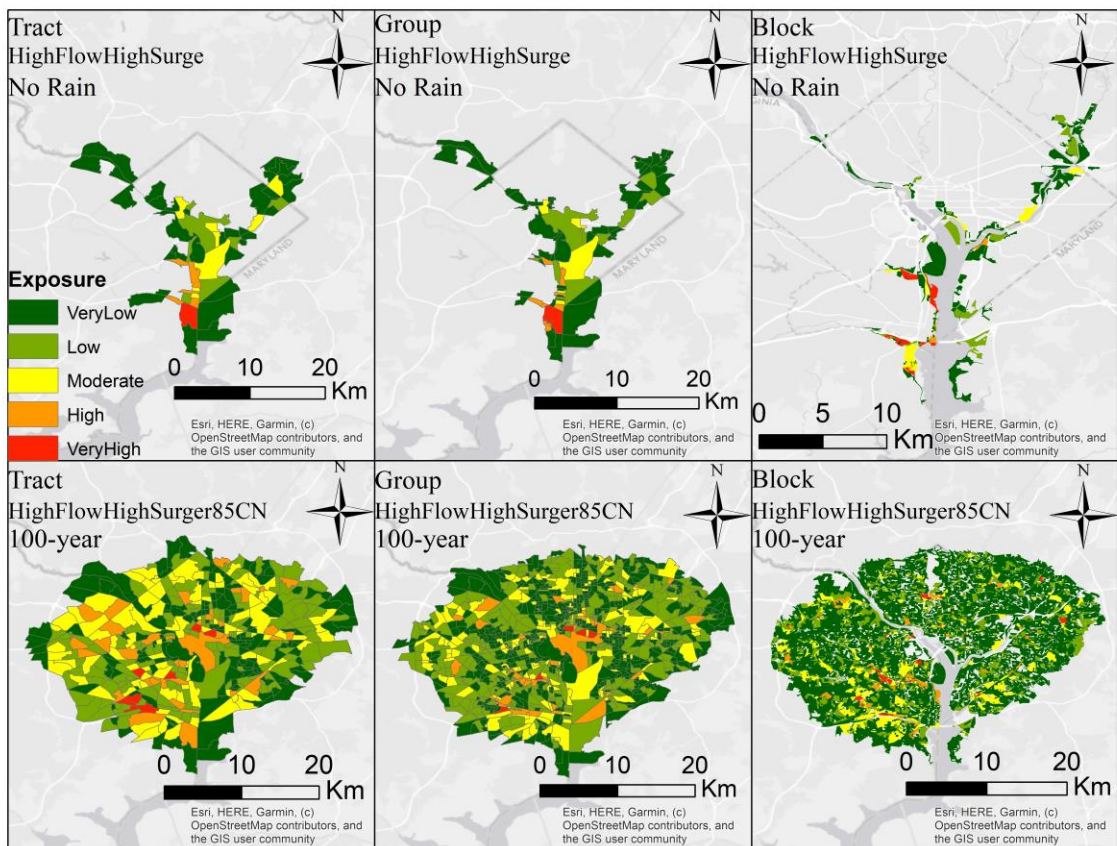
Figure 19 Spatial distribution of flood exposure index in each scale

For the no rain scenario, Figure 19 indicated that the exposure was higher in the Virginia side of the Potomac River in each scale. The middle and the north-east part of the study area had lower exposure levels. These findings could be explained by flood depth grids Figure 13 and Fairfax and Alexandria counties having more inundated

valuable single and multi-family dwellings (RES1, RES3B, RES3E, RES3F) than the rest of inundated locations. Larger inundation areas in Fairfax County and Alexandria City could be interpreted by the susceptibility of low-lying areas near the Potomac River to coastal flood events (Mitigation Advisory Committee 2017). Additionally, lower damages were observed in the coastal parts of DC because only a few residential buildings were inside of the inundation boundary. Figure 13 illustrated that the inundation area was larger and flood depth height was higher in the Virginia side of the Potomac River compared to the rest of the inundated area in the no rain scenario. The distribution of the exposure levels was similar in each scale, yet the block level analysis highlighted more areas experiencing higher flood damages. In addition, the coarser scale exposure index did mask some considerably damaged blocks since they aggregate the economic losses in several blocks to represent damage in the group and tract scales. For instance, one block, which is located in the south bank of the Anacostia River in the south-east of the DC, indicated a high level exposure in the no rain scenario although the corresponding tract and group were classified as a moderate level of exposure.

For the rain scenario, tract and group scales demonstrated similar distributions of high and very high exposure levels. However, the block level distribution indicated additional areas that had very high exposure in the study area especially in Prince George's, Montgomery, and Fairfax counties. The damage values were maximum in the blocks that had a high value single and multi-family dwellings as well as temporary lodgings. In tract and group, same locations in north and north-west of the National Capital Region in DC, Alexandria and Arlington counties had the highest exposure. Tract

level showed two additional locations in Arlington county which had very high exposure

levels. Similar to no rain scenario, those differences might be explained by the

methodology of calculating damage values by summing the economic loss values of

blocks to indicate total damage in groups and tracts. There were blocks in several

locations which had very high damage whereas neighborhood blocks did not. Therefore,

they showed these severe damage values in the block level assessment but not in coarser

scale summations. For both scenarios, the spatial distribution of the flood exposure index

indicated that flooding in the Potomac River caused more damage compared to other

streams, rivers and tributaries in the Washington, DC Metropolitan Area, such as

Anacostia River, Four Mile Run, Cameron Run, etc. Hence, locations in the banks of

Potomac River generally indicated more severe damage than the other ones. This may be

explained by the larger size and volume of water of Potomac River (Commission 2008).

In addition, the results of the rain scenario indicated severe damages in the locations with

denser infrastructure, such as Arlington County and DC, while no rain scenario caused

more damage on the banks of the Potomac River due to coastal storm surges.

2.4.3 Flood Socio-Economic Vulnerability Assessment (FSOEVI)

The SOVI, Exposure index, and FSOEVI scores were illustrated in Figure 20 and

Figure 21 for "High Flow High Surge No Rain" and "High Flow High Surge 100 year

85CN" scenarios. The geographic aggregation levels, which have very high or high levels

of SOVI and exposure, were shown with dark umber color and defined as the highly

socioeconomic vulnerable to flood events. Figure 20 indicated that the number of

geographic aggregation levels under compound flood risk less in the no rain scenario.

In no rain scenario, (Figure 20) tract and block-level analysis demonstrated high FSOEVI, while group level did not due to the highly and very highly vulnerable population that experienced lower damage values. Two groups located in the west bank of the Potomac River exposed to high (high & very high) flood damage but had moderate levels of FSOEVI. The north-west of the study area and the Maryland side of the Potomac River showed low FSOEVI levels on each scale. For each scale, the south-western part was highlighted with high FSOEVI levels. The Tract level analysis found one tract which had a high FSOEVI level in Alexandria City. For the block-level analysis, the high FSOEVI scores were found in the same location with the tract levels. However, one more location in the south bank of Cameron Run in Fairfax County, which had very high exposure and SOVI, was also captured by block levels assessment.
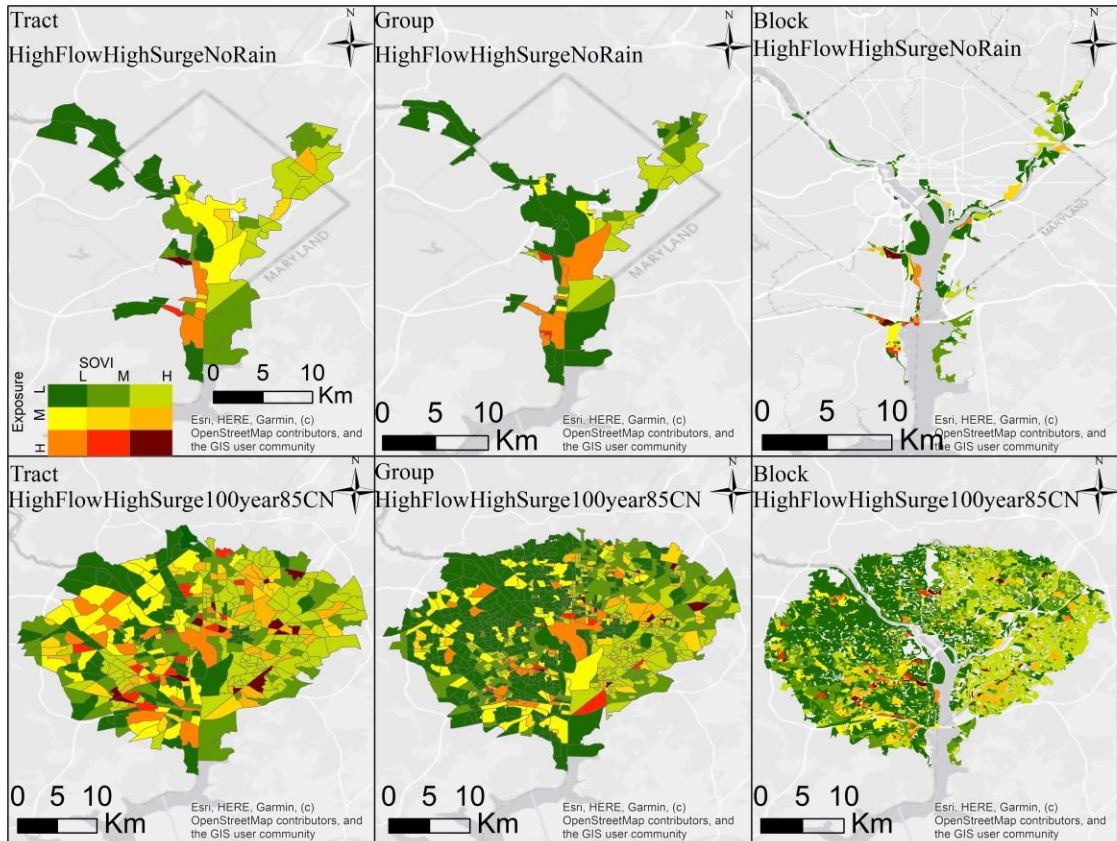
Figure 20 Spatial distributions of the FSOEVI results in the Washington, DC Metropolitan Area

The findings of rain scenario (Figure 20) indicated different distributions in disparate scales. Block and group level results showed more parallel distributions compared to tract level. For instance, in group and block levels, most of the geographic aggregation levels in the north-west of the study area appeared as less vulnerable than the rest of the Washington, DC metropolitan area. However, the tract level distribution of FSOEVI showed several moderately vulnerable locations in the north-west, especially around the north-west of Arlington County. Unlike no rain scenario, the populations with

high FSOEVI were more distributed to the entire area. 13, 10 geographic aggregations found under high risk from three different counties and cities in coarser scale analyses while block-level results highlighted 45 different locations from six different counties and cities. The blocks with high FSOEVI were found in Alexandria City, DC, Prince George's, and Montgomery counties. In tract and group scales, no aggregation levels classified as high FSOEVI in Montgomery County (Figure 20, Figure 21, Figure 22). Figure 21 summarized comparison of the total number of a socioeconomically vulnerable population to compound flood hazard and the number of socially vulnerable populations for two different scenarios.
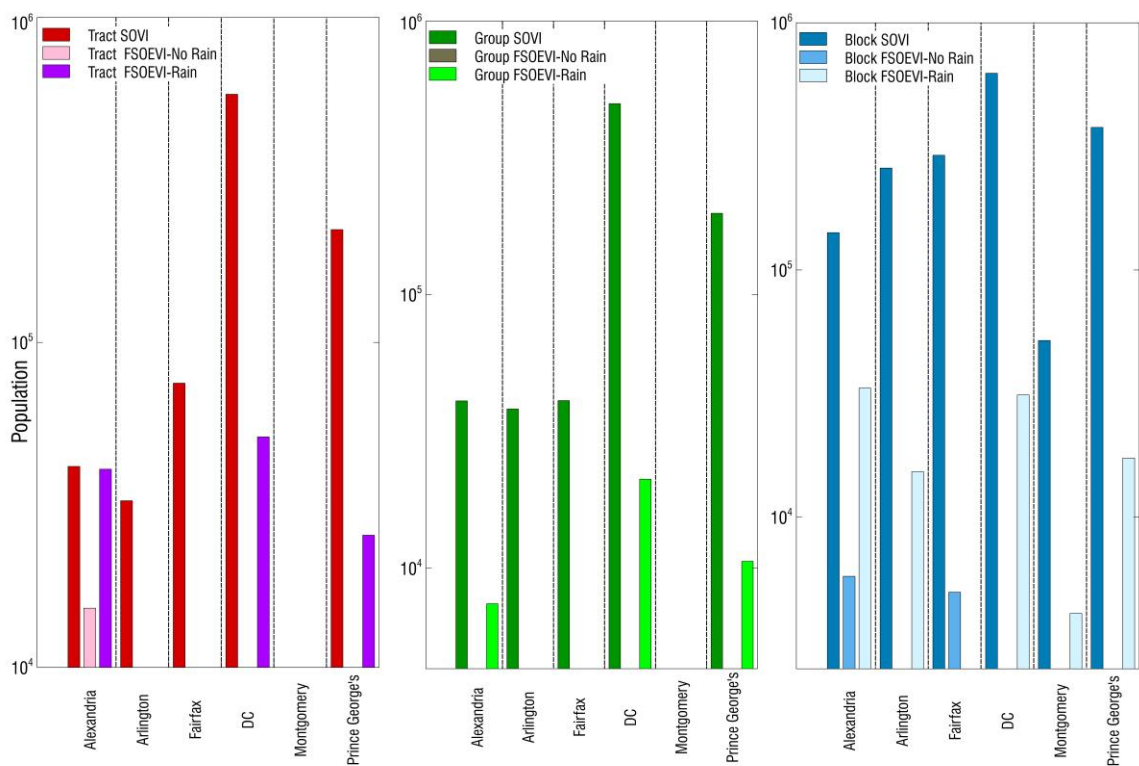
Figure 21 Comparison of the spatial distribution of vulnerable population in tract, group, and block

Figure 21 demonstrated that the high spatial variances were observed in each

scale in terms of the population vulnerable to flood. In tract and group levels, vulnerable

population to flood was only found in Alexandria, Arlington, Prince George's, and DC

while block level analysis indicated some vulnerable population in Fairfax and

Montgomery counties as well in the rain scenario. In no rain scenario, only Alexandria

City was detected to have a highly vulnerable population to flood. The differences of

results for each scale are parallel between rain and no rain scenarios, including finer scale

that highlighted more locations as vulnerable. The main difference was for the block

scale not only in Alexandria City but also in Fairfax where some geographic aggregation

levels were determined as vulnerable to flood. Figure 22 illustrated the ratio between the population vulnerable to flood and the socially vulnerable population.
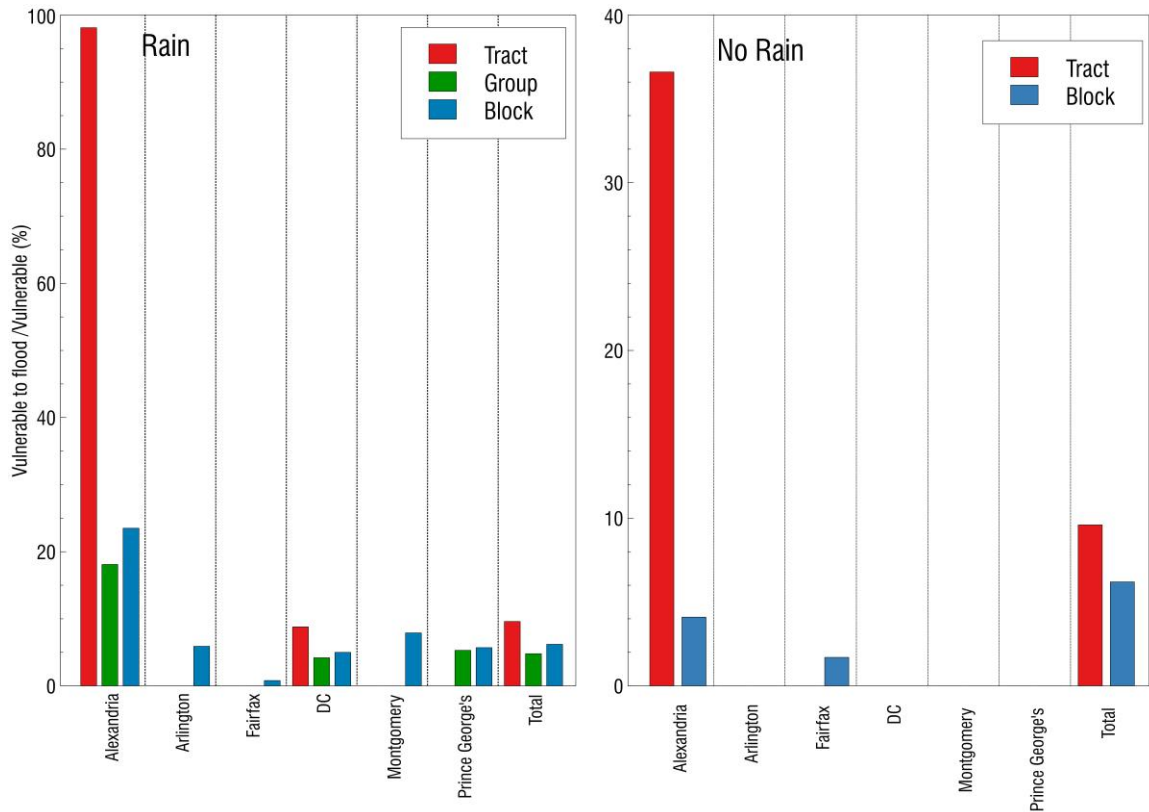
Figure 22 Vulnerable to flood/ Socially vulnerable (%)

Figure 22 illustrated that the ratio of vulnerable population to flood was the highest in Alexandria City for both scenarios in each scale. The ratio was much lower in scenarios with no rain because there was no inundation in most of the land. In tract level, almost all socially vulnerable populations (98%) were also found vulnerable to flood in Alexandria City for rain scenario. For no rain scenario, 36 % of the vulnerable population were classified as vulnerable to flood. There was no tract found vulnerable to flood in

Arlington and Fairfax counties in any scenarios. Group level analysis indicated that any of the groups which had vulnerable populations experienced flood damage in no rain scenario. However, it was found that different portions of the socially vulnerable population were revealed as vulnerable to flood as well in the rain scenario in Alexandria City, DC, and Prince George's County with ratios of 18%, 4%, and 5%, respectively. Similar to tract level, there was no vulnerability found to flood in Arlington, Fairfax and Montgomery counties. Block level analysis illustrated high spatial variability in terms of vulnerable population to flood. Unlike tract and group levels, portions of the vulnerable population in the Montgomery, Fairfax and Arlington counties were also found vulnerable to flood. Only block level assessment could capture that substantial vulnerable population to flood in those counties. Consistent with the other scales, the highest portion of the vulnerable population was identified in Alexandria City for both scenarios (no rain: 4%, rain: 23.5%). The lowest ratio was determined in Fairfax County for both scenarios. On the Maryland side of the study area, 8% and 5% of the vulnerable population was classified as vulnerable to flood in Montgomery and Prince George's counties, respectively.

The comparison of the compound flood vulnerability in three scales suggested that more population was found as highly vulnerable to flood in tract level than block level. The reason is the cross-scale relationship among the geographic aggregation levels. Populations in the tract levels are almost five times larger than block level. When several blocks indicating high vulnerabilities were located in the same tract, the corresponding tract could be classified as vulnerable although the rest of blocks did not show high levels

of vulnerability in the same tract. In fact, those vulnerable blocks only account for a small

portion of the population in tract level. Thus, the assessment in tract level can be

misleading in locations that have complex demographic and socio-economic structure

(Lawrence 2002; Boulant et al. 2016; Nijman and Wei 2020), such as Washington, DC

metropolitan area. However, finer level analyses demonstrated more vulnerable locations

than other scales' spatial variances. These findings are consistent with the literature (van

Zandt et al. 2012; Remo et al. 2016).

Despite the disadvantages of block level analysis, such as limited data availability

(Cutter et al. 2012; van Zandt et al. 2012; Fatemi et al. 2017) and being relatively small to

be utilized in the planning efforts (Remo et al. 2016), the complexity of the data of

vulnerability factors (Rygel et al. 2006; Pricope et al. 2019) and the results of the hazards

could be better explained by micro-scale analysis (Cutter et al. 2012; Frazier et al. 2013).

Furthermore, risk distributions in finer scales might be useful in metropolitan areas since

the high-level localized variation of both distributions of biophysical and social

dimensions of the risk may support the coordination of the emergency planning within

the area (Lawrence 2002; Boulant et al. 2016; Nijman and Wei 2020). Similarly, in our

study, block level analysis was able to capture more locations with substantial compound

flood vulnerabilities, which were found as moderate or low levels of vulnerability in the

coarser scales. Consistent with our results, a similar study conducted in the entire Illinois

state (Remo et al. 2016) , which also aimed to identify flood vulnerability by merging

flood damage and social vulnerability index at the county, jurisdictional and block levels,

found that a number of block-level that shows high vulnerability is larger than the other

coarser scales. Although there are some methodological differences with that study, including merging the SOVI and the exposure terms, considering different types of losses, the main outcomes were that aggregation of flood vulnerabilities on coarser scales may lead to not being able to highlight some locations with considerable vulnerabilities.

Tract and group scales may be claimed as the aggregation levels which have the most uncertainty levels in terms of damage and exposure values among all scales due to aggregation of losses. Yet, the data availability is higher in those two scales compared to block scale, which has the least uncertainty regarding exposure. Thus, each scale seems to have its own advantages and disadvantages to be used in this framework to quantify compound flood socioeconomic vulnerability. However, since the socioeconomic structure and demographics vary significantly within the metropolitan areas (Lawrence 2002; Boulant et al. 2016; Nijman and Wei 2020), the finer scale social vulnerability assessment are more powerful tools to indicate those complexity of the population of the metropolitan areas. Therefore, finer scale analysis should be implemented for better representation of vulnerable population to flood.

Total vulnerable to flood/socially vulnerable ratios were found 10%, 5%, and 6% in tract, group, and block scales, respectively for rain scenarios. Same ratios were found as 37% for tract and 3% for block scales in no rain scenarios. Furthermore, less than 5% of the total population was determined as a vulnerable population to flood in all scales in the study area for both scenarios. Those portions of the population vulnerable to flood were located in less than 3% of the total land in the Washington, Dc Metropolitan area for both scenarios.

All results in every geographic aggregation level were justified with very high and high levels of exposure and social vulnerability levels. In addition, results of tract and group-level analysis showed some similar patterns because they utilized the same dataset even though they had different variables. Another reason for some differences in the results can be the scale. Since damage values were summed for each census block for a definition of group and tract levels, distributions of exposure index vary. In some cases, the census block had high flood damage, but the other blocks around it do not have much damage. Therefore, when damage values were summed to get group and tract level, they may have lower damages in total when comparing with others in the study area.

2.5 Conclusion

This study aimed to evaluate the urban compound flood risk of the residential population at three different scales (Figure 22) in the Washington, DC metropolitan area that is an important geographical location to provide robust information to planners and decision-makers in three different scales by assessing socio-economic drivers of flood risk. 41 variables were defined from the literature considering data availability for tract, group, and block scales. Then, flood hazard was modeled by the HEC-RAS 2D model to represent the variability of impacts of compound urban flood for seven scenarios. Flood depth information, which was acquired from the flood hazard module, was used for flood damage estimation with HAZUS-MH. Two of seven scenarios were chosen to quantify socioeconomic flood vulnerability. With the normalization of those estimated damage values, the Exposure Index was calculated. Then, the SOVI and Exposure Index results were combined to introduce the FSOEVI distribution in the study area. After the method

was applied, flood risk and its drivers were represented spatially to highlight the riskiest locations. This analysis provides scientific insights on compound flooding in the cities along tidal areas and can be implemented for risk analysis of other coastal metropolitan cities with the associated flood driver inputs.

It was found that the south-east shows higher, while north-west indicated lower social vulnerability levels in the study area. The vulnerable population was more spatially distributed in block scale results. The results of loss estimation suggested that the locations in DC experienced the most severe damages in all scenarios with rain due to denser residential infrastructure. In no rain scenario, Alexandria City and Fairfax County demonstrated the highest damage owing to their low-lying coastal areas and high value residential buildings. The normalized values of flood damages, which was defined as an exposure index in this study, for two selected scenarios indicating riverine and coastal flooding together with and without 100-year storm were compared. In no rain scenario, the results illustrated that the south-west side of the study area was exposed to more severe damages on residential buildings and vehicles. The more severe damages were found on the banks of Potomac River due to the fact that storm surges cause more damage than riverine flood. For the rain scenario, exposure index results were more evenly distributed over the areas because the rain scenario lead larger inundated areas in more locations.

In the spatial distribution of FSOEVI, which was defined with a combination of exposure and social vulnerability terms, the residential population located at the south-west of the study area tended to highlight more risk in no rain scenario. On the other

hand, the 100-year compound flood scenario identified some hotspots in DC, Arlington, Alexandria, and Fairfax Counties. This finding suggests that the distribution of the population who have more compound flood vulnerability, significantly depends on characteristics of the event. The multiscale comparison suggested that block scale comparison was able to capture more locations with high vulnerabilities and considerable amount of flood damages compared to coarser scales. Therefore, it is important to assess flood socioeconomic vulnerability in the finest scale possible to be able to notice vulnerable locations effectively in the metropolitan areas. Since planning for mitigation and vulnerability reduction efforts are generally conducted in coarser scale, there is a risk of not being able to cover all vulnerable locations and populations. Finer scale assessments may help decision-makers to highlight additional locations which are not able to be found in a coarser scale analysis. Understanding of the distributions of those identified vulnerable populations could facilitate pre- and post-disaster emergency response efforts (Remo et al. 2016; Gu et al. 2018; Karunarathne and Lee 2020). All results explained above can aid decision-makers from different administration levels to quantify risk and plan mitigation and adaptation actions for the residential population in one of the most important locations of the U.S. In addition, presented framework in this study can easily be applied some other coastal metropolitan areas under compound flood risk, such as New York and Baltimore MD.

Both results and the framework from this study could be improved for the flood damage and integrated risk analysis during urban flooding from multiple flood drivers. For example, all information related to the population for block level was obtained from

the 2010 decennial census, which is the latest dataset available. However, this data may

be counted as a bit outdated in comparison with tract and group level studies which were

utilizing data from 2018. It is known that data from census 2020 is going to be published

soon. For this reason, it is recommended to apply this framework by using the new

population data. That would make SOVI analysis more robust and representative of

today's population features. Addition of climate change and further development

scenarios could facilitate the efforts of vulnerability reduction in the future as well. In

that way, both SOVI and exposure distributions would be projected, and change over

time may be assessed. Furthermore, with projected flood risk levels, the mitigation

actions can be planned better for the future.

CONCLUSIONS

The first aim of the study was to introduce the Social Vulnerability Index for agricultural communities and quantify the overall flood risk of the agricultural communities in the Potomac River Watershed. 13 different parameters were defined to assess spatial distribution of the social vulnerability levels in the Potomac River Watershed. The temporal distribution of physical damage to crops from a 100-year flood event were calculated for 365 days. The spatiotemporal distributions of physical damage and spatial distribution of social vulnerabilities were combined to evaluate spatiotemporal distribution of the agricultural communities in the Potomac River Watershed.

The Social Vulnerability Index (SOVI) results indicated that agricultural communities in Highland and Prince George's counties were more vulnerable than the rest of the basin. In addition, 23% of the counties were found to be as vulnerable as most of the agricultural communities in Texas, Florida, Georgia, Arizona, and Mississippi, which were highlighted as one of the most vulnerable agricultural communities in the U.S.

The results of temporal distribution of flood damages from the 100-year flood event, which is classified as major flood event, demonstrated that flood damages were higher in the summer and fall seasons. Furthermore, the maximum damage was observed

in late September in the entire Potomac River Watershed. This finding can aid decision makers to allocate more resources for resilience actions in late September.

The spatiotemporal distributions of the overall flood risk illustrated that agricultural communities in the Shenandoah County were identified as the most vulnerable agricultural communities in most likely months to experience major flood hazards (September and October) in the Potomac River Watershed. Additionally, the agricultural communities in Hampshire, Shenandoah, and St Mary's counties had high vulnerability levels to floods in different times of the year. To conclude, the socially vulnerable agricultural communities may experience severe flood damages only in specific times of the year. In most of the cases, the communities who may need extra support for adaptation vary throughout the year. Therefore, mitigation actions need to be planned based on both spatial and temporal distribution of the risk of flooding across agricultural communities.

The second aim of the study was to quantify the urban compound flood risk in residential populations at three different scales to provide decision-makers robust information about both physical and social dimensions of risk in the Washington, DC metropolitan area. 41 different vulnerability factors were selected for urban population by both considering data availability and suitability to study area for census tract, group, and block scales. The compound flood hazard was evaluated for two different compound flood scenarios, which represent coastal surge and riverine flood with and without rainfall events. Flood depth information, which was acquired from the flood hazard module, was used for flood damage estimation for socioeconomic losses with HAZUS-MH. Then,

SOVI and exposure index were merged to introduce the Flood Socioeconomic Vulnerability Index (FSOEVI).

The Social Vulnerability Index (SOVI) was calculated and compared for each scale. The spatial distributions of socially vulnerable populations indicated similar results in each scale. The south-east of the study area was highlighted as more vulnerable. Generally, populations located in the inner city were more vulnerable than the ones located in suburbs and exurbs. This finding can be explained by the fact that the wealthier population, which were defined as more resilient to flood hazard, generally lives in suburbs and exurbs. Therefore, the populations in the inner city were found less resilient compared to suburbs and exurbs. However, there were some locations in the inner city with low levels of vulnerability. The multiscale comparison showed that block scale analysis was able to reveal more locations with high vulnerability levels. Thus, coarser scale analysis was not sensitive to capture the complexity of demographics and distributions of socioeconomic structure of the population in the metropolitan area.

The findings of the Exposure Index showed that residential populations located in the south-west of the study area had more population vulnerable to compound flood. The general distribution of risk for the no rain scenario demonstrated that the populations located near the banks of the Potomac River were more vulnerable compared to other locations. For the compound flood event with significant rain, the risk was more distributed across the study area. Some hotspots with highly vulnerable populations were determined in DC, Arlington County, Alexandria City, and Fairfax County. Therefore, it can be concluded that distributions of the risk were significantly dependent on

characteristics of the compound flood event, which is inclusion of rainfall event in our case. The multiscale comparison suggest that block scale analysis was able to reveal more locations with high vulnerability levels. Thus, it is important to evaluate flood vulnerabilities in the finest scale in order to discover vulnerable locations in the metropolitan areas. Although planning for vulnerability reduction efforts were generally performed in coarser scales, there is a risk of not being able to capture all vulnerable populations. It can be concluded that flood vulnerability assessments in the finest scale aid decision makers to highlight additional locations with substantial vulnerability levels.

To conclude, the study was aimed to quantify the different type of flood risks by combining physical and socio-economic dimensions on urban and agricultural populations. This objective was achieved by using tools including the comprehensive social vulnerability assessment, HAZUS-MH, and HEC-RAS 2D. All results aforementioned can help decision-makers, planners, and risk managers to quantify, observe, evaluate, and mitigate risk of flood on assets and communities better. The presented framework for the urban study can easily be applied in other coastal metropolitan areas in the U.S. For the agriculture framework, presented method can be performed in the states leading the agricultural economy in the U.S. such as California, Iowa, Texas, Nebraska to aid decision makers to plan mitigation efforts.

APPENDIX

Appendix A

The parameters used for flood urban vulnerability are shown in the Table 9.

Table 9A1 SOVI parameters for urban SOVI

Parameter/Correlation	Definition	References
PerFem (+)	% Female population	(Cutter et al. 2003; Fekete 2009; Cutter et al. 2012; van Zandt et al. 2012; Rufat et al. 2015; Remo et al. 2016; Fernandez et al. 2016; Roder et al. 2017; Gu et al. 2018; Rufat et al. 2019; Pricope et al. 2019; Chakraborty et al. 2020; Khajehei et al. 2020; Medina et al. 2020)
PerSensAge (+)	% age 5 years and under& 65 years and over	(Clark et al. 1998; Cutter et al. 2003; Fekete 2009; Cutter et al. 2012; van Zandt et al. 2012; Felsenstein and Lichter 2014; Bergstrand et al. 2015; KC et al. 2015; Rufat et al. 2015; Remo et al. 2016; Roder et al. 2017; Schuster-Wallace et al. 2018; Gu et al. 2018; Rufat et al. 2019; Pricope et al. 2019; Chakraborty et al. 2020; Khajehei et al. 2020; Medina et al. 2020)
MedAge (-)	Median Age	(Cutter et al. 2003; Bergstrand et al. 2015; Fernandez et al. 2016; Fatemi et al. 2017; Rasch 2017; Rufat et al. 2019; Chakraborty et al. 2020; Khajehei et al. 2020)
PerBlack (+)	% African American population	(Clark et al. 1998; Cutter et al. 2003, 2012; van Zandt et al. 2012; Bergstrand et al. 2015; KC et al. 2015; Rufat et al. 2015; Remo et al. 2016; Rufat et al. 2019; Pricope et al. 2019; Chakraborty et al. 2020; Khajehei et al. 2020)
PerAs (+)	% Asian population	(Clark et al. 1998; Cutter et al. 2003, 2012; van Zandt et al. 2012; Bergstrand et al. 2015; KC et al. 2015; Rufat et al. 2015; Remo et al. 2016; Rufat et al. 2019; Pricope et al. 2019; Chakraborty et al. 2020; Khajehei et al. 2020)
PerAm (+)	% Native American population	(Clark et al. 1998; Cutter et al. 2003, 2012; van Zandt et al. 2012; Bergstrand et al. 2015; KC et al. 2015; Rufat et al. 2015; Remo et al. 2016; Rufat et al. 2019; Pricope et al. 2019;

Parameter/Correlation	Definition	References
		Chakraborty et al. 2020; Khajehei et al. 2020)
PerHaw (+)	% Native Hawaiian population	(Cutter et al. 2012; van Zandt et al. 2012; KC et al. 2015; Rufat et al. 2015; Remo et al. 2016; Pricope et al. 2019; Chakraborty et al. 2020)
PerHis (+)	% Hispanic population	(Clark et al. 1998; Cutter et al. 2003; van Zandt et al. 2012; Bergstrand et al. 2015; KC et al. 2015; Rufat et al. 2015; Remo et al. 2016; Rufat et al. 2019; Pricope et al. 2019; Chakraborty et al. 2020; Khajehei et al. 2020)
PerFemEmp (+)	% Female Employment	(Cutter et al. 2003; Bergstrand et al. 2015; Chakraborty et al. 2020; Khajehei et al. 2020)
PerPop12thGrade (+)	% Adult educational attainment less than 12th	(Clark et al. 1998; Cutter et al. 2003; Fekete 2009; van Zandt et al. 2012; Bergstrand et al. 2015; KC et al. 2015; Fernandez et al. 2016; Schuster-Wallace et al. 2018; Gu et al. 2018; Rufat et al. 2019; Chakraborty et al. 2020; Khajehei et al. 2020; Medina et al. 2020)
PerIncom (-)	Per capita income	(Clark et al. 1998; Cutter et al. 2003; KC et al. 2015; Roder et al. 2017; Rufat et al. 2019; Khajehei et al. 2020)
PerUnemp (+)	% Unemployed	(Cutter et al. 2003; van Zandt et al. 2012; KC et al. 2015; Fernandez et al. 2016; Roder et al. 2017; Khajehei et al. 2020; Medina et al. 2020)
PerPopPov (+)	% Population under poverty level	(Cutter et al. 2003; van Zandt et al. 2012; Bergstrand et al. 2015; KC et al. 2015; Fatemi et al. 2017; Rufat et al. 2019; Chakraborty et al. 2020; Khajehei et al. 2020)
PerHouPov (+)	% Households under the poverty level	(Cutter et al. 2003; van Zandt et al. 2012; Bergstrand et al. 2015)
PerDis (+)	% Disabled population	(Clark et al. 1998; Bergstrand et al. 2015; Rufat et al. 2015, 2019; Pricope et al. 2019; Chakraborty et al. 2020)
PerDiswpov (+)	% Disabled population below poverty level	(Bergstrand et al. 2015; Rufat et al. 2019; Chakraborty et al. 2020)
PerNoVehic (+)	% Housing without vehicle	(van Zandt et al. 2012; Felsenstein and Lichter 2014; Bergstrand et al. 2015; Rufat et al. 2019; Chakraborty et al. 2020; Khajehei et al. 2020; Medina et al. 2020)

Parameter/Correlation	Definition	References
Incless35K (+)	% Population earning less than 35K in the last 12 months	(Cutter et al. 2003; Remo et al. 2016)
Incless40K (+)	% Population earning less than 40K in the last 12 months	(Cutter et al. 2003; Remo et al. 2016)
PerwthoutEarn (+)	% Population without earnings	(Remo et al. 2016)
MedHouInc (-)	Median household income	(Thakuy et al. 2011; Schuster-Wallace et al. 2018)
AggInc (-)	Aggregate Income	(Thakuy et al. 2011; Schuster-Wallace et al. 2018)
PerNoHealth (+)	% Population without health insurance	(Bergstrand et al. 2015)
PerAsis (+)	% Population with Food Stamp assistance	(Fatemi et al. 2017; Roder et al. 2017)
PerVac (-)	% Vacant housing	(Remo et al. 2016; Rufat et al. 2019; Medina et al. 2020)
PerMob (+)	% Mobile housing	(Cutter et al. 2003, 2012; van Zandt et al. 2012; KC et al. 2015; Fatemi et al. 2017; Rufat et al. 2019; Khajehei et al. 2020)
PerRent (+)	% Renters occupied	(Fekete 2009; van Zandt et al. 2012; Bergstrand et al. 2015; KC et al. 2015; Remo et al. 2016; Fernandez et al. 2016; Gu et al. 2018; Rufat et al. 2019; Pricope et al. 2019)

Parameter/Correlation	Definition	References
MedVal (-)	Median house value	(Clark et al. 1998; Cutter et al. 2003, 2012; Bergstrand et al. 2015; Fatemi et al. 2017; Rufat et al. 2019; Khajehei et al. 2020)
AvgValue (-)	Average home value	(Clark et al. 1998; Cutter et al. 2003, 2012; Bergstrand et al. 2015; Fatemi et al. 2017; Rufat et al. 2019; Khajehei et al. 2020)
MedGrossRent (-)	Median gross rent	(Clark et al. 1998; Cutter et al. 2003; Bergstrand et al. 2015; Rufat et al. 2019; Khajehei et al. 2020)
AvgCashRen (-)	Average cash rent	(Clark et al. 1998; Cutter et al. 2003; Bergstrand et al. 2015; Rufat et al. 2019; Khajehei et al. 2020)
PerLimEng (+)	% speaking English as a second language with limited English proficiency	(van Zandt et al. 2012; Bergstrand et al. 2015; KC et al. 2015; Rufat et al. 2015; Fatemi et al. 2017; Chakraborty et al. 2020)
PerRatInctoPov (+)	% Population Ratio of Income to Poverty level less than 1.0	(Clark et al. 1998; Chakraborty et al. 2020)
GINI (+)	GINI Index	(Thakuy et al. 2011; Felsenstein and Lichter 2014; Rasch 2017)
PerwthoutSocSec (+)	% Population no social security income	(Cutter et al. 2003; Bergstrand et al. 2015; Rufat et al. 2015; Fatemi et al. 2017; Khajehei et al. 2020)
PerFemHou (+)	% Female headed householders	(Cutter et al. 2003; Rufat et al. 2019; Khajehei et al. 2020)
PerFemHouAlo (+)	% Female headed householders living alone	(Schuster-Wallace et al. 2018; Gu et al. 2018; Chakraborty et al. 2020)
PerFemHwChild (+)	% Female householder with	(van Zandt et al. 2012; Bergstrand et al. 2015; Roder et al. 2017)

Parameter/Correlation	Definition	References
	children	
PerChilwFam (-)	% Children living with family	(van Zandt et al. 2012; Bergstrand et al. 2015; Roder et al. 2017)
PerServ (-)	% Population works in service industry	(Cutter et al. 2003; Bergstrand et al. 2015; Rufat et al. 2019; Khajehei et al. 2020)
PerExtrac (-)	% Population works in extractive industry	(Clark et al. 1998; Cutter et al. 2003; Bergstrand et al. 2015; Rufat et al. 2019; Khajehei et al. 2020)

REFERENCES

Abdur Rashid Sarker M, Alam K, Gow J (2013) Assessing the determinants of rice farmers' adaptation strategies to climate change in Bangladesh. Int J Clim Chang Strateg Manag 5:382–403. https://doi.org/10.1108/IJCCSM-06-2012-0033

Abebe Y, Kabir G, Tesfamariam S (2018) Assessing urban areas vulnerability to pluvial flooding using GIS applications and Bayesian Belief Network model. J Clean Prod 174:1629–1641. https://doi.org/10.1016/j.jclepro.2017.11.066

Abson DJ, Dougill AJ, Stringer LC (2012) Using Principal Component Analysis for information-rich socio-ecological vulnerability mapping in Southern Africa. Appl Geogr 35:515–524. https://doi.org/10.1016/j.apgeog.2012.08.004

Adger WN (2006) Vulnerability. Glob Environ Chang 16:268–281. https://doi.org/10.1016/j.gloenvcha.2006.02.006

Ahsan MN, Warner J (2014) The socioeconomic vulnerability index: A pragmatic approach for assessing climate change led risks-A case study in the south-western coastal Bangladesh. Int J Disaster Risk Reduct 8:32–49. https://doi.org/10.1016/j.ijdrr.2013.12.009

Alakkari S, Dingliana J (2018) Principal Component Analysis Techniques for Visualization of Volumetric Data. In: Advances in Principal Component Analysis. pp 99–120

Antolini F, Tate E, Dalzell B, et al (2020) Flood Risk Reduction from Agricultural Best Management Practices. JAWRA J Am Water Resour Assoc 56:161–179. https://doi.org/10.1111/1752-1688.12812

Armaş I, Gavriş A (2013) Social vulnerability assessment using spatial multi-criteria analysis (SEVI model) and the Social Vulnerability Index (SoVI model) – a case study for Bucharest, Romania. Nat Hazards Earth Syst Sci 13:1481–1499. https://doi.org/10.5194/nhess-13-1481-2013

Arrighi C, Campo L (2019) Effects of digital terrain model uncertainties on high-resolution urban flood damage assessment. J Flood Risk Manag 12:. https://doi.org/10.1111/jfr3.12530

Awere KG, Jakpa JT, Owusu AB (2016) Smallholder farmers' vulnerability to floods in

the Tolon District, Ghana. Interdiscip Environ Rev 17:286.
https://doi.org/10.1504/IER.2016.10001112

Ayyub BM, Braileanu HG, Qureshi N (2012) Prediction and Impact of Sea Level Rise on Properties and Infrastructure of Washington, DC. Risk Anal 32:1901–1918.
https://doi.org/10.1111/j.1539-6924.2011.01710.x

Baky MA Al, Islam M, Paul S (2020) Flood Hazard, Vulnerability and Risk Assessment for Different Land Use Classes Using a Flow Model. Earth Syst Environ 4:225–244.
https://doi.org/10.1007/s41748-019-00141-w

Balica SF, Douben N, Wright NG (2009) Flood vulnerability indices at varying spatial scales. Water Sci Technol 60:2571–2580. https://doi.org/10.2166/wst.2009.183

Balica SF, Popescu I, Beevers L, Wright NG (2013) Parametric and physically based modelling techniques for flood risk and vulnerability assessment: A comparison. Environ Model Softw 41:84–92. https://doi.org/10.1016/j.envsoft.2012.11.002

Barroca B, Bernardara P, Mouchel JM, Hubert G (2006) Indicators for identification of urban flooding vulnerability. Nat Hazards Earth Syst Sci 6:553–561.
https://doi.org/10.5194/nhess-6-553-2006

Bathi JR, Das HS (2016) Vulnerability of coastal communities from storm surge and flood disasters. Int J Environ Res Public Health 13:239.
https://doi.org/10.3390/ijerph13020239

Bathrellos GD, Skilodimou HD, Soukis K, Koskeridou E (2018) Temporal and spatial analysis of flood occurrences in the drainage basin of Pinios River (Thessaly, Central Greece). Land 7:1–18. https://doi.org/10.3390/land7030106

Battista J, Bernard B, Derosier A, et al (1998) Water Quality in the Potomac River Basin

Bergstrand K, Mayer B, Brumback B, Zhang Y (2015) Assessing the Relationship Between Social Vulnerability and Community Resilience to Hazards. Soc Indic Res 122:391–409. https://doi.org/10.1007/s11205-014-0698-3

Bertilsson L, Wiklund K, de Moura Tebaldi I, et al (2018) Urban flood resilience – A multi-criteria index to integrate flood resilience into urban planning. J. Hydrol.

Bhattacharya N, Lamond J, Proverbs D, Hammond F (2011) Impact of flooding on the value of commercial properties in the UK. Interdiscip approaches to disaster risk reduction, Dev suitable communities cities

Bjarnadottir S, Li Y, Stewart MG (2011) Social vulnerability index for coastal communities at risk to hurricane hazard and a changing climate. Nat Hazards 59:1055–

1075. https://doi.org/10.1007/s11069-011-9817-5

Boulant J, Brezzi M, Veneri P (2016) Income Levels And Inequality in Metropolitan Areas: A Comparative Approach in OECD Countries

Bradshaw CJA, Sodhi NS, Peh KSH, Brook BW (2007) Global evidence that deforestation amplifies flood risk and severity in the developing world. Glob Chang Biol 13:2379–2395. https://doi.org/10.1111/j.1365-2486.2007.01446.x

Brémond P, Grelot F, Agenais A-L (2013) Flood damage assessment on agricultural areas: review and analysis of existing methods

Brooks N, Adger WN, Kelly PM (2005) The determinants of vulnerability and adaptive capacity at the national level and the implications for adaptation. Glob Environ Chang 15:151–163. https://doi.org/10.1016/j.gloenvcha.2004.12.006

Cannon T, Twigg J, Rowell J (2003) Social Vulnerability , Sustainable Livelihoods and Disasters Report to DFID Conflict and Humanitarian Assistance Department. World 1–63

Centers for Disease for Control and Prevention (2015) Planning for an Emergency: Strategies for Identifying and Engaging At-Risk Groups

Chakraborty L, Rus H, Henstra D, et al (2020) A place-based socioeconomic status index: Measuring social vulnerability to flood hazards in the context of environmental justice. Int J Disaster Risk Reduct 43:101394. https://doi.org/10.1016/j.ijdrr.2019.101394

Chau VN, Cassells S, Holland J (2015) Economic impact upon agricultural production from extreme flood events in Quang Nam, central Vietnam. Nat Hazards 75:1747–1765. https://doi.org/10.1007/s11069-014-1395-x

Chauhan N, Shukla R, Joshi PK (2020) Assessing inherent vulnerability of farming communities across different biogeographical zones in Himachal Pradesh, India. Environ Dev 33:100506. https://doi.org/10.1016/j.envdev.2020.100506

Chen H, Liang Q, Liang Z, et al (2019a) Remote-sensing disturbance detection index to identify spatio-temporal varying flood impact on crop production. Agric For Meteorol 269–270:180–191. https://doi.org/10.1016/j.agrformet.2019.02.002

Chen H, Liang Z, Liu Y, et al (2017) Integrated remote sensing imagery and two-dimensional hydraulic modeling approach for impact evaluation of flood on crop yields. J Hydrol 553:262–275. https://doi.org/10.1016/j.jhydrol.2017.08.001

Chen W, Wang X, Deng S, et al (2019b) Integrated urban flood vulnerability assessment using local spatial dependence-based probabilistic approach. J Hydrol 575:454–469.

https://doi.org/10.1016/j.jhydrol.2019.05.043

Cho SY, Chang H (2017) Recent research approaches to urban flood vulnerability, 2006–2016. Nat. Hazards 88:633–649

Clark GE, Moser SC, Ratick SJ, et al (1998) ASSESSING THE VULNERABILITY OF COASTAL COMMUNITIES TO EXTREME STORMS: THE CASE OF REVERE, MA., USA

Commission NCP (2008) Report on Flooding andStormwater in Washington, DC. Washington DC

Couasnon A, Eilander D, Muis S, et al (2020) Measuring compound flood potential from river discharge and storm surge extremes at the global scale. Nat Hazards Earth Syst Sci 20:489–504. https://doi.org/10.5194/nhess-20-489-2020

Crichton D (2002) UK and Global Insurance Responses to Flood Hazard. Water Int. 27:119–131

Crow HA (2014) Assessment of The FEMA HAZUS-MH 2.0 Crop Loss Tool Fremont County, Iowa 2011

Cutrell AK, Rozelle J, Hines SH (2018) FEMA Standard Operating Procedure for Hazus Flood Level 2 Analysis Hazus Flood Model

Cutter SL (1996) Vulnerability to environmental hazards. Prog Hum Geogr 20:529–539. https://doi.org/10.1177/030913259602000407

Cutter SL, Boruff BJ, Shirley WL (2003) Social Vulnerability to Environmental Hazards n. Soc Sci Q 84:242–261. https://doi.org/10.1111/1540-6237.8402002

Cutter SL, Mitchell JT, Scott MS (2012) Revealing the vulnerability of people and places: A case study of Georgetown county, South carolina. Hazards, Vulnerability Environ Justice 90:83–114. https://doi.org/10.4324/9781849771542

de la Paix MJ, Lanhai L, Xi C, et al (2013) Soil degradation and altered flood risk as a consequence of deforestation. L Degrad Dev 24:478–485. https://doi.org/10.1002/ldr.1147

De Risi R, De Paola F, Turpie J, Kroeger T (2018) Life Cycle Cost and Return on Investment as complementary decision variables for urban flood risk management in developing countries. Int J Disaster Risk Reduct 28:88–106. https://doi.org/10.1016/j.ijdrr.2018.02.026

Deely SC, Dodman DC, Hardoy JC, Johnson CC (2010) World Disasters Report 2010: Focus on Urban Risk. Disasters 213

Dumenu WK, Takam Tiamgne X (2020) Social vulnerability of smallholder farmers to climate change in Zambia: the applicability of social vulnerability index. SN Appl Sci 2:436. https://doi.org/10.1007/s42452-020-2227-0

Duy PN, Chapman L, Tight M (2019) Resilient transport systems to reduce urban vulnerability to floods in emerging-coastal cities: A case study of Ho Chi Minh City, Vietnam. Travel Behav Soc 15:28–43. https://doi.org/10.1016/j.tbs.2018.11.001

Dwyer A, Zoppou C, Nielsen O (2004) Quantifying Social Vulnerability: A methodology for identifying those at risk to natural hazards

Eakin H, Luers AL (2006) Assessing the Vulnerability of Social-Environmental Systems. Annu Rev Environ Resour 31:365–394. https://doi.org/10.1146/annurev.energy.30.050504.144352

Eem S, Yang B, Jeon H (2018) Simplified Methodology for Urban Flood Damage Assessment at Building Scale using Open Data. J Coast Res 85:1396–1400. https://doi.org/10.2112/si85-280.1

Erena SH, Worku H (2019) Urban flood vulnerability assessments: the case of Dire Dawa city, Ethiopia. Nat Hazards 97:495–516. https://doi.org/10.1007/s11069-019-03654-9

FAO (2017) The impact of of natural hazards and disasters on agriculture, food security and nutrition

Fatemi F, Ardalan A, Aguirre B, et al (2017) Social vulnerability indicators in disasters: Findings from a systematic review. Int. J. Disaster Risk Reduct. 22:219–227

Fekete A (2009) Validation of a social vulnerability index in context to river-floods in Germany. Nat Hazards Earth Syst Sci 9:393–403. https://doi.org/10.5194/nhess-9-393-2009

Felsenstein D, Lichter M (2014) Social and economic vulnerability of coastal communities to sea-level rise and extreme flooding. Nat Hazards 71:463–491. https://doi.org/10.1007/s11069-013-0929-y

FEMA (2020) FEMA Flood Map Service Center. In: Natl. Flood Hazard Layer. https://msc.fema.gov/portal/home. Accessed 20 Oct 2020

FEMA FEMA (2013) Multi-hazard loss estimation methodology, flood model, HAZUS, technical manual. Dep Homel Secur Emerg Prep Response Dir FEMA, Mitig Div Washington, DC 569

Fernandez P, Mourato S, Moreira M (2016) Social vulnerability assessment of flood risk using GIS-based multicriteria decision analysis. A case study of Vila Nova de Gaia.

Geomatics, Nat Hazards Risk 7:1367–1389.
https://doi.org/10.1080/19475705.2015.1052021

Frazier TG, Thompson CM, Dezzani RJ (2013) Development of a spatially explicit vulnerability-resilience model for community level hazard mitigation enhancement. pp 13–24

Füssel H-M (2007) Vulnerability: A generally applicable conceptual framework for climate change research. Glob Environ Chang 17:155–167.
https://doi.org/10.1016/j.gloenvcha.2006.05.002

Ganguly KK, Nahar N, Hossain BM (2019) A machine learning-based prediction and analysis of flood affected households: A case study of floods in Bangladesh. Int J Disaster Risk Reduct 34:283–294. https://doi.org/10.1016/j.ijdrr.2018.12.002

Gonsalves RE (2014) Rapid Damage and LossAssessment (DaLA) December 24-25 , 2013 Floods A report by the Government of Saint Vincent and the Grenadines. 24

Goodchild MF, Smith MJ De, Longley P (2007) Geospatial Analysis Comprehensive Guide to Principles, Techniques and Software Tools. Leicester

Gu H, Du S, Liao B, et al (2018) A hierarchical pattern of urban social vulnerability in Shanghai, China and its implications for risk management. Sustain Cities Soc 41:170–179. https://doi.org/10.1016/j.scs.2018.05.047

Hadipour V, Vafaie F, Kerle N (2019) An indicator-based approach to assess social vulnerability of coastal areas to sea-level rise and flooding: A case study of Bandar Abbas city, Iran. Ocean Coast Manag 105077.
https://doi.org/10.1016/j.ocecoaman.2019.105077

Hall JW, Sayers PB, Dawson RJ (2005) National-scale Assessment of Current and Future Flood Risk in England and Wales. Nat Hazards 36:147–164.
https://doi.org/10.1007/s11069-004-4546-7

Hinkel J, Lincke D, Vafeidis AT, et al (2014) Coastal flood damage and adaptation costs under 21st century sea-level rise. Proc Natl Acad Sci U S A 111:3292–3297.
https://doi.org/10.1073/pnas.1222469111

Holand IS, Lujala P, Rød JK (2011) Social vulnerability assessment for Norway: A quantitative approach. Nor Geogr Tidsskr - Nor J Geogr 65:1–17.
https://doi.org/10.1080/00291951.2010.550167

Hoque MAA, Tasfia S, Ahmed N, Pradhan B (2019) Assessing spatial flood vulnerability at kalapara upazila in Bangladesh using an analytic hierarchy process. Sensors (Switzerland) 19

Huang D, Zhang R, Huo Z, et al (2012) An assessment of multidimensional flood vulnerability at the provincial scale in China based on the DEA method. Nat Hazards 64:1575–1586. https://doi.org/10.1007/s11069-012-0323-1

Huizinga J, De Moel H, Szewczyk W (2017) Methodology and the database with guidelines. https://doi.org/10.2760/16510

ILO (2017) Understanding the drivers of rural vulnerability

Interstate Commission on the Potomac River Basin (2020) Potomac Basin Facts - ICPRB. https://www.potomacriver.org/potomac-basin-facts/. Accessed 19 Oct 2020

Interstate Commission on the Potomac River Basin (2018) Potomac River Basin Comprehensive Water Resources Plan

Jha RK, Gundimeda H (2019) An integrated assessment of vulnerability to floods using composite index – A district level analysis for Bihar, India. Int J Disaster Risk Reduct 35:101074. https://doi.org/10.1016/j.ijdrr.2019.101074

Jiménez-Jiménez SI, Ojeda-Bustamante W, Ontiveros-Capurata RE, Marcial-Pablo M de J (2020) Rapid urban flood damage assessment using high resolution remote sensing data and an object-based approach. Geomatics, Nat Hazards Risk 11:906–927. https://doi.org/10.1080/19475705.2020.1760360

Jose R, Apura RJ, Dela Torre DM, et al (2017) Assessing the vulnerability of agricultural crops to riverine floods in kalibo, philippines using composite index method. In: GISTAM 2017 - Proceedings of the 3rd International Conference on Geographical Information Systems Theory, Applications and Management. SciTePress, pp 184–194

Karagiorgos K, Thaler T, Heiser M, et al (2016) Integrated flash flood vulnerability assessment: Insights from East Attica, Greece. J. Hydrol. 541:553–562

Karamouz M, Fereshtehpour M, Ahmadvand F, Zahmatkesh Z (2016) Coastal flood damage estimator: An alternative to FEMA's HAZUS platform. J Irrig Drain Eng 142:. https://doi.org/10.1061/(ASCE)IR.1943-4774.0001017

Karunarathne AY, Lee G (2020) Developing a multi-facet social vulnerability measure for flood disasters at the micro-level assessment. Int J Disaster Risk Reduct 49:. https://doi.org/10.1016/j.ijdrr.2020.101679

Kawasaki A, Kawamura G, Zin WW (2020) A local level relationship between floods and poverty: A case in Myanmar. Int J Disaster Risk Reduct 42:. https://doi.org/10.1016/j.ijdrr.2019.101348

Kaźmierczak A, Cavan G (2011) Surface water flooding risk to urban communities:

Analysis of vulnerability, hazard and exposure. Landsc Urban Plan 103:185–197. https://doi.org/10.1016/j.landurbplan.2011.07.008

KC B, Shepherd JM, Gaither CJ (2015) Climate change vulnerability assessment in Georgia. Appl Geogr 62:62–74. https://doi.org/10.1016/j.apgeog.2015.04.007

Khajehei S, Ahmadalipour A, Shao W, Moradkhani H (2020) OPEN A Place-based Assessment of Flash Flood Hazard and Vulnerability in the Contiguous United States. 1–12. https://doi.org/10.1038/s41598-019-57349-z

Khan NA, Gao Q, Abid M, Shah AA (2020) Mapping farmers' vulnerability to climate change and its induced hazards: evidence from the rice-growing zones of Punjab, Pakistan. Environ Sci Pollut Res. https://doi.org/10.1007/s11356-020-10758-4

Klaus S, Kreibich H, Merz B, et al (2016) Large-scale, seasonal flood risk analysis for agricultural crops in Germany. Environ Earth Sci 75:1289. https://doi.org/10.1007/s12665-016-6096-1

Kotzee I, Reyers B (2016) Piloting a social-ecological index for measuring flood resilience: A composite index approach. Ecol Indic 60:45–53. https://doi.org/10.1016/j.ecolind.2015.06.018

Lawrence RJ (2002) Inequalities in urban areas: innovative approaches to complex issues. Scand J Public Health 30:34–40. https://doi.org/10.1177/14034948020300030601

Lee JS, Choi H Il (2018) Comparison of flood vulnerability assessments to climate change by construction frameworks for a composite indicator. Sustain 10:. https://doi.org/10.3390/su10030768

Ma D, Chen J, Zhang W, et al (2007) Farmers' vulnerability to flood risk: A case study in the Poyang Lake Region. J Geogr Sci 17:269–284. https://doi.org/10.1007/s11442-007-0269-5

Magombeyi MS, Taigbenu AE (2008) Crop yield risk analysis and mitigation of smallholder farmers at quaternary catchment level: Case study of B72A in Olifants river basin, South Africa. Phys Chem Earth 33:744–756. https://doi.org/10.1016/j.pce.2008.06.050

Mandal R (2014) Flood, cropping pattern choice and returns in agriculture: A study of Assam plains, India. Econ Anal Policy 44:333–344. https://doi.org/10.1016/j.eap.2014.08.001

Mansur A V., Brondízio ES, Roy S, et al (2016) An assessment of urban vulnerability in the Amazon Delta and Estuary: a multi-criterion index of flood exposure, socio-economic conditions and infrastructure. Sustain Sci 11:625–643. https://doi.org/10.1007/s11625-

016-0355-7

Maroof MAS (2016) Assessing the influence of parameters for agricultural flood loss estimation in the Middle Cedar River Watershed, Iowa. University of Iowa

Mavhura E, Manyena B, Collins AE (2017) An approach for measuring social vulnerability in context: The case of flood hazards in Muzarabani district, Zimbabwe. Geoforum 86:103–117. https://doi.org/10.1016/j.geoforum.2017.09.008

McEntire D (2011) Understanding and reducing vulnerability: From the approach of liabilities and capabilities. Disaster Prev Manag An Int J 20:294–313. https://doi.org/10.1108/09653561111141736

Medina N, Abebe YA, Sanchez A, Vojinovic Z (2020) Assessing Socioeconomic Vulnerability after a Hurricane : A Combined Use of an Index-Based approach and Principal Components Analysis. Sustain 12:. https://doi.org/10.3390/su12041452

Merz B, Kreibich H, Schwarze R, Thieken A (2010) Assessment of economic flood damage. Nat Hazards Earth Syst Sci 10:1697–1724. https://doi.org/10.5194/nhess-10-1697-2010

Messner F, Meyer V (2006) Flood Damage, Vulnerability and Risk Perception-Challenges for Flood Damage Research. In: Schanze Jochenand Zeman E and MJ (ed) Flood Risk Management: Hazards, Vulnerability and Mitigation Measures. Springer Netherlands, Dordrecht, pp 149–167

Middelmann-Fernandes MH (2010) Flood damage estimation beyond stage-damage functions: An Australian example. J Flood Risk Manag 3:88–96. https://doi.org/10.1111/j.1753-318X.2009.01058.x

Mitigation Advisory Committee (2017) Northern Virginia Hazard Mitigation Plan

Mohanty MP, H V, Yadav V, et al (2020) A new bivariate risk classifier for flood management considering hazard and socio-economic dimensions. J Environ Manage 255:109733. https://doi.org/10.1016/j.jenvman.2019.109733

Monterroso A, Conde C, Gay C, et al (2014) Two methods to assess vulnerability to climate change in the Mexican agricultural sector. Mitig Adapt Strateg Glob Chang 19:445–461. https://doi.org/10.1007/s11027-012-9442-y

Munyai RB, Musyoki A, Nethengwe NS (2019) An assessment of flood vulnerability and adaptation: A case study of Hamutsha-Muungamunwe village, Makhado municipality. Jamba J. Disaster Risk Stud. 11

Muthusamy M, Casado MR, Salmoral G, et al (2019) A remote sensing based integrated

approach to quantify the impact of fluvial and pluvial flooding in an urban catchment. Remote Sens. 11

Myers M (1997) Trends in Floods. In: Pielke RA (ed) Workshop on the Social and Economic Impacts of Weather Proceedings, National Center for Atmospheric Research. National Center for Atmospheric Research, Boulder,CO, pp 77–86

National Weather Service High Water Level Terminology. https://www.weather.gov/aprfc/terminology#:~:text=NWS High Water Level Terminology&text=Stage - the level of the,for measurement of water level. Accessed 20 Oct 2020

National Weather Service (2016) Flood Frequency

Nelson V, Meadows K, Cannon T, et al (2002) Uncertain predictions, invisible impacts, and the need to mainstream gender in climate change adaptations. Gend Dev 10:51–59. https://doi.org/10.1080/13552070215911

Nga PH, Takara K, Cam Van N (2018) Integrated approach to analyze the total flood risk for agriculture: The significance of intangible damages – A case study in Central Vietnam. Int J Disaster Risk Reduct 31:862–872. https://doi.org/10.1016/j.ijdrr.2018.08.001

Nicholas KA, Durham WH (2012) Farm-scale adaptation and vulnerability to environmental stresses: Insights from winegrowing in Northern California. Glob Environ Chang 22:483–494. https://doi.org/10.1016/j.gloenvcha.2012.01.001

Nijman J, Wei YD (2020) Urban inequalities in the 21st century economy. Appl Geogr 117:102188. https://doi.org/10.1016/j.apgeog.2020.102188

Oubennaceur K, Chokmani K, Nastev M, et al (2019) Flood risk mapping for direct damage to residential buildings in Quebec, Canada. Int J Disaster Risk Reduct 33:44–54. https://doi.org/10.1016/j.ijdrr.2018.09.007

Ouma YO, Tateishi R (2014) Urban flood vulnerability and risk mapping using integrated multi-parametric AHP and GIS: Methodological overview and case study assessment. Water (Switzerland) 6:1515–1545. https://doi.org/10.3390/w6061515

Oxfam America (2009) Exposed: Social Vulnerability and Climate Change in the US Southeast. 24

Pantaleoni E, Engel BA, Johannsen CJ (2007) Identifying agricultural flood damage using Landsat imagery. Precis Agric 8:27–36. https://doi.org/10.1007/s11119-006-9026-5

Paprotny D, Vousdoukas MI, Morales-Nápoles O, et al (2020) Pan-European

hydrodynamic models and their ability to identify compound floods. Nat Hazards 101:933–957. https://doi.org/10.1007/s11069-020-03902-3

Pinos J, Orellana D, Timbe L (2020) Assessment of microscale economic flood losses in urban and agricultural areas: case study of the Santa Bárbara River, Ecuador. Nat Hazards 103:2323–2337. https://doi.org/10.1007/s11069-020-04084-8

Pinter N, Huthoff F, Dierauer J, et al (2016) Modeling residual flood risk behind levees, Upper Mississippi River, USA. Environ Sci Policy 58:131–140. https://doi.org/10.1016/j.envsci.2016.01.003

Prahl BF, Boettle M, Costa L, et al (2018) Damage and protection cost curves for coastal floods within the 600 largest European cities. Sci Data 5:. https://doi.org/10.1038/sdata.2018.34

Pricope NG, Halls JN, Rosul LM (2019) Modeling residential coastal flood vulnerability using finished-floor elevations and socio-economic characteristics. J Environ Manage 237:387–398. https://doi.org/10.1016/j.jenvman.2019.02.078

Rahman MS, Di L (2020) A systematic review on case studies of remote-sensing-based flood crop loss assessment. Agric 10:. https://doi.org/10.3390/agriculture10040131

Rasch R (2017) Income Inequality and Urban Vulnerability to Flood Hazard in Brazil*. Soc Sci Q 98:299–325. https://doi.org/10.1111/ssqu.12274

Rehman S, Sahana M, Hong H, et al (2019) A systematic review on approaches and methods used for flood vulnerability assessment: framework for future research. Nat Hazards 96:975–998. https://doi.org/10.1007/s11069-018-03567-z

Reid S, Smit B, Caldwell W, Belliveau S (2007) Vulnerability and adaptation to climate risks in Ontario agriculture. Mitig Adapt Strateg Glob Chang 12:609–637. https://doi.org/10.1007/s11027-006-9051-8

Remo JWF, Pinter N, Mahgoub M (2016) Assessing Illinois's flood vulnerability using Hazus-MH. Nat Hazards 81:265–287. https://doi.org/10.1007/s11069-015-2077-z

Roder G, Sofia G, Wu Z, Tarolli P (2017) Assessment of Social Vulnerability to floods in the floodplain of northern Italy. Weather Clim Soc 9:717–737. https://doi.org/10.1175/WCAS-D-16-0090.1

Roncancio DJ, Nardocci AC (2016) Social vulnerability to natural hazards in São Paulo, Brazil. Nat Hazards 84:1367–1383. https://doi.org/10.1007/s11069-016-2491-x

Rosenzweig C, Tubiello FN, Goldberg R, et al (2002) Increased crop damage in the US from excess precipitation under climate change. Glob Environ Chang 12:197–202.

https://doi.org/10.1016/S0959-3780(02)00008-0

Rufat S, Tate E, Burton CG, Maroof AS (2015) Social vulnerability to floods: Review of case studies and implications for measurement. Int J Disaster Risk Reduct 14:470–486. https://doi.org/10.1016/j.ijdrr.2015.09.013

Rufat S, Tate E, Emrich CT, Antolini F (2019) How Valid Are Social Vulnerability Models? Ann Am Assoc Geogr 109:1131–1153. https://doi.org/10.1080/24694452.2018.1535887

Rygel L, O'Sullivan D, Yarnal B (2006) A method for constructing a social vulnerability index: An application to hurricane storm surges in a developed country. Mitig Adapt Strateg Glob Chang 11:741–764. https://doi.org/10.1007/s11027-006-0265-6

Sam AS, Kumar R, Kächele H, Müller K (2017) Vulnerabilities to flood hazards among rural households in India. Nat Hazards 88:1133–1153. https://doi.org/10.1007/s11069-017-2911-6

Schuster-Wallace CJ, Murray SJ, McBean EA (2018) Integrating Social Dimensions into Flood Cost Forecasting. Water Resour Manag 32:3175–3187. https://doi.org/10.1007/s11269-018-1983-8

Shen Y, Morsy MM, Huxley C, et al (2019) Flood risk assessment and increased resilience for coastal urban watersheds under the combined impact of storm tide and heavy rainfall. J Hydrol 579:. https://doi.org/10.1016/j.jhydrol.2019.124159

Sherly MA, Karmakar S, Parthasarathy D, et al (2015) Disaster Vulnerability Mapping for a Densely Populated Coastal Urban Area: An Application to Mumbai, India. Ann Assoc Am Geogr 105:1198–1220. https://doi.org/10.1080/00045608.2015.1072792

Shrestha BB, Perera EDP, Kudo S, et al (2019) Assessing flood disaster impacts in agriculture under climate change in the river basins of Southeast Asia. Springer Netherlands

Shrestha R, Di L, Yu EG, et al (2017) Regression model to estimate flood impact on corn yield using MODIS NDVI and USDA cropland data layer. J Integr Agric 16:398–407. https://doi.org/10.1016/S2095-3119(16)61502-2

Singh O, Singh H (2015) The response of farmers to the flood hazard under rice–wheat ecosystem in Somb basin of Haryana, India: an empirical study. Nat Hazards 75:795–811. https://doi.org/10.1007/s11069-014-1341-y

Sowmya K, John CM, Shrivasthava NK (2015) Urban flood vulnerability zoning of Cochin City, southwest coast of India, using remote sensing and GIS. Nat Hazards 75:1271–1286. https://doi.org/10.1007/s11069-014-1372-4

Spielman SE, Tuccillo J, Folch DC, et al (2020) Evaluating social vulnerability indicators: criteria and their application to the Social Vulnerability Index. Nat Hazards 100:417–436. https://doi.org/10.1007/s11069-019-03820-z

Sridhar V, Ali SA, Lakshmi V (2019) Assessment and validation of total water storage in the Chesapeake Bay watershed using GRACE. J Hydrol Reg Stud 24:100607. https://doi.org/10.1016/j.ejrh.2019.100607

Stafford S, Abramowitz J (2017) An analysis of methods for identifying social vulnerability to climate change and sea level rise: a case study of Hampton Roads, Virginia. Nat Hazards 85:1089–1117. https://doi.org/10.1007/s11069-016-2622-4

Sumi SJ (2020) Compound Urban Flooding: The Emerging Hazard for Large Metropolitan Areas

Suryanto S, Rahman A (2019) Application of livelihood vulnerability index to assess risks for farmers in the Sukoharjo Regency and Klaten Regency, Indonesia. Jàmbá J Disaster Risk Stud 11:. https://doi.org/10.4102/jamba.v11i1.739

Tapia-Silva F-O, Itzerott S, Foerster S, et al (2011) Estimation of flood losses to agricultural crops using remote sensing. Phys Chem Earth, Parts A/B/C 36:253–265. https://doi.org/10.1016/j.pce.2011.03.005

Tapsell SM, Penning-Rowsell EC, Tunstall SM, Wilson TL (2002) Vulnerability to flooding: health and social dimensions. Philos Trans R Soc London Ser A Math Phys Eng Sci 360:1511–1525. https://doi.org/10.1098/rsta.2002.1013

Tella A, Balogun AL (2020) Ensemble fuzzy MCDM for spatial assessment of flood susceptibility in Ibadan, Nigeria. Nat Hazards. https://doi.org/10.1007/s11069-020-04272-6

Thakuy JK, Singh KS, Ramanathan A, Gossel W (2011) Geospatial Techniqhes for Managing Enviromental Resouces. 308

U.S. Army Corps of Engineering (2016) HEC-RAS 5.0 2D Modeling User's Manual

U.S. Census Bureau (2019a) Census Reporter Profile page for Washington-Arlington-Alexandria, DC-VA-MD-WV Metro Area. https://censusreporter.org/profiles/31000US47900-washington-arlington-alexandria-dc-va-md-wv-metro-area/. Accessed 18 Oct 2020

U.S. Census Bureau (2019b) Census Reporter Profile page for Washington, DC. https://censusreporter.org/profiles/16000US1150000-washington-dc/. Accessed 18 Oct 2020

Ullah F, Saqib SE, Ahmad MM, Fadlallah MA (2020) Flood risk perception and its determinants among rural households in two communities in Khyber Pakhtunkhwa, Pakistan. Nat Hazards 104:225–247. https://doi.org/10.1007/s11069-020-04166-7

UNDP (2004) Reducing Disaster Risk: a Challenge for Development-a Global Report

United States Census Bureau (2019) Glossary. https://www.census.gov/programs-surveys/geography/about/glossary.html. Accessed 22 Oct 2020

US Army Corps of Engineers (1985) AGDAM Agricultural Flood Damage Analysis User's Manual

USDA NASS (2019) United States Summary and State Data. 2012 Census Agric 1:

Van Ootegem L, Verhofstadt E, Van Herck K, Creten T (2015) Multivariate pluvial flood damage models. Environ Impact Assess Rev 54:91–100. https://doi.org/10.1016/j.eiar.2015.05.005

van Zandt S, Peacock WG, Henry DW, et al (2012) Mapping social vulnerability to enhance housing and neighborhood resilience. Hous Policy Debate 22:29–55. https://doi.org/10.1080/10511482.2011.624528

Vásquez-León M (2009) Hispanic Farmers and Farmworkers: Social Networks, Institutional Exclusion, and Climate Vulnerability in Southeastern Arizona. Am Anthropol 111:289–301. https://doi.org/10.1111/j.1548-1433.2009.01133.x

Vega-Serratos BE, Domínguez-Mora R, Posada-Vanegas G (2018) Evaluación estacional del riesgo por inundación en zonas agrícolas. Tecnol y ciencias del agua 09:92–127. https://doi.org/10.24850/j-tyca-2018-03-04

Vozinaki AEK, Karatzas GP, Sibetheros IA, Varouchakis EA (2015) An agricultural flash flood loss estimation methodology: the case study of the Koiliaris basin (Greece), February 2003 flood. Nat Hazards 79:899–920. https://doi.org/10.1007/s11069-015-1882-8

Wahl T, Jain S, Bender J, et al (2015) Increasing risk of compound flooding from storm surge and rainfall for major US cities. Nat Clim Chang 5:1093–1097. https://doi.org/10.1038/nclimate2736

Walkling B, Haworth BT (2020) Flood risk perceptions and coping capacities among the retired population, with implications for risk communication: A study of residents in a north Wales coastal town, UK. Int J Disaster Risk Reduct 51:. https://doi.org/10.1016/j.ijdrr.2020.101793

Weerasinghe KM, Gehrels H, Arambepola NMSI, et al (2018) Qualitative Flood Risk

assessment for the Western Province of Sri Lanka. In: Procedia Engineering. Elsevier Ltd, pp 503–510

Wilby RL, Keenan R (2012) Adapting to flood risk under climate change. Prog Phys Geogr 36:348–378. https://doi.org/10.1177/0309133312438908

Win S, Zin WW, Kawasaki A, San ZMLT (2018) Establishment of flood damage function models: A case study in the Bago River Basin, Myanmar. Int J Disaster Risk Reduct 28:688–700. https://doi.org/10.1016/j.ijdrr.2018.01.030

Wu Z, Shen Y, Wang H (2019) Assessing Urban Areas' Vulnerability to Flood Disaster Based on Text Data: A Case Study in Zhengzhou City. Sustain 11:4548. https://doi.org/10.3390/su11174548

Xian S, Lin N, Hatzikyriakou A (2015) Storm surge damage to residential areas: a quantitative analysis for Hurricane Sandy in comparison with FEMA flood map. Nat Hazards 79:1867–1888. https://doi.org/10.1007/s11069-015-1937-x

Yang Q, Zhang S, Dai Q, Yao R (2020) Improved Framework for Assessing Vulnerability to Different Types of Urban Floods. Sustainability 12:7668. https://doi.org/10.3390/su12187668

Yang W, Xu K, Lian J, et al (2018) Multiple flood vulnerability assessment approach based on fuzzy comprehensive evaluation method and coordinated development degree model. J Environ Manage 213:440–450. https://doi.org/10.1016/j.jenvman.2018.02.085

Yerramilli S (2012) A Hybrid Approach of Integrating HEC-RAS and GIS Towards the Identification and Assessment of Flood Risk Vulnerability in the City of Jackson, MS. Am J Geogr Inf Syst 1:7–16. https://doi.org/10.5923/j.ajgis.20120101.02

Zahran S, Brody SD, Peacock WG, et al (2008) Social vulnerability and the natural and built environment: A model of flood casualties in Texas. Disasters 32:537–560. https://doi.org/10.1111/j.1467-7717.2008.01054.x

Zarafshani K, Sharafi L, Azadi H, Van Passel S (2016) Vulnerability Assessment Models to Drought: Toward a Conceptual Framework. Sustainability 8:588. https://doi.org/10.3390/su8060588

Zhang N, Huang H (2013) Social vulnerability for public safety: A case study of Beijing, China. Chinese Sci Bull 58:2387–2394. https://doi.org/10.1007/s11434-013-5835-x

Zheng N, Takara K, Tachikawa Y, Kozan O (2008) Analysis of Vulnerability to Flood Hazard Based on Land Use and Population Distribution in the Huaihe River Basin, China. Annu Disasaster Prev Resour Institute, Kyoto Univ 83–91

Zhou Q, Mikkelsen PS, Halsnæs K, Arnbjerg-Nielsen K (2012) Framework for economic pluvial flood risk assessment considering climate change effects and adaptation benefits. J Hydrol 414–415:539–549. https://doi.org/10.1016/j.jhydrol.2011.11.031

Zscheischler J, Westra S, Van Den Hurk BJJM, et al (2018) Future climate risk from compound events. Nat. Clim. Chang. 8:469–477

BIOGRAPHY

Tuğkan Tanır was born in Ankara, Turkey. He received a Bachelor of Science in Environmental Engineering from Middle East Technical University (METU) in 2016. He worked as a Consulting Engineer in several drought management projects. He joined the MS program of the Civil, Environmental, and Infrastructure Engineering Department at George Mason University (GMU) in Fall-2018.